

Radiative and Electroweak Penguin B Decays

A. Ishikawa¹, U. Haisch², T. Feldmann³, and J. Yamaoka⁴

¹*Tohoku University*

**E-mail: akimasa@epx.phys.tohoku.ac.jp*

²*University of Oxford*

**E-mail: Ulrich.Haisch@physics.ox.ac.uk*

³*University of Siegen*

**E-mail: thorsten.feldmann@uni-siegen.de*

⁴*Pacific Northwest National Laboratory*

.....
This is a chapter of the B2TiP book.

	<i>Contents</i>	PAGE
1	Radiative and Electroweak Penguin B Decays	2
1.1	Introduction	2
1.1.1	Theoretical Basics	2
1.2	Radiative penguin decays	5
1.2.1	Inclusive $B \rightarrow X_q \gamma$ decays	5
1.2.2	Measurements of $B \rightarrow X_s \gamma$	9
1.2.3	Measurement of $B \rightarrow X_d \gamma$	11
1.2.4	Exclusive $b \rightarrow q \gamma$ decays	12
1.2.5	Measurement of $B \rightarrow V \gamma$	16
1.2.6	Importance of PID for $b \rightarrow d \gamma$	17
1.3	EW penguin decays	19
1.3.1	Inclusive $B \rightarrow X_q \ell^+ \ell^-$ decay	19
1.3.2	Measurement of $B \rightarrow X_s \ell^+ \ell^-$	22
1.3.3	Exclusive $b \rightarrow q \ell^+ \ell^-$ Decays	24
1.3.4	Measurement of $B \rightarrow K^{(*)} \ell^+ \ell^-$	26
1.3.5	$b \rightarrow q \tau^+ \tau^-$ and Lepton Flavor Non-Universality	28
1.3.6	Tests of Lepton Flavor Universality in $b \rightarrow s \ell^+ \ell^-$ and $B_q \rightarrow \tau^+ \tau^-$	31
1.3.7	Future Interplay of Inclusive and Exclusive $b \rightarrow s \ell^+ \ell^-$ Measurements	32
1.4	Double-radiative decays	33
1.4.1	Searches for $B_q \rightarrow \gamma \gamma$	36
1.4.2	$B \rightarrow X_s \gamma \gamma$ decay	37
1.4.3	$B \rightarrow K^{(*)} \nu \bar{\nu}$ Transitions and Missing Energy Signals	38
1.4.4	Search for $B_q \rightarrow \nu \bar{\nu}$ or Invisible Final States	46
1.5	Conclusions	47

1. Radiative and Electroweak Penguin B Decays

Editors: T. Feldmann, U. Haisch, A. Ishikawa and J. Yamaoka

Additional section writers: W. Altmannshofer, G. Bell, C. Bobeth, S. Cunliffe, T. Huber, J. Kamenik, A. Kokulu, E. Kou, E. Manoni, M. Misiak, G. Paz, D. Straub, S. Wehle, R. Zwicky

1.1. Introduction

Flavor-changing neutral current (FCNC) $b \rightarrow s$ and $b \rightarrow d$ processes continue to be of great importance to precision flavor physics. The Belle II physics program in this area will focus on processes and measurements, such as fully-inclusive measurements of $B \rightarrow X_{s,d}\gamma$ and $B \rightarrow X_{s,d}\ell^+\ell^-$, as well as decays such as $B_{d,s} \rightarrow \gamma\gamma$, $B \rightarrow K^{(*)}\nu\bar{\nu}$ and $B_{d,s} \rightarrow \tau^+\tau^-$.

Secondly, Belle II will provide an independent test of anomalies recently uncovered by the LHCb and Belle experiments in the angular analysis of $B \rightarrow K^*\mu^+\mu^-$ [1–3], in the determination of $R_K = \text{Br}(B^+ \rightarrow K^+\mu^+\mu^-)/\text{Br}(B^+ \rightarrow K^+e^+e^-)$ [4], and $R_K^* = \text{Br}(B^0 \rightarrow K^{*0}\mu^+\mu^-)/\text{Br}(B^0 \rightarrow K^{*0}e^+e^-)$ [5]. Some of these measurements have also been performed by the CMS and ATLAS experiments, although with less sensitivity [6–8]. Complementary to the LHCb results, Belle II has access to processes such as $B \rightarrow K^{(*)}\tau^+\tau^-$ and $B \rightarrow K^{(*)}\nu\bar{\nu}$.

1.1.1. Theoretical Basics.

Effective Hamiltonian. After decoupling the top quark, the Higgs boson and the electroweak (EW) gauge bosons, flavor-changing weak interactions relevant for the $b \rightarrow q\gamma$ transitions with $q = d, s$ can be described in the Standard Model (SM) by the following effective Hamiltonian (see e.g. [9, 10])

$$\mathcal{H}_{\text{eff}}^{\text{SM}} = -\frac{4G_F}{\sqrt{2}} \lambda_t^{(q)} \left[\sum_{i=1}^8 C_i Q_i + \kappa_q \sum_{i=1}^2 C_i (Q_i - Q_i^u) \right]. \quad (1)$$

Here G_F is the Fermi constant and we have defined $\kappa_q = \lambda_u^{(q)}/\lambda_t^{(q)} = (V_{uq}^* V_{ub})/(V_{tq}^* V_{tb})$. The crucial difference between the transitions with d -quarks and s -quarks in the final state stems from the distinct Cabibbo-Kobayashi-Maskawa (CKM) hierarchy

$$\begin{aligned} \lambda_u^{(s)} : \lambda_c^{(s)} : \lambda_t^{(s)} &= \mathcal{O}(\lambda^4 : \lambda^2 : \lambda^2), \\ \lambda_u^{(d)} : \lambda_c^{(d)} : \lambda_t^{(d)} &= \mathcal{O}(\lambda^3 : \lambda^3 : \lambda^3), \end{aligned} \quad (2)$$

with the Wolfenstein parameter $\lambda \simeq 0.23$ governing the size of branching ratios and the respective hierarchies of different decay topologies.

Expressions for the current-current ($Q_{1,2}$), four-quark (Q_{3-6}), photonic dipole (Q_7) and gluonic dipole (Q_8) operators can be found for instance in [10]. Let us quote here the most

important ones:

$$\begin{aligned}
Q_1 &= (\bar{q}_L \gamma_\mu T^a c_L)(\bar{c}_L \gamma^\mu T^a b_L), \\
Q_2 &= (\bar{q}_L \gamma_\mu c_L)(\bar{c}_L \gamma^\mu b_L), \\
Q_7 &= \frac{e}{16\pi^2} m_b (\bar{q}_L \sigma^{\mu\nu} b_R) F_{\mu\nu}, \\
Q_8 &= \frac{g_s}{16\pi^2} m_b (\bar{q}_L \sigma^{\mu\nu} T^a b_R) G_{\mu\nu}^a,
\end{aligned} \tag{3}$$

where e and g_s are the electromagnetic and strong coupling, $F_{\mu\nu}$ and $G_{\mu\nu}^a$ the $U(1)_{\text{em}}$ and $SU(3)_c$ field-strength tensors, T^a are colour matrices and the indices L, R denote the chirality of the quark fields. The operators $Q_{1,2}^u$ appearing in (1) are obtained from $Q_{1,2}$ by replacing c -quark by u -quark fields.

The Wilson coefficients C_i in (1) contain the short-distance (SD) dynamics, i.e. physics from high energies, and can thus be calculated in perturbation theory. In the SM, they are first evaluated at the scale $\mu_w = \mathcal{O}(m_W)$ and then evolved down to $\mu_b = \mathcal{O}(m_b)$ using the renormalisation group equations (RGEs) in the effective theory. At present, all the low-energy Wilson coefficients $C_i(\mu_b)$ relevant for $b \rightarrow q\gamma$ are known to next-to-next-to-leading order (NNLO) in QCD, and include a resummation of logarithmically-enhanced effects of $\mathcal{O}(\alpha_s^2)$ contributions [11].

In the case of the radiative decays into two charged leptons $b \rightarrow q\ell^+\ell^-$ with $\ell = e, \mu, \tau$, the SM operator basis in (1) has to be extended by two additional operators

$$\begin{aligned}
Q_9 &= (\bar{q}_L \gamma_\mu b_L)(\bar{\ell} \gamma^\mu \ell), \\
Q_{10} &= (\bar{q}_L \gamma_\mu b_L)(\bar{\ell} \gamma^\mu \gamma_5 \ell),
\end{aligned} \tag{4}$$

while for the $b \rightarrow q\nu\bar{\nu}$ transitions only the single operator

$$Q_L = (\bar{q}_L \gamma_\mu b_L) \sum_\ell (\bar{\nu}_{\ell L} \gamma^\mu \nu_{\ell L}), \tag{5}$$

is relevant. Also in the case of the $b \rightarrow q\ell^+\ell^-$ modes the relevant low-energy Wilson coefficients $C_i(\mu_b)$ are known to NNLO accuracy within the SM [12–14], while in the case of $b \rightarrow q\nu\bar{\nu}$ only the next-to-leading order (NLO) corrections are fully known [15, 16].¹

The effect of physics beyond the SM (BSM) to radiative and rare $b \rightarrow q$ transitions can enter (1) in essentially two ways: (i) through modified values for the high-scale Wilson coefficients C_i not necessarily aligned with the flavor coefficients $\lambda_t^{(q)}$ and/or (ii) through additional operators with different chirality and/or flavor structures compared to the SM.

Hadronic Effects. As it stands, the effective Hamiltonian (1) only describes the weak decays at the parton level. The physics associated to long-distance (LD) dynamics requires to evaluate hadronic matrix elements

$$\langle X_{d,s}\gamma(\ell^+\ell^-) | Q_i | B \rangle, \tag{6}$$

of the operators Q_i which contain non-perturbative QCD effects. A particular subtlety arises from the fact that in case of purely hadronic operators, the final state can also be generated

¹The smallness of NNLO effects in $B_s \rightarrow \mu^+\mu^-$ [17] suggests that also in the case of $b \rightarrow q\nu\bar{\nu}$ such contributions should have a very limited phenomenological impact. NLO EW effects similar to those studied in [18, 19] are instead more relevant.

by (real or virtual) photon radiation from internal lines during the hadronic transition. The theoretical description of hadronic corrections to the partonic decay crucially depends on the way these transitions are probed in terms of one or the other hadronic observable. In all cases one exploits the fact that the mass m_b of the decaying b -quark is significantly larger than the typical hadronic scale set by (multiples of) the fundamental QCD scale $\Lambda_{\text{QCD}} = \mathcal{O}(200 \text{ MeV})$.

For fully-inclusive observables, the heavy-quark expansion (HQE) is equivalent to a local operator product expansion (OPE) [20, 21], by which total decay rates can be expressed in terms of forward B -meson matrix elements of local operators. Here the partonic decay represents the leading term in a simultaneous expansion in powers of Λ_{QCD}/m_b and $\alpha_s(m_b)$ and only two non-trivial matrix elements appear up to $\mathcal{O}(\Lambda_{\text{QCD}}^2/m_b^2)$ in the expansion, one of which can be extracted from spectroscopy. The OPE breaks down when one tries to calculate differential inclusive decay distributions near phase-space boundaries. A twist expansion involving forward matrix elements of non-local light-cone operators (so-called shape functions) is then required to properly account for non-perturbative effects [22–24]. It was generally believed that all non-local operators reduce to local ones when the differential decay distributions are integrated over the entire phase-space, but then shown in [25, 26] for $B \rightarrow X_s \gamma$ that this is not always the case. These non-local power corrections can be expressed in terms of subleading shape functions, which makes them in principle calculable. In practice however the precise impact of non-local power corrections is difficult to estimate given the limited knowledge about the functional forms of the subleading shape functions.

In case of exclusive decay observables, B -meson decays into low-energetic hadrons can be described in Heavy Quark Effective Theory (HQET). At first approximation, the relevant hadronic quantities are given by $B \rightarrow X$ transition form factors which can be obtained with reasonable accuracy from lattice-QCD simulations, see [27] and references therein. In recent years, various lattice results became available e.g. $B \rightarrow \pi$ form factors [28, 29], $B \rightarrow K$ form factors [30, 31], $B \rightarrow K^*$ and $B_s \rightarrow \phi$ form factors [32, 33]. The lattice simulations are performed for high-momentum transfer, $q^2 \geq 14 \text{ GeV}^2$, i.e. small hadronic recoil. Predictions for smaller values of q^2 are then obtained by employing well-motivated extrapolations.

In many cases (notably for $B \rightarrow V \gamma$ decays), however, we are interested in situations where the energy transfer E_{recoil} to light hadrons in the final state is large of the order of $m_b/2$. In these cases, the systematic heavy-mass expansion leads to the concept of QCD-(improved) factorisation (QCDF) (cf. [34, 35]). The predictive power of QCDF is limited by hadronic uncertainties related to the transition form factors and the light-cone distribution amplitudes for the leading Fock states in the involved hadrons, as well as by power corrections in Λ_{QCD}/m_b . Form factors at large hadronic recoil can, for instance, be calculated with QCD light-cone sum rules (LCSRs), for a review see e.g. [36, 37]. Recent LCSR estimates include twist-three radiative and twist-four tree-level contributions, but have an accuracy of not better than 10%, which implies an uncertainty of at least 20% on the level of branching ratios (see for instance [38] for a recent discussion). More troublesome is the issue of power corrections. A naive dimensional estimate indicates that such contributions should be of the order of $\Lambda_{\text{QCD}}/E_{\text{recoil}}$, but the exact number is hard to quantify.

1.2. Radiative penguin decays

98

1.2.1. Inclusive $B \rightarrow X_q \gamma$ decays.

(Contributing authors: M. Misiak and G. Paz)

99

100

Experimental Status. The inclusive $B \rightarrow X_q \gamma$ decays provide important constraints on masses and interactions of many possible BSM scenarios such as models with extended Higgs sectors or supersymmetric (SUSY) theories. Measurements of their CP-averaged and isospin-averaged branching ratios by BaBar [39–42] and Belle [43, 44] lead to the following combined results

$$\text{Br}_{s\gamma}^{\text{exp}} = (3.27 \pm 0.14) \cdot 10^{-4}, \quad (7)$$

$$\text{Br}_{d\gamma}^{\text{exp}} = (1.41 \pm 0.57) \cdot 10^{-5}. \quad (8)$$

They are in perfect agreement with the corresponding SM predictions [45, 46]

$$\text{Br}_{s\gamma}^{\text{SM}} = (3.36 \pm 0.23) \cdot 10^{-4}, \quad (9)$$

$$\text{Br}_{d\gamma}^{\text{SM}} = (1.73^{+0.12}_{-0.22}) \cdot 10^{-5}. \quad (10)$$

The results in (7) to (10) correspond to the photon energy cut $E_\gamma > E_0 = 1.6 \text{ GeV}$ in the decaying meson rest frame. The measurements have been performed at $E_0 \in [1.7, 2.0] \text{ GeV}$ for $\text{Br}_{s\gamma}$, and at $E_0 \simeq 2.24 \text{ GeV}$ for $\text{Br}_{d\gamma}$. Next, extrapolations down to $E_\gamma > E_0 = 1.6 \text{ GeV}$ were applied. Such extrapolations are unavoidable because the experimental background subtraction errors rapidly grow with decreasing E_0 , while the theoretical non-perturbative uncertainties grow with increasing E_0 .

In the average for $\text{Br}_{s\gamma}^{\text{exp}}$ given in (7), only the measurements at $E_0 = 1.9 \text{ GeV}$ have been chosen as an input, and the extrapolation factors from [47] have been used. The question whether uncertainties in these factors have been properly estimated awaits a devoted study [48–50], especially in view of the upcoming more precise measurements at Belle II. The necessary extrapolation for $\text{Br}_{d\gamma}^{\text{exp}}$ (8) was performed in [51], following the method of [47]. In this case, the precision is much less of an issue given the large uncertainties in the original experimental result [40].

Basic Formulas. Theoretical calculations of $\text{Br}_{q\gamma}$ within and beyond the SM are based on the equality

$$\Gamma(\bar{B} \rightarrow X_q \gamma) = \Gamma(b \rightarrow X_q^p \gamma) + \delta\Gamma_{\text{non-per}}, \quad (11)$$

where $\Gamma(b \rightarrow X_q^p \gamma)$ stands for the perturbative b -quark decay rate with only charmless partons in the final state X_s^p (strangeness = -1) or X_d^p (strangeness = 0). As long as E_0 is large ($E_0 \simeq m_b/2$) but not too close to the endpoint ($m_b - 2E_0 \gg \Lambda_{\text{QCD}}$), the non-perturbative effects accounted for by $\delta\Gamma_{\text{non-per}}$ remain under control, and constitute a correction at the few percent level [26, 52]. However, to discuss their size in a meaningful manner, one needs to get rid of $m_{b,\text{pole}}^5$ from the leading perturbative contribution $\Gamma(b \rightarrow X_q^p \gamma)$, as on-shell masses of quarks are ill-defined. For this purpose, a normalization to the semi-leptonic decay rate can be used. The SM results quoted in (9) to (10) have been derived

124 from the formula [53]

$$\text{Br}_{q\gamma} = \text{Br}_{c\ell\nu} \xi_q \frac{6\alpha}{\pi C} \left[P_q(E_0) + N_q(E_0) \right], \quad (12)$$

125 where $\xi_q = |V_{tq}^* V_{tb}/V_{cb}|^2$ is the relevant CKM factor, $\alpha = \alpha(0)$ is the electromagnetic coupling
 126 constant renormalized at $q^2 = 0$, $\text{Br}_{c\ell\nu}$ stands for the CP-averaged and isospin-averaged
 127 branching ratio of the semi-leptonic $\bar{B} \rightarrow X_c \ell \bar{\nu}$ decay, and C represents the so-called semi-
 128 leptonic phase-space factor

$$C = \left| \frac{V_{ub}}{V_{cb}} \right|^2 \frac{\Gamma(\bar{B} \rightarrow X_c \ell \bar{\nu})}{\Gamma(\bar{B} \rightarrow X_u \ell \bar{\nu})}. \quad (13)$$

129 The function $P_q(E_0)$ is defined by the ratio

$$\frac{\Gamma(b \rightarrow X_q^p \gamma) + \Gamma(\bar{b} \rightarrow X_q^p \gamma)}{|V_{cb}/V_{ub}|^2 \Gamma(b \rightarrow X_u^p e \bar{\nu})} = \xi_q \frac{6\alpha}{\pi} P_q(E_0). \quad (14)$$

130 In the $q = s$ case, the non-perturbative effects accounted for by $N_s(1.6 \text{ GeV})$ in (12) enhance
 131 the central value of $\text{Br}_{s\gamma}^{\text{SM}}$ by around 3% [54], while the corresponding uncertainty amounts to
 132 about $\pm 5\%$ [26]. In the $q = d$ case, one encounters additional sources of uncertain hadronic
 133 effects that originate from the CKM-unsuppressed $b \rightarrow du\bar{u}\gamma$ transitions [52]. We shall come
 134 back to the issue of non-perturbative corrections after discussing the dominant perturbative
 135 term $P_q(E_0)$.

136 *Theoretical Calculations of $P_s(E_0)$.* For $b \rightarrow s\gamma$, the CKM element ratio κ_s in (1) is small,
 137 changing $\text{Br}_{s\gamma}^{\text{SM}}$ by less than 0.3%. Barring this effect and the higher-order EW ones, $P_s(E_0)$
 138 is given within the SM by

$$P_s(E_0) = \sum_{i,j=1}^8 C_i^{\text{eff}}(\mu_b) C_j^{\text{eff}}(\mu_b) K_{ij}, \quad (15)$$

139 where C_i^{eff} are certain linear combinations of the Wilson coefficients C_i (cf. [45]). They differ
 140 from C_i only for $i = 7, 8$, and are fixed by the requirement that the leading-order (LO) $b \rightarrow s\gamma$
 141 and $b \rightarrow sg$ amplitudes are proportional to C_7^{eff} and C_8^{eff} .

142 To match the experimental precision, the symmetric matrix K_{ij} needs to be determined
 143 up to $\mathcal{O}(\alpha_s^2)$ in its perturbative expansion

$$K_{ij} = \sum_{n=0}^{\infty} \left(\frac{\alpha_s(\mu_b)}{4\pi} \right)^n K_{ij}^{(n)}. \quad (16)$$

144 The quantities $K_{ij}^{(0)}$ and $K_{ij}^{(1)}$ are already known in a practically complete manner, with the
 145 latest contributions coming from [55, 56]. As far as $K_{ij}^{(2)}$ are concerned, it is sufficient to
 146 restrict to the operators listed in (3) because the remaining ones are negligible at the NNLO
 147 level due to their small Wilson coefficients and other suppression factors. Currently complete
 148 NNLO expressions are available for $K_{77}^{(2)}$ [57–59] and $K_{78}^{(2)}$ [60, 61] only. For $K_{ij}^{(2)}$ with
 149 $i, j \in \{1, 2, 8\}$, the two-body final-state contributions are known in a complete manner, while
 150 the three-body and four-body contributions have been evaluated [62–64] in the Brodsky-
 151 Lepage-Mackenzie (BLM) [65] approximation.

152 It remains to discuss $K_{17}^{(2)}$ and $K_{27}^{(2)}$. The BLM approximations for these quantities are
 153 known since a long time [62, 66]. The same is true for effects due to non-vanishing quark

masses in loops on the gluon lines [67]. However, the generic non-BLM parts of $K_{17}^{(2)}$ and $K_{27}^{(2)}$ have been found so far only in two limiting cases for the c -quark mass, namely $m_c \gg m_b/2$ [68, 69] and $m_c = 0$ [45]. An interpolation between these two limits was performed in [45], leading to the conclusion that the considered non-BLM corrections are sizable, enhancing $\text{Br}_{s\gamma}^{\text{SM}}$ by about 5%.

An uncertainty of $\pm 3\%$ due to the interpolation in m_c was included in the error budget of (9). It was added in quadrature to the other three uncertainties of $\text{Br}_{s\gamma}^{\text{SM}}$: non-perturbative ($\pm 5\%$), higher-order ($\pm 3\%$) and parametric ($\pm 2\%$). Future improvements in the accuracy of the perturbative calculations of $P_s(E_0)$ will require determining $K_{17}^{(2)}$ and $K_{27}^{(2)}$ for the physical value of m_c without any interpolation.

The Case of $\text{Br}_{d\gamma}^{\text{SM}}$. Extending the NNLO calculation to the case of $\text{Br}_{d\gamma}^{\text{SM}}$, one needs to take into account that, contrary to κ_s , the ratio κ_d is not numerically small. The global CKM fit in [70] implies that

$$\kappa_d = (0.007^{+0.015}_{-0.011}) + i(-0.404^{+0.012}_{-0.014}). \quad (17)$$

Due to the small value of $\text{Re } \kappa_d$, terms proportional to $|\kappa_d|^2$ turn out to give the dominant effects in the CP-averaged $\text{Br}_{d\gamma}^{\text{SM}}$. In such terms, perturbative two-body and three-body final-state contributions arise only at $\mathcal{O}(\alpha_s^2)$ and $\mathcal{O}(\alpha_s)$, respectively. They vanish for $m_c = m_u$, which implies that they are suppressed by $m_c^2/m_b^2 \simeq 0.1$. As a result, the main κ_d effect comes from four-body final states, namely from the $b \rightarrow du\bar{u}\gamma$ mode that appears already at tree level.

One way to calculate these contributions consist in evaluating the $b \rightarrow du\bar{u}\gamma$ diagrams including a common light-quark mass m_q inside the collinear logarithms [64], and then to vary m_b/m_q between $10 \sim m_B/m_K$ and $50 \sim m_B/m_\pi$ to estimate the uncertainty. Such an approach leads to an effect of 2% to 11% on $\text{Br}_{d\gamma}$. A more involved analysis with the help of fragmentation functions gives an almost identical range [52]. As a result, the SM prediction for $\text{Br}_{d\gamma}$ in (10) is essentially insensitive to which of the two methods is used. The central value in that equation corresponds to the first method with $m_b/m_q = 50$.

Non-Perturbative Effects in $B \rightarrow X_q\gamma$. In discussing the non-perturbative effects in $B \rightarrow X_q\gamma$, one has to distinguish contributions from the interference of Q_7 with itself, and contributions from other operators. It is convenient to express the quantity $N_s(E_0)$ that was defined in (12) in terms of the Wilson coefficients, by analogy to (15)

$$N_s(E_0) = \sum_{i,j=1}^8 C_i^{\text{eff}}(\mu_b) C_j^{\text{eff}}(\mu_b) S_{ij}. \quad (18)$$

For E_0 far from the endpoint region, S_{77} is parameterized by matrix elements of higher-dimensional local operators. These matrix elements are universal in the sense that they contribute also to semi-leptonic B decays. In consequence, one finds

$$S_{77} = \sum_{n=2}^{\infty} \frac{1}{m_b^n} \sum_k c_{k,n} \langle O_{k,n} \rangle. \quad (19)$$

The $\langle O_{k,n} \rangle$ matrix elements scale as Λ_{QCD}^n , which implies that the power corrections start at power $\Lambda_{\text{QCD}}^2/m_b^2$. The coefficients $c_{k,2}$ were calculated up to $\mathcal{O}(\alpha_s)$ in [71, 72]. Their $\mathcal{O}(\alpha_s^0)$

parts [73, 74] turn out to vanish due to accidental cancellation of corrections of this order to the radiative and semi-leptonic $B \rightarrow X_u \ell \bar{\nu}$ decays. The quantity S_{77} affects the SM prediction for $\text{Br}_{s\gamma}$ (9) by around -0.3% only, which includes the effect of the $\mathcal{O}(\alpha_s^0)$ coefficients $c_{k,3}$ [75]. The coefficients $c_{k,4}$ and $c_{k,5}$ have also been calculated at $\mathcal{O}(\alpha_s^0)$ [76], but the corresponding matrix elements are poorly constrained, and the resulting small correction has been neglected in (9).

In the endpoint region, the (Q_7, Q_7) interference part of the photon energy spectrum is described by the following symbolic factorization formula:

$$\frac{d\Gamma_{77}}{dE_\gamma} \sim H \cdot J \otimes S + \frac{1}{m_b} \sum_i H \cdot J \otimes s_i + \frac{1}{m_b} \sum_i H \cdot j_i \otimes S + \mathcal{O}\left(\frac{\Lambda_{\text{QCD}}^2}{m_b^2}\right). \quad (20)$$

The hard functions H and jet functions J, j_i are calculable in perturbation theory. The shape functions S and s_i are non-perturbative and given in terms of non-local matrix elements. At the leading power, there is only a single shape function S . It is universal in the sense that it also appears for the endpoint region of semi-leptonic B decays [22–24]. The subleading shape functions s_i contribute also to the endpoint region of semi-leptonic B decays, but in a different linear combination. For the first term in (20), H [58] and J [77] are known up to $\mathcal{O}(\alpha_s^2)$. For the second term, H and J are known explicitly at $\mathcal{O}(\alpha_s^0)$ only [78–80] (see also [81]). For the third term, H is known at $\mathcal{O}(\alpha_s^0)$ and j_i at $\mathcal{O}(\alpha_s)$ [82]. As one integrates over the photon energy in (20), the shape functions reduce to local operators, and one obtains (19). Measurements of the $B \rightarrow X_s \gamma$ photon spectrum are being used in calculations that are necessary to extract $|V_{ub}|$ from $B \rightarrow X_u \ell \bar{\nu}$ [23, 49, 83–85]. These computations currently do not include uncertainties stemming from the resolved photon contributions (see below).

Non-perturbative effects from other pairs of operators are more complicated. Apart from “direct” photon contribution arising from diagrams in which the photon couples directly to the weak vertex, there are also “resolved” photon contribution in which the photon couples to light partons. For example, Q_8 gives rise to the process $b \rightarrow sg \rightarrow s\bar{q}q\gamma$, and Q_2 leads to the process $b \rightarrow s\bar{c}c \rightarrow sg\gamma$. Such effects were discussed in the literature [25, 54, 86–91] but were only studied systematically in [26]. Taking them into account, the photon spectrum in the endpoint region can be factorized symbolically as [26]

$$\frac{d\Gamma}{dE_\gamma} \sim H \cdot J \otimes S + H \cdot J \otimes s \otimes \bar{J} + H \cdot J \otimes s \otimes \bar{J} \otimes \bar{J}. \quad (21)$$

The first term in (21) is the direct photon contribution, similar to (20), while the terms in the second line correspond to the resolved photon contributions that start at order Λ_{QCD}/m_b . The jet functions \bar{J} are perturbative. The soft functions s are non-perturbative and, unlike the shape functions, they contain non-localities in two light-cone directions.

In the integrated rate, the resolved photon contributions leads to $\Gamma \sim \bar{J} \otimes h$, where h are non-local matrix elements. At power Λ_{QCD}/m_b , the only non-vanishing contributions to the integrated rate arise from S_{27} , S_{78} , and S_{88} . Conservative modelling gives a total of around 5% non-perturbative uncertainty in $\text{Br}_{s\gamma}^{\text{SM}}$ from the resolved photon contributions at $E_0 = 1.6 \text{ GeV}$. Direct photon contributions to S_{ij} are smaller, and can be included in the 5% uncertainty estimate.

reco. method	tagging	effi.	S/B	q	p_B	A_{CP}	Δ_{0+}	ΔA_{CP}
sum-of-exclusive	none	high	moderate	s or d	yes	yes	yes	yes
fully-inclusive	had. B	very low	very good	s and d	yes	yes	yes	yes
	SL B	very low	very good	s and d	no	yes	yes	yes
	L	moderate	good	s and d	no	yes	no	no
	none	very high	very bad	s and d	no	no	no	no

Table 1: Observables accessible in $B \rightarrow X_q \gamma$ and the corresponding reconstruction methods. The table uses abbreviations for reconstruction (reco.), hadronic (had.), semi-leptonic and leptonic (SL and L), efficiency (effi.), signal to background ratio (S/B), if the spectator quark may be specified (q), and if the momentum of the signal B meson is measured (p_B).

The resolved photon contributions are more important in the case of the CP asymmetry 227

$$A_{CP} = \frac{\Gamma(\bar{B} \rightarrow X_s \gamma) - \Gamma(B \rightarrow X_{\bar{s}} \gamma)}{\Gamma(\bar{B} \rightarrow X_s \gamma) + \Gamma(B \rightarrow X_{\bar{s}} \gamma)}. \quad (22)$$

As shown in [92], they dominate over perturbative effects [93–96]. One finds a CP asymmetry in the range $[-0.6\%, 2.8\%]$ compared to around 0.5% from perturbative effects alone. Resolved photon contributions also imply that the difference between the CP asymmetries for charged and neutral B mesons are sensitive to new-physics effects [92].

Currently, the main source of uncertainty in $\text{Br}_{s\gamma}^{\text{SM}}$ is the resolved photon contribution. The extraction of HQET parameters from $B \rightarrow X_c \ell \bar{\nu}$, as done in [97], can help to better control the S_{27} contribution. By better measuring the isospin asymmetry (IA) 234

$$\Delta_{0+} = \frac{\Gamma(B^0 \rightarrow X_s \gamma) - \Gamma(B^+ \rightarrow X_s \gamma)}{\Gamma(B^0 \rightarrow X_s \gamma) + \Gamma(B^+ \rightarrow X_s \gamma)}, \quad (23)$$

one can furthermore hope to pin down the S_{78} contributions since these quantities are directly related [26, 98]. New Belle II measurements can therefore help to suppress non-perturbative uncertainties in the SM predictions for $B \rightarrow X_s \gamma$. 237

1.2.2. Measurements of $B \rightarrow X_s \gamma$. (Contributing author: A. Ishikawa) 238

There are two methods to reconstruct $B \rightarrow X_q \gamma$ decays. They will be referred to as the sum-of-exclusive method and the fully-inclusive method. In the sum-of-exclusive method, the hadronic system is reconstructed from many exclusive decays containing a kaon, such as $K n \pi$, $K \eta m \pi$ or $3 K m \pi$, where $n \geq 1$ and $m \geq 0$. Hadronic candidates are then combined with a hard photon to reconstruct B -meson candidates. In the fully-inclusive method, the other B meson is fully reconstructed either in a hadronic final state (hadronic tag), or with an energetic lepton (semi-leptonic tag) from the B -meson decay. 246

The two reconstruction methods have their own pros and cons, and provide access to different observables, as summarised in Table 1. Only the sum-of-exclusive method can specify that the transition was $b \rightarrow s$ (or $b \rightarrow d$), whereas the fully-inclusive method can only ever measure sum of $b \rightarrow s$ and $b \rightarrow d$ transitions. Reconstructing the other B -meson decay determines the charges of b quark and/or spectator quark (d or u) in the signal B meson, which is required to measure direct CP violation and/or isospin violation. 252

The branching ratio of $B \rightarrow X_s \gamma$ was measured by BaBar [39, 41, 42, 99], Belle [43, 100] and CLEO [101]. The uncertainties of the measured branching ratios are systematically dominated. Given the expected large Belle II data sample a reduction of systematic uncertainties is of the utmost importance. For instance, at Belle the dominant source of systematic uncertainties in the inclusive analysis with lepton tagging is from hadrons faking photons. At Belle II it should be possible to reduce this uncertainty by dedicated studies of the cluster shape in the calorimeter. A conservative estimation gives that the total systematic uncertainty with a photon energy threshold of 1.8 GeV can be reduced from 6% to 4%.

So far all measurements required a photon energy greater than 1.6 GeV, extrapolating to the full range of photon energy with the threshold of 1.6 GeV assuming a theoretical model. At Belle II, the branching ratio with the photon energy threshold of 1.6 GeV is directly measurable, removing the need to perform the extrapolation and in turn the corresponding source of systematic uncertainty. Lowering the photon energy threshold will however increase the size of the systematic uncertainty due to hadronic backgrounds.

The photon spectrum in the B -meson rest frame can be directly measured with a fully-inclusive analysis with hadronic tagging, since the momentum of the B meson is known. Note that unfolding of the Doppler effect due to a finite B -meson momentum in the $\Upsilon(4S)$ rest frame is needed in case a fully-inclusive analysis with lepton tagging is performed. The hadronic tagging provides a straightforward approach to measure the moments of the photon energy spectrum. The uncertainty on the branching ratio measured with hadronic tagging is dominated by statistics at Belle due to the limited number of tagged B mesons. In view of the large data set at Belle II instead systematic uncertainties will dominate. In fact, like in the case of lepton tagging, the dominant source of systematic uncertainty arises from misreconstruction of hadrons as photons. As a result the uncertainties of the branching ratio measurements with hadronic tagging will be comparable and strongly correlated with the uncertainty in the lepton tagging analysis.

The branching ratio measurement with the sum-of-exclusive method has compared to the fully-inclusive analysis different systematics. The dominant sources of systematic uncertainties will be due to fragmentation and missing decay modes. Given the large data set it should however possible to reduce the latter source of uncertainty by including additional decay modes, but even then the accuracy of the branching ratio measurement via the sum-of-exclusive method is expected to be slightly lower than the uncertainty provided by fully-inclusive analyses.

As already mentioned around (23), measurements of the IAs, possible both with the sum-of-exclusive method and the fully-inclusive method with hadronic tagging, can be used to reduce the theoretical uncertainties in $B \rightarrow X_q \gamma$ related to non-local power corrections. BaBar measured $\Delta_{0+}(B \rightarrow X_s \gamma) = (-0.6 \pm 5.8 \pm 0.9 \pm 2.4)\%$ [102] and $\Delta_{0+}(B \rightarrow X_{s+d} \gamma) = (-6 \pm 15 \pm 7)\%$ [39] with partial data sets of 81.9 fb^{-1} and 210 fb^{-1} , respectively. In these measurements, the first error is statistical, the second is systematic and the third is due to a production ratio of $B^+ B^-$ and $B^0 \bar{B}^0$ from $\Upsilon(4S)$ decay (f_{+-}/f_{00}).

The dominant uncertainty of $\Delta_{0+}(B \rightarrow X_s \gamma)$ at Belle II will be of systematic origin and related to the ratio f_{+-}/f_{00} . The most promising method to measure f_{+-}/f_{00} without assuming isospin invariance in hadronic B decays is the use of double semi-leptonic decays,

$\bar{B} \rightarrow D^* \ell^- \bar{\nu}$, as has been done by BaBar. Belle II measurements of $\Delta_{0+}(B \rightarrow X_{s+d}\gamma)$ will instead be statistically limited.

Direct CP violation in $B \rightarrow X_{s+d}\gamma$ has also been measured in an inclusive analysis with lepton tagging. Belle has measured this quantity with the full data set and the result is dominated by statistics, $A_{\text{CP}}(B \rightarrow X_{s+d}\gamma) = (1.6 \pm 3.9 \pm 0.9)\%$ for $E_\gamma > 2.1$ GeV [103]. At Belle II with 50 ab^{-1} the statistical uncertainty will amount to 0.5%. The dominant source of systematic uncertainty from the asymmetry of the background can be assessed using increased data in background regions (so-called sidebands). A conservative estimation shows that a systematic uncertainty of 0.4% is reachable.

Both the sum-of-exclusive reconstruction and the fully-inclusive reconstruction with hadronic tagging can determine the flavor and isospin of the parent in $B \rightarrow X_q\gamma$ decays. Such a separation is needed in order to study the direct CP violation and the difference of direct CP violation between the charged and neutral B mesons $\Delta A_{\text{CP}}(B \rightarrow X_q\gamma) = A_{\text{CP}}(B^+ \rightarrow X_q^+\gamma) - A_{\text{CP}}(B^0 \rightarrow X_q^0\gamma)$.

As stated earlier the theoretical uncertainty of the CP asymmetry (22) is dominated by the contribution from resolved photons [92]. Precise measurement of A_{CP} hence allow to constrain the size of non-local power corrections. The existing measurements of A_{CP} by BaBar and Belle with 429 fb^{-1} and 140 fb^{-1} use the sum-of-exclusive method and find $(1.7 \pm 1.9 \pm 1.0)\%$ [104] and $(0.2 \pm 5.0 \pm 3.0)\%$ [105], respectively. In [104] BaBar also measured ΔA_{CP} obtaining $(5.0 \pm 3.9 \pm 1.5)\%$ for $E_\gamma > 2.1$ GeV.

Belle II can measure both A_{CP} and ΔA_{CP} using the same technique as BaBar yet with a much larger data set. A reduction of the systematic uncertainties is therefore crucial at Belle II. The systematic uncertainty due to the detector asymmetry can be reduced, in part by taking the difference of A_{CP} and in part due to the statistics of the larger data sample, since it is in practice determined from sideband events. The bias from the asymmetry due to peaking background can be expressed as a product of the number of peaking background events and the difference of A_{CP} between signal and peaking background. BaBar conservatively took all of the $B\bar{B}$ background events as contributing to the uncertainty due to peaking backgrounds. At Belle II it should be possible to obtain a more realistic estimate, since the CP asymmetries of both charged and neutral $B \rightarrow X_s\gamma$ decays and the dominant peaking backgrounds can be measured precisely. As a result the achievable accuracy of the measurement of ΔA_{CP} is determined by the statistical uncertainty for which a precision of 0.4% is expected. BaBar and Belle usually assumed that the direct CP violation does not depend on the specific X_s decay mode while Belle II can also test this assumption with its large data set.

Belle II will also perform a measurement of $\Delta A_{\text{CP}}(B \rightarrow X_{s+d}\gamma)$ using the fully-inclusive reconstruction with hadronic tagging. With 711 fb^{-1} about 300 ± 27 signal events are expected at Belle with the neutral B fraction of 52% which corresponds to a 16% precision on ΔA_{CP} . At Belle II, the statistical uncertainty is still dominant even after including a factor of two improvement in the hadronic tagging efficiency.

1.2.3. Measurement of $B \rightarrow X_d\gamma$.

(Contributing author: A. Ishikawa)

In contrast to $B \rightarrow X_s \gamma$ the inclusive $B \rightarrow X_d \gamma$ decay is experimentally largely unexplored. In consequence, Belle II is in the near-term future the only place to study the various $B \rightarrow X_d \gamma$ observables.

Since a fully-inclusive analysis is impossible in the presence of the large $B \rightarrow X_s \gamma$ background, a measurement of $B \rightarrow X_d \gamma$ has to rely on the sum-of-exclusive method. BaBar has managed to reconstructed $7X_d$ decay modes, 2π , 3π and 4π modes with at most one neutral pion and $\pi^\pm \eta (\rightarrow \gamma\gamma)$ mode and applied a hadronic mass cut of 2.0 GeV. At Belle II the statistical uncertainties will at some point be smaller than the systematic ones, and the increase in luminosity can be exploited to achieve a better understanding of the hadronic spectrum as well as the fragmentation of the X_d system, including missing modes to reduce the systematic uncertainties as done by B -factories in the sum-of-exclusive measurement of $B \rightarrow X_s \gamma$. In fact, the dominant systematic uncertainty from missing modes can be reduced to 10% by adding reconstructed decay modes, such as final states having five pions, two π^0 , two kaons and an η plus multiple pions or an η' plus multiple pions, as well as by applying a looser hadronic mass cut. The second and third largest uncertainties are of statistical origin (6%) and the systematic uncertainty due to fragmentation (5%). The total uncertainty on $\text{Br}_{d\gamma}$ is expected to be around 14% with 50 ab^{-1} of integrated luminosity.

The observables $\Delta_{0+}(B \rightarrow X_d \gamma)$, $A_{\text{CP}}(B \rightarrow X_d \gamma)$ and $\Delta A_{\text{CP}}(B \rightarrow X_d \gamma)$ have up to now not been measured. In the asymmetries large parts of the systematic uncertainties cancel out and therefore the corresponding measurements will be statistically limited at Belle II. With 50 ab^{-1} of data the precision on $\Delta_{0+}(B \rightarrow X_d \gamma)$ can be estimated to be about 14%. The accuracy of A_{CP} is expected to be slightly worse than that of Δ_{0+} since flavor tagging of the other B^0 meson is needed for flavor non-eigenstate $B^0 \rightarrow X_{d\bar{d}}^0 \gamma$ decays. By taking into account a effective flavor tagging efficiency of 30% and using the product of the mixing probability in the $B^0 \bar{B}^0$ system, $\chi_d = 0.1875$, the anticipated precision of $A_{\text{CP}}(B \rightarrow X_d \gamma)$ is 5%. The quoted uncertainty is dominated by the statistical uncertainty on $A_{\text{CP}}(B^+ \rightarrow X_{u\bar{d}}^+ \gamma)$, while the accuracy of a future ΔA_{CP} measurement is dominated by the statistical uncertainty on $A_{\text{CP}}(B^0 \rightarrow X_{d\bar{d}}^0 \gamma)$ and amounts to roughly 11%.

1.2.4. Exclusive $b \rightarrow q \gamma$ decays. (Contributing authors: E. Kou and R. Zwicky)

Preliminaries. Radiative decays into light vector mesons $B_{(q,s)} \rightarrow V \gamma$ with $V = K^*, \rho, \omega, \phi$, represent prototypes of FCNC transitions. Promising candidates are $B_{(q,s)} \rightarrow (K^*, \phi) \gamma$ for the $b \rightarrow s$ and $B_{(q,s)} \rightarrow (\rho/\omega, \bar{K}^*) \gamma$ for the $b \rightarrow d$ transitions.

To first approximation only the matrix elements of the photonic dipole operator Q_7 in (3) enter, which are described by hadronic transition form factors for the $b \rightarrow q$ tensor currents. The remaining operators describe LD physics contributions, from internal emission of the photon during the hadronic transition, and thus generically involve strong-interaction phases. There are three basic LD topologies. One originating from the gluonic dipole operator Q_8 and two from four-quark operators Q_{1-6} , referred to as weak annihilation (WA) and quark loop (QL) topologies in the following. The WA topology is only relevant if the valence quarks in the initial B and light vector meson matches the flavor structure of the respective four-quark operator in (1). In the QL topology two quarks from the four-quark operators with the same flavor are contracted to a closed loop from which the external photon and/or additional gluons can be radiated.

In QCDF the LD processes have been shown to factorize at LO in Λ_{QCD}/m_b and $\mathcal{O}(\alpha_s)$ [106–108]. A LCSR computation for the contribution of Q_8 at leading twist has been performed in [109], where also a discussion of the relation to QCDF can be found. WA has been computed in the LCSR approach in [110–112]. The computation of QL in LCSR is involved, and a hybrid treatment of QCDF and LCSR has been presented in [112]. LD c -quark loop contributions are a topic in their own right and will be discussed in more detail later on.

Unlike their semi-leptonic counterparts, $B_{(q,s)} \rightarrow V\ell^+\ell^-$ to be discussed in Section 1.3.3, $B_{(q,s)} \rightarrow V\gamma$ decays do not lend themselves to a rich angular analysis. Instead, they are described by two helicity amplitudes corresponding to the two possible photon polarizations. Schematically, one has

$$H_{\mp} \propto \lambda_t^{(d,s)} \left\{ \frac{m_b}{m_{(d,s)}} \right\} C_7 (1 + \delta_{\text{fac}}) T_1(0) + \sum_{U=u,c} \lambda_U^{(d,s)} L_{\mp}^U(0), \quad (24)$$

where $T_1(0)$ is the relevant $B \rightarrow V$ transition form factor, δ_{fac} denotes factorisable QCD corrections and L_{\mp}^U stands for the previously discussed LD contributions (including the Wilson coefficients of the hadronic operators).

While in the SM the polarization of the photon is predominantly left-handed, leading to the hierarchy $H_- \gg H_+$, in BSM models with right-handed currents this does not necessarily have to be the case. In fact, LHCb reported recently the first direct observation (with 5.2σ significance) of the photon polarization in $b \rightarrow s\gamma$ through a measurement of angular correlations in $B^{\pm} \rightarrow K^{\pm}\pi^{\mp}\pi^{\pm}\gamma$ [113]. This raises the question by how much Belle II can improve on this and future LHCb measurements. Concerning the sensitivity of the photon polarization to new physics, one should compare the prospects that exclusive $b \rightarrow s\gamma$ measurements have to those that arise from $B \rightarrow K^*\ell^+\ell^-$. Relevant articles in this context are for instance [114–117].

The branching ratios for $B \rightarrow V\gamma$ decays are proportional to $|H_+|^2 + |H_-|^2$, where the form factor $T_1(0)$ in (24) provide a major part of the theoretical uncertainties. Numerically, they are estimated to be of $\mathcal{O}(4 \cdot 10^{-5})$ for the $b \rightarrow s$ transitions, while those for the $b \rightarrow d$ transitions are further suppressed by a factor of $\lambda^2 \simeq 0.05$. In contrast, WA turns out to be sizable for the $b \rightarrow d\gamma$ modes [118] as a result of the CKM hierarchies (2).

Observables. Because of the rather large hadronic uncertainties of more than 20%, the branching ratios $B \rightarrow V\gamma$ are not considered to be the most promising candidates for discovering BSM physics. On the other hand, since the uncertainties of individual modes are strongly correlated, considering ratios of branching ratios such as $R_{K^*\gamma/\phi\gamma} = \text{Br}(B \rightarrow K^*\gamma) / \text{Br}(B_s \rightarrow \phi\gamma)$ is advantageous both from a theoretical and experimental point of view. The SM prediction for this ratio reads [112]²

$$R_{K^*\gamma/\phi\gamma}^{\text{SM}} = 0.78 \pm 0.18, \quad (25)$$

²The quoted theory uncertainty is improvable as correlations have only partially been taken into account in [112].

while the LHCb collaboration measured $R_{K^*\gamma/\phi\gamma}^{\text{exp}} = 1.23 \pm 0.12$ [119, 120]. The observed deviation of 2σ cannot be regarded as statistically significant, but it would be interesting to understand if there can be a correlation to the discrepancies observed by LHCb in $B \rightarrow K^*\mu^+\mu^-$ and $B_s \rightarrow \phi\mu^+\mu^-$ (see e.g. [1, 2, 121–123]). Another ratio of interest is $R_{\rho\gamma/K^*\gamma}$, which has been used for the first determinations of $|V_{td}/V_{ts}|$ [106, 108, 124]. After the precision measurements of B_s – \bar{B}_s mixing, the extractions of $|V_{td}/V_{ts}|$ via $R_{\rho\gamma/K^*\gamma}$ are however no longer competitive.

Other observables which are sensitive to BSM contributions to (1) are the IAs, and the direct and indirect CP-asymmetries. The IAs can be defined as

$$a_I^{\bar{0}-} = \frac{c_V^2 \Gamma(\bar{B}^0 \rightarrow \bar{V}^0 \gamma) - \Gamma(B^- \rightarrow V^- \gamma)}{c_V^2 \Gamma(\bar{B}^0 \rightarrow \bar{V}^0 \gamma) + \Gamma(B^- \rightarrow V^- \gamma)}, \quad (26)$$

where $c_{\rho^0} = \sqrt{2}$ and $c_{K^{*0}} = 1$ are isospin-symmetry factors. The IAs are essentially driven by two effects, both of them involving LD physics: (i) photon emission from the spectator quark which probes the different charge factors for u -quarks and d -quarks and (ii) matrix elements of isotriplet combinations of hadronic operators in the effective Hamiltonian (1). In order to accumulate more statistics one can define CP-averaged IAs through $\bar{a}_I = (a_I^{\bar{0}-} + a_I^{0+})/2$. Subtleties concerning the CP-averaging of the IAs are discussed in Section 6.3 of [112].

Early analyses of the IAs in the framework of QCDF can be found in [106, 108, 125]. It turns out that the dominant SM contribution to (26) for $B \rightarrow K^*\gamma$ arises as a subleading effect in the HQE and involves the Wilson coefficients of Q_{1-6} . Compared to this, the effect of Q_8 is numerically suppressed, but in QCDF suffers from endpoint divergences of convolution integrals, which leads to rather large uncertainties. The problem of endpoint divergences can be avoided by determining the relevant matrix elements directly in the LCSR approach which has been performed for the contributions of Q_8 in [109] and for the QL topologies in [112].

For exclusive $b \rightarrow d\gamma$ transitions, the situation is somewhat different because the current-current operators $Q_{1,2}^u$ enter with unsuppressed CKM factors $\lambda_u^{(d)}$. Their relatively large annihilation contribution thus interferes with the naively factorizing contribution from the electromagnetic operator Q_7 proportional to $\lambda_t^{(d)}$. The resulting strong dependence of the IA of $B \rightarrow \rho\gamma$ on $\cos\phi_2$ was noted in [106, 108] where approximate formulas can be found.

The most up-to-date theoretical predictions for the IAs are [112]

$$\begin{aligned} \bar{a}_I^{\text{SM}}(K^*\gamma) &= (4.9 \pm 2.6) \% , \\ \bar{a}_I^{\text{SM}}(\rho\gamma) &= (5.2 \pm 2.8) \% . \end{aligned} \quad (27)$$

Notice that the former prediction is consistent with the HFAG average $\bar{a}_I^{\text{exp}}(K^*\gamma) = (5.2 \pm 2.6)\%$ [126], whereas the latter is in slight tension $\bar{a}_I^{\text{exp}}(\rho\gamma) = (30_{+16}^{-13})\%$, albeit with considerable uncertainty. The closeness of the two values in (27) is a consequence of the CKM angle ϕ_2 being roughly 90° which suppresses the above-mentioned interference term. This can be exploited to define the observable [112]

$$1 - \delta_{a_I} = \frac{\bar{a}_I(\rho\gamma)}{\bar{a}_I(K^*\gamma)} \sqrt{\frac{\bar{\Gamma}(B \rightarrow \rho\gamma)}{\bar{\Gamma}(B \rightarrow K^*\gamma)}} \left| \frac{V_{ts}}{V_{td}} \right|, \quad (28)$$

where δ_{a_I} is close to zero, and the quantity $(1 - \delta_{a_I})^{\text{SM}} = 0.90 \pm 0.11$ shows a reduced uncertainty with respect to the individual CP-averaged IAs (27). The experimental average $\delta_{a_I}^{\text{exp}} = -4.0 \pm 3.5$ [112] can be improved at Belle II through more statistics as well as taking into account experimental correlations. The sensitivity of (28) to BSM physics has been studied in [112] in a model-independent fashion.

At Belle II, one can study the time-dependent CP asymmetries [127]

$$A_{\text{CP}}(t) = \frac{\Gamma(\bar{B} \rightarrow f\gamma) - \Gamma(B \rightarrow f\gamma)}{\Gamma(\bar{B} \rightarrow f\gamma) + \Gamma(B \rightarrow f\gamma)} = \frac{S_{f\gamma} \sin(\Delta m_q t) - C_{f\gamma} \cos(\Delta m_q t)}{\cosh\left(\frac{\Delta\Gamma_q t}{2}\right) - H_{f\gamma} \sinh\left(\frac{\Delta\Gamma_q t}{2}\right)}, \quad (29)$$

where f ought to be a CP eigenstate as otherwise the effect washes out. Note that the width difference $\Delta\Gamma_q$ can be safely neglected for B_d but that is not the case for B_s . This feature leads to the new observables $H_{f\gamma}$ [128]. The mixing-induced asymmetries $S_{f\gamma}$ arise from the interference between $B(\bar{B}) \rightarrow f\gamma$ and $B(\bar{B}) \rightarrow \bar{B}(B) \rightarrow f\gamma$ amplitudes and read

$$S_{V\gamma} = \frac{2\text{Im}\left[\frac{q}{p}(\bar{H}_+ H_+^* + \bar{H}_- H_-^*)\right]}{|H_+|^2 + |H_-|^2 + |\bar{H}_+|^2 + |\bar{H}_-|^2}, \quad (30)$$

where p, q relate the physical and flavor eigenstates, H_{\pm} have been defined in (24), and \bar{H}_{\pm} are the corresponding amplitudes of the conjugate decay. At Belle II, one can expect a significant improvement in the determination of $A_{\text{CP}}(t)$ in the channels such as $f = K_S\pi^0, \pi^+\pi^-$ mediated by K^* and ρ resonances, which will be discussed in some more detail.

Before embarking on the discussion of LD contributions, we first give predictions for (30) including SD effects only. Using $q/p \simeq e^{-2i\phi_1}$, one obtains

$$\begin{aligned} S_{K^*(K_S\pi^0)\gamma}^{\text{SM,SD}} &= -2 \frac{m_s}{m_b} \sin 2\phi_1, \\ S_{\rho^0(\pi^+\pi^-)\gamma}^{\text{SM,SD}} &= 0. \end{aligned} \quad (31)$$

The quantity $S_{\rho^0(\pi^+\pi^-)\gamma}^{\text{SM,SD}}$ vanishes because the CP-odd oscillation phase ϕ_1 cancels exactly against the phase from the helicity amplitude. Examples of BSM models which can induce sizable right-handed currents consistent with the constraint from $\text{Br}(B \rightarrow X_s\gamma)$ include left-right symmetric models [127, 129, 130] and a supersymmetric (SUSY) $SU(5)$ grand unified theory with right-handed neutrinos [130]. A model-independent study can be found in [114].

LD QCD contributions denoted by L_U in (24) modify the predictions (31) and arise first at $\mathcal{O}(\Lambda_{\text{QCD}}/m_b)$. The dominant corrections are expected to stem from c -quark loops [131], because such effects are due to the current-current operators $Q_{1,2}$ in (1) that have large Wilson coefficients. By using the corresponding contribution of the inclusive decays it has been concluded in the latter work that the LD contamination in (31) could be as large as 10%. By performing a kinematic decomposition it can however be shown that $H_- \gg H_+$ holds at leading twist for any local transition operator [109, 132]. The hierarchy of helicity amplitudes can therefore only be broken by higher-twist effects, and one such contributions comes from gluon exchange between the c -quark loop and the vector meson. An explicit evaluation of the LD corrections due to c -quark loops [118, 128, 133] yields a correction of $\mathcal{O}(1\%)$, which is considerably smaller than the inclusive calculation would suggest (see also [134]). Further evidence for the smallness of LD c -quark effects arises from the fact that the corrections to the helicity hierarchy are of $\mathcal{O}(m_V^2/m_b^2)$. This indicates that the hierarchy

is more badly broken by excited (i.e. heavier) vector meson states. Vertex corrections are treated in QCDF [106, 107] and automatically obey $H_- \gg H_+$. The evaluation of the vertex corrections beyond factorisation is challenging and remains a future task. Including both SD and LD contributions, the quantities in (31) turn into [118, 135]

$$\begin{aligned} S_{K^*(K_S\pi^0)\gamma}^{\text{SM}} &= (-2.3 \pm 1.6)\%, \\ S_{\rho^0(\pi^+\pi^-\gamma)}^{\text{SM}} &= (0.2 \pm 1.6)\%. \end{aligned} \quad (32)$$

The photon polarization is one of the most challenging measurements in B physics today and various modes have been proposed to further improve the precision — see [114] for more details. LHCb has already applied many of the proposed methods and Belle II should be able to further extend these studies. For instance at Belle II it should be possible to expand the recent LHCb analysis [113] of angular correlations in $B^\pm \rightarrow K^\pm \pi^\mp \pi^\pm \gamma$ [136, 137] by including the neutral modes as well as performing a Dalitz analysis [138]. The angular analysis of $B \rightarrow K^* e^+ e^-$ has been performed by LHCb [139] at very low q^2 where the photonic dipole operator Q_7 and its chirality-flipped partner Q'_7 dominate. A similar analysis should be possible at Belle II and furthermore, the use the angular distribution of the converted photon from $B \rightarrow K^* \gamma$ is under discussion [140].

The direct CP asymmetries $C_{f\gamma}$ require weak CP-odd and strong CP-even phase differences of two amplitudes and are therefore by default sensitive to CP-odd phases beyond the SM. CP-even phases instead originate from LD QCD effects. In the SM the direct CP asymmetry for $b \rightarrow s\gamma$ is small, since there is no CP-odd phase at $\mathcal{O}(\lambda^3)$. These observables can thus serve as null-tests. As an example we quote $C_{\phi(\rightarrow KK)\gamma}^{\text{SM}} = (0.5 \pm 0.5)\%$ from [128]. For the $b \rightarrow d\gamma$ modes on the other hand the t -quark loop diagram induces a sizable CP-odd phase. For example, in [141] a direct CP asymmetry of 15% is predicted for $B_d \rightarrow \pi^+ \pi^- \gamma$ within the SM.

1.2.5. Measurement of $B \rightarrow V\gamma$.

(Contributing author: A. Ishikawa)

The $b \rightarrow s\gamma$ transition has been first observed by CLEO via $B \rightarrow K^* \gamma$ in 1993 [142]. Even two decades later this decay is still an important tool to search for new physics. The three most important observables in this channel are the photon polarization, the isospin and the CP asymmetries.

The K^* mesons are reconstructed from either of the $K^-\pi^0$, $K_s^0\pi^-$, $K^-\pi^+$ and $K_s^0\pi^0$ decays. The B -meson candidate is reconstructed by combining the K^* candidate and a hard photon reconstructed from an electromagnetic cluster in the electromagnetic calorimeter (ECL) which is not associated with any charged tracks in the tracking system. Exclusive modes are much cleaner than the fully-inclusive mode thanks to requirements imposed on the difference in energy, ΔE , and the beam-constrained mass, M_{bc} . The $K^-\pi^0$, $K_s^0\pi^-$ and $K^-\pi^+$ modes are flavor eigenstates which can be used for measurements of A_{CP} while $K_s^0\pi^0$ with flavor tagging of the other B meson can be used to measure the time-dependent CP asymmetry (29) which is sensitive to the polarization of the final-state photon.

At Belle II with 5 ab^{-1} [Uli: 5/ab or 50/ab?] of data the measurement of $\bar{a}_I(K^*\gamma)$ will be systematically limited. The dominant uncertainty is due to f_{+-}/f_{00} and amounts to 0.5%. Notice that this uncertainty is smaller by a factor of five than that of the most up-to-date SM prediction (27). Measurements of the direct CP asymmetries will instead still be statistically limited. The corresponding uncertainties are estimated to be 0.2% and 0.3% for

$A_{\text{CP}}(B^0 \rightarrow K^{*0}\gamma)$ and $A_{\text{CP}}(B^+ \rightarrow K^{*+}\gamma)$, respectively, which constitutes a factor of eight improvement compared to Belle. Notice that the theoretical uncertainty of the corresponding SM prediction $A_{\text{CP}}^{\text{SM}}(B^0 \rightarrow K^{*0}\gamma) = (0.3 \pm 0.1)\%$ [117] is smaller than the statistical uncertainty reachable at Belle II. A precision measurement of $A_{\text{CP}}^{\text{SM}}(B^0 \rightarrow K^{*0}\gamma)$ is nevertheless an important goal since it will allow to set stringent constraints on the imaginary part of the Wilson coefficient of Q_7 [117, 143], which otherwise is difficult to bound. Like A_{CP} also the measurement of ΔA_{CP} will be statistically limited at Belle II and the projected uncertainty amounts to 0.4% with 50 ab^{-1} of luminosity.

The $b \rightarrow d\gamma$ process was first observed in 2006 [144] by Belle through the exclusive $B \rightarrow \rho\gamma$ and $B^0 \rightarrow \omega^0\gamma$ decays. All the branching ratios, isospin asymmetries, direct and time-dependent CP asymmetries have been measured subsequently [145–147], but the achieved precision is not high enough to set stringent limits on new physics. This lack in precision is unfortunate since the measured value of $\bar{a}_I(\rho\gamma)$ shows a slight tension with the SM prediction, a fact that has already been mentioned in the context of (27). Thanks to the good particle identification (PID) system and the large integrated luminosity to be recorded at Belle II, precise measurement of $B \rightarrow (\rho, \omega)\gamma$ will be possible for the first time, which is crucial in view of the aforementioned tension.

The ρ and ω mesons are reconstructed from two-pion and three-pion final states. Hard photon candidates are combined with the light mesons to form B -meson candidates. A dominant continuum background can be suppressed by a multivariate analysis with event shape variables. The large $b \rightarrow s\gamma$ background which peaks in ΔE and M_{bc} can be significantly suppressed by the new PID system, using the iTOP for the barrel region and the ARICH for the forward endcap region.

Assuming that the current central experimental value of $\bar{a}_I(\rho\gamma)$ is confirmed, Belle II can observe a 5σ deviation from the SM prediction already with 6 ab^{-1} . With 50 ab^{-1} of data the statistical uncertainty (1.7%) will dominate the measurement with the largest systematic uncertainties are from f_{+-}/f_{00} (0.5%) and background modelling (0.5%). In total a precision of 1.9% on $\bar{a}_I(\rho\gamma)$ will be achievable at Belle II, which compares favourably with the current theoretical SM uncertainty of 2.8% as quoted in (27).

The CP asymmetries in the case of charged and neutral B mesons are measured in different ways. The mode $B^+ \rightarrow \rho^+\gamma$ is self-flavor tagging thus allowing for a straightforward measurement of the direct CP asymmetry. In contrast, $B^0 \rightarrow \rho^0\gamma$ is not a flavor eigenstate, but a time-dependent measurement with flavor tagging allows to extract both A_{CP} and the S parameter. With 50 ab^{-1} of data one can expect to reach a precision of 3.0%, 3.8% and 6.4% for $A_{\text{CP}}(B^+ \rightarrow \rho^+\gamma)$, $A_{\text{CP}}(B^0 \rightarrow \rho^0\gamma)$ and $S_{\rho^0\gamma}$, respectively.

1.2.6. Importance of PID for $b \rightarrow d\gamma$.

(Contributing author: S. Cunliffe)

In both the inclusive analysis of $B \rightarrow X_d\gamma$ (described in Section 1.2.3) and exclusive analyses (Section ??), particle identification (PID) information plays an important role. Specifically PID is necessary to reduce the problematic background originating from misidentified kaons from $B \rightarrow X_s\gamma$ processes. For example, in the case of the dominant process $B^0 \rightarrow K^{*0}\gamma$ where the excited kaon decays to the charged final state: $K^{*0} \rightarrow K^+\pi^-$. This process is roughly a factor 100 larger than the dominant $b \rightarrow d\gamma$ process, namely $B^0 \rightarrow \rho^0\gamma$ with $\rho^0 \rightarrow \pi^+\pi^-$.

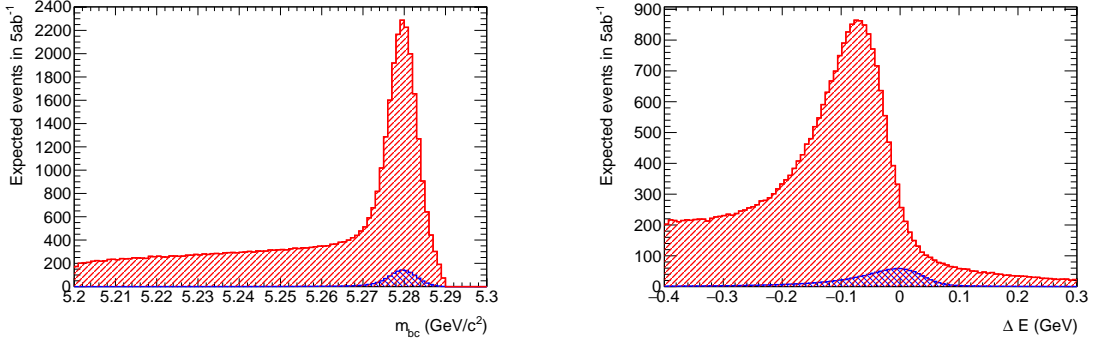


Fig. 1: Distributions of M_{bc} and ΔE for correctly identified $B^0 \rightarrow \rho^0\gamma$ signal events (blue) overlaid with misidentified $B \rightarrow K^*\gamma$ where the kaon from the K^{*0} decay is misreconstructed as a pion (red). With no PID selection cut the background swamps the signal.

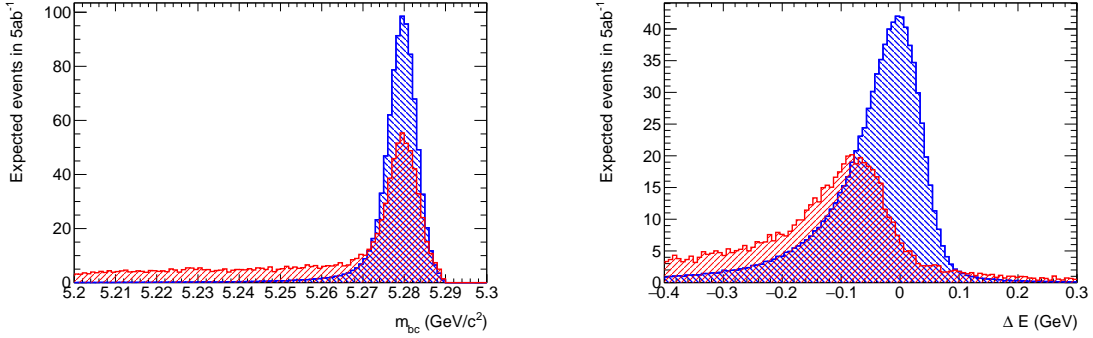


Fig. 2: Same as Figure 1 but employing PID information. After a simple optimization the background is reduced significantly.

A study based on full Belle II simulation is performed to quantify the performance of PID. Samples of 1 million events of both $B^0 \rightarrow \rho^0\gamma$ and $B^0 \rightarrow K^{*0}\gamma$ are generated. After performing a full detector reconstruction a simple pre-selection criteria is applied to both samples. An optimization for a cut on the pion probability (defined in Section ??) is performed to maximise the figure of merit, $S/\sqrt{S+B}$. Here S is the number of correctly identified $B^0 \rightarrow \rho^0\gamma$ events, and B is the number of $B^0 \rightarrow K^{*0}\gamma$ where the kaon track was misreconstructed as a pion. Both S and B are scaled to the expected number of events in 5ab^{-1} of data. The value of the optimal selection cut is found to give a figure of merit well above 10.

Figures 1 and 2 show overlaid distributions of the beam constrained-mass, M_{bc} , and energy difference, ΔE , for both samples before, and after the selection cut at the optimal point. The importance of PID is evident from the two figures.

The above study is repeated using a simulation of the Belle detector, in order to compare to the associated Belle PID performance. The Belle optimisation is performed for the analogous PID likelihood variables described in Section 5.2.1 of [148]. The Belle II PID system is found to provide an improvement in the figure of merit by approximately 30%.

1.3. EW penguin decays1.3.1. Inclusive $B \rightarrow X_q \ell^+ \ell^-$ decay. (Contributing authors: G. Bell and T. Huber)

Inclusive $B \rightarrow X_q \ell^+ \ell^-$ decays provide information on the quark flavor sector that is complementary to inclusive $b \rightarrow q \gamma$ and exclusive $b \rightarrow q \ell^+ \ell^-$ transitions. In contrast to $B \rightarrow X_q \gamma$, an angular analysis of the decay products entails a richer dependence on the SD Wilson coefficients. Compared to exclusive $b \rightarrow q \ell^+ \ell^-$ decays, on the other hand, hadronic uncertainties are under better theoretical control for the inclusive modes. Measurements of the $B \rightarrow X_q \ell^+ \ell^-$ decay distributions at Belle II will thus complement the LHCb studies of the exclusive $b \rightarrow q \ell^+ \ell^-$ transitions, thereby providing important cross-checks of the deviations found by LHCb and Belle in $B \rightarrow K^* \mu^+ \mu^-$ and related modes [2–4, 149].

The two main kinematic variables in inclusive $B \rightarrow X_s \ell^+ \ell^-$ decays are the di-lepton invariant mass squared $m_{\ell\ell}^2 = q^2$ and $z = \cos \theta$, where θ is the angle between the three-momenta of the positively charged lepton ℓ^+ and the initial B meson in the di-lepton center-of-mass frame. In terms of these variables, the double differential decay width takes the form of a second-order polynomial in z [150],

$$\frac{d^2\Gamma}{dq^2 dz} = \frac{3}{8} [(1+z^2)H_T(q^2) + 2zH_A(q^2) + 2(1-z^2)H_L(q^2)]. \quad (33)$$

The functions H_T , H_A , and H_L represent three independent observables. H_A is up to a rational factor equivalent to the forward-backward asymmetry [151], while the q^2 spectrum is given by the sum of H_T and H_L :

$$\begin{aligned} \frac{dA_{\text{FB}}}{dq^2} &= \int_{-1}^{+1} dz \frac{d^2\Gamma}{dq^2 dz} \text{sgn}(z) = \frac{3}{4} H_A(q^2), \\ \frac{d\Gamma}{dq^2} &= \int_{-1}^{+1} dz \frac{d^2\Gamma}{dq^2 dz} = H_T(q^2) + H_L(q^2). \end{aligned} \quad (34)$$

The observables mainly depend on the Wilson coefficients C_7 , C_9 and C_{10} . Taking only these three coefficients into account and suppressing a common prefactor $G_F^2 m_b^5 |V_{ts}^* V_{tb}|^2 / (48\pi^3)$, one has (with $\hat{s} = q^2/m_b^2$)

$$\begin{aligned} H_T(q^2) &= 2\hat{s}(1-\hat{s})^2 \left[\left| C_9 + \frac{2}{\hat{s}} C_7 \right|^2 + |C_{10}|^2 \right], \\ H_L(q^2) &= (1-\hat{s})^2 \left[|C_9 + 2C_7|^2 + |C_{10}|^2 \right], \\ H_A(q^2) &= -4\hat{s}(1-\hat{s})^2 \text{Re} \left[C_{10} \left(C_9 + \frac{2}{\hat{s}} C_7 \right) \right]. \end{aligned} \quad (35)$$

The di-lepton invariant mass spectrum is dominated by charmonium resonances (J/ψ , $\psi(2S)$, etc.), which are usually removed by kinematic cuts. This leads to the so-called perturbative di-lepton invariant mass regions: the low- q^2 region for $1 \text{ GeV}^2 < q^2 < 6 \text{ GeV}^2$ and the high- q^2 region for $q^2 > 14.4 \text{ GeV}^2$. Within these regions, one expects that the theoretical uncertainties can be controlled to around 10%.

In the low- q^2 region, the observables can be computed within a local OPE in the heavy-quark limit. The perturbative calculation is well advanced and higher-order QCD [12, 152–160] and EW [160–163] corrections are available to NNLO and NLO, respectively. The leading

power corrections of order $\Lambda_{\text{QCD}}^2/m_b^2$ [74, 164–166], $\Lambda_{\text{QCD}}^3/m_b^3$ [167, 168] and $\Lambda_{\text{QCD}}^2/m_c^2$ [54] are also known.

In the high- q^2 region, on the other hand, the heavy-mass expansion breaks down at the endpoint of the q^2 spectrum. For the integrated high- q^2 spectrum, however, there exists an effective expansion in inverse powers of $m_b^{\text{eff}} = m_b (1 - \sqrt{\hat{s}_{\text{min}}})$ instead of m_b . This expansion converges less rapidly, and the convergence behaviour depends on the value of the q^2 cut, $\hat{s}_{\text{min}} = q_{\text{min}}^2/m_b^2$ [158].

The differential decay width is furthermore affected by QED corrections, which lead to two major modifications. First, the electron and muon channels get different contributions of the form $\ln(m_b^2/m_\ell^2)$, which stem from collinear photon emissions. Second, the simple z -dependence of the double differential decay distribution in (33) gets modified and becomes a complicated function of z [163]. In the presence of QED radiation, the observables (35) are therefore defined by taking appropriate projections of the double differential rate [163]. In order to compare theoretical predictions with experimental data, it is important that the experimental analyses use the same prescriptions.

The theoretical uncertainties can be further reduced by normalizing the observables to the inclusive semi-leptonic $B \rightarrow X_c \ell \bar{\nu}$ decay rate. The SM predictions for the $B \rightarrow X_s \mu^+ \mu^-$ observables then become

$$\begin{aligned} H_T[1, 6]_{\mu\mu} &= (4.03 \pm 0.28) \cdot 10^{-7}, \\ H_L[1, 6]_{\mu\mu} &= (1.21 \pm 0.07) \cdot 10^{-6}, \\ H_A[1, 6]_{\mu\mu} &= (-0.42 \pm 0.16) \cdot 10^{-7}, \\ \text{Br}[1, 6]_{\mu\mu} &= (1.62 \pm 0.09) \cdot 10^{-6}, \\ \text{Br}[> 14.4]_{\mu\mu} &= (2.53 \pm 0.70) \cdot 10^{-7}. \end{aligned} \tag{36}$$

Here the notation $O[q_0, q_1]$ with $O = H_T, H_L, H_A, \text{Br}$ means that the relevant observable has been integrated over $q^2 \in [q_0^2, q_1^2]$. The complete list of theory predictions can be found in [163]. To tame the large uncertainty in the high- q^2 branching ratio, which mainly stems from poorly known parameters in the power corrections, a normalization to the semi-leptonic $B \rightarrow X_u \ell \bar{\nu}$ rate with the same cut in q^2 was proposed [168],

$$\mathcal{R}(s_0) = \frac{\int_{\hat{s}_0}^1 d\hat{s} \frac{d\Gamma_{B \rightarrow X_s \ell^+ \ell^-}}{d\hat{s}}}{\int_{\hat{s}_0}^1 d\hat{s} \frac{d\Gamma_{B \rightarrow X_u \ell \bar{\nu}}}{d\hat{s}}}. \tag{37}$$

Employing this normalization results in

$$\mathcal{R}(14.4)_{\mu\mu} = (2.62 \pm 0.30) \cdot 10^{-3}. \tag{38}$$

Unfortunately, the achieved precision cannot yet be exploited, because the BaBar [169, 170] and Belle [171–173] measurements suffer from sizable experimental uncertainties in the ballpark of 30%. Furthermore, all measurements performed at the B -factories are based on a sum over exclusive final states, which makes a direct comparison to the theoretical predictions non-trivial. The latest published measurement of the branching ratio by Belle [172] is based on a sample of $152 \cdot 10^6$ $B\bar{B}$ events only, which corresponds to less than 30% of its total

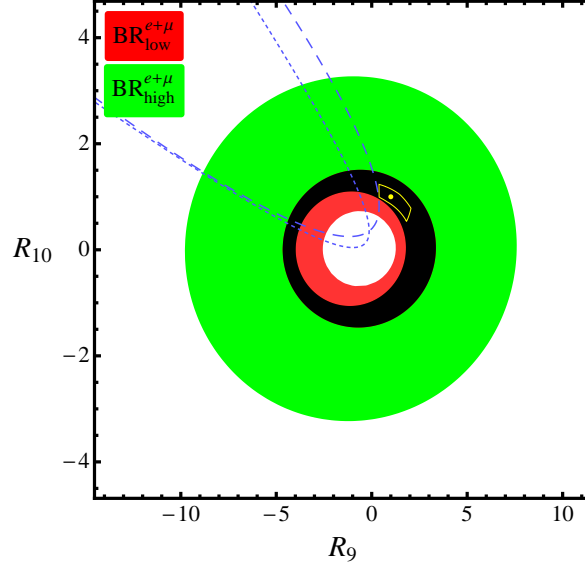


Fig. 3: 95% confidence level (CL) constraints on the Wilson coefficient ratios $R_{9,10} = C_{9,10}/C_{9,10}^{\text{SM}}$. Shown are the branching ratio constraints at low- q^2 (red) and high- q^2 (green), together with their overlap (black). The region outside the dashed parabola shaped regions is allowed by the Belle measurement of the forward-backward asymmetry. The yellow dot is the SM point and the yellow contour is the future Belle II reach. See [163] for further details.

dataset. BaBar has more recently presented an analysis using its entire dataset ($471 \cdot 10^6 B\bar{B}$ 643 events) [170]. The weighted averages of the experimental results read [163] 644

$$\begin{aligned} \text{Br}[1, 6]_{\ell\ell}^{\text{exp}} &= (1.58 \pm 0.37) \cdot 10^{-6}, \\ \text{Br}[> 14.4]_{\ell\ell}^{\text{exp}} &= (4.8 \pm 1.0) \cdot 10^{-7}, \end{aligned} \quad (39)$$

for the low- q^2 and high- q^2 region, respectively. In addition, Belle presented a measure- 645 ment of the forward-backward asymmetry [173] and BaBar a measurement of the CP 646 asymmetry [170]. 647

Belle II can significantly improve upon this situation and with its two orders of magnitude 648 larger data sample, it might for the first time be possible to perform a complete angular 649 analysis of $B \rightarrow X_s \ell^+ \ell^-$ decays. In the beginning, Belle II will still have to rely on the sum- 650 over-exclusive method, but a fully-inclusive analysis based on the recoil technique may be 651 feasible in the long term. 652

The prospects for future improvements on the experimental side calls for refinements of 653 the SM predictions. Some of the important questions to be addressed are: 654

- (i) In the absence of a fully-inclusive analysis, one has to revisit the theoretical issues that 655 arise from semi-inclusive analyses. In particular, a cut on the hadronic invariant mass 656 $M_{X_s} \lesssim 1.8 \text{ GeV}$ affects the low- q^2 region and induces additional theoretical uncertainties. 657 The theoretical description in this “shape-function region” is similar to $B \rightarrow X_u \ell \nu$ and 658 $B \rightarrow X_s \gamma$ decays [174, 175]. An analysis of the effects from sub-leading shape functions 659

was presented in [176], and a prediction for the position of the zero of the forward-backward asymmetry in the presence of the M_{X_s} cut was given in [177]. Similar studies for other observables as well as a detailed analysis of the impact of the M_{X_s} cut on the extraction of the Wilson coefficients are yet to be performed.

(ii) Similar to inclusive $B \rightarrow X_s \gamma$ decays (see Section 1.2.1), a systematic analysis of hadronic non-local power corrections includes resolved contributions in which the virtual photon couples to light partons instead of connecting directly to the effective weak interaction vertex. These contributions stay non-local even when the hadronic mass cut is released and therefore represent an irreducible uncertainty independent of the cut. A detailed analysis that quantifies this uncertainty is currently in progress [178].

(iii) To estimate the impact of the charmonium resonances on the low- q^2 and high- q^2 regions, one may attempt to model the resonance structure explicitly. The current implementation via the Krüger-Sehgal approach [179] uses dispersion relations for the electromagnetic vacuum polarization. The model is based on the assumption that the $c\bar{c}$ loop and the $b \rightarrow s$ transition factorize, which is not justified on theoretical grounds. Since LHCb measurements of $B^+ \rightarrow K^+ \mu^+ \mu^-$ indeed suggest that non-factorizable corrections substantially modify the interference, theoretical investigations that go beyond the Krüger-Sehgal approach seem to be required.

(iv) The ratio $R_{X_s} = \text{Br}_{\mu\mu}/\text{Br}_{ee}$, in analogy to the quantity $R_{K^{(*)}}$ in the exclusive modes, is among the “golden modes” proposed for the early Belle II run. A measurement of R_{X_s} will shed light on possible hints for lepton flavor non-universality recently observed by LHCb [4, 5]. Given the expected Belle II precision, a careful reanalysis of photon radiation will become important since collinear QED corrections represent the leading source of lepton flavor universality breaking in the SM. As the size of these contributions is sensitive to the imposed experimental cuts, a close interaction between experiment and theory is needed.

(v) The latest analyses of $B \rightarrow X_d \ell^+ \ell^-$ decays date back more than ten years [180, 181]. An update with a decomposition into angular observables, including higher-order QCD and QED bremsstrahlung corrections, appears to be timely. Due to the different hierarchy of CKM elements, one expects larger CP-violating effects in $b \rightarrow d \ell^+ \ell^-$ than in $b \rightarrow s \ell^+ \ell^-$ transitions.

The experimental data can be used to constrain new-physics effects in a model-independent fashion, i.e. by constraining the Wilson coefficients. For the case of C_9 and C_{10} the current situation as well as the potential impact of future Belle II measurements is illustrated in Figure 3 [150, 163]. From the figure it is evident that the new-physics potential of $B \rightarrow X_s \ell^+ \ell^-$ decays has not yet been fully exploited. Furthermore, right-handed currents — which have been extensively studied in exclusive transitions — were not included in the latest theory studies, and the synergy and complementarity of inclusive and exclusive $b \rightarrow s \ell^+ \ell^-$ analyses is yet to be explored. To this purpose, detailed Monte Carlo studies could be used in conjunction with realistic theory predictions to estimate how much statistics is needed at Belle II to reach or exceed the sensitivity of the LHCb measurements on the exclusive modes. Such analyses could build on the studies [150, 163].

1.3.2. Measurement of $B \rightarrow X_s \ell^+ \ell^-$.

(Contributing author: A. Ishikawa)

All existing measurements of the inclusive $B \rightarrow X_s \ell^+ \ell^-$ mode have employed the sum-of-exclusive method [169–173]. In this method the hadronic system X_s is reconstructed from $K n \pi$ final states with $n \leq 4$, allowing for at most one neutral pion. The X_s system is combined with the di-electron or di-muon pair to reconstruct the B meson. The B meson is identified by its ΔE and M_{bc} distributions. Since the decay does not contain hard photons, the ΔE resolution is much better than that in $B \rightarrow X_s \gamma$. This allows one to adopt a tight ΔE selection which compared to the $B \rightarrow X_s \gamma$ analysis suppresses the likelihood of multiple candidates in a single event and the self-cross-feed. A hadronic mass selection is applied to reduce combinatorial backgrounds, i.e. $M_{X_s} < 1.8 \text{ GeV}$ at BaBar [170] and $M_{X_s} < 2.1 \text{ GeV}$ [171] or $M_{X_s} < 2.0 \text{ GeV}$ [172, 173] at Belle. Our study of the prospects of the $B \rightarrow X_s \ell^+ \ell^-$ measurements at Belle II are based on a cut of $M_{X_s} < 2.0 \text{ GeV}$, but we emphasize that this selection can be loosened in order to better understand the X_s spectrum and to reduce theoretical uncertainties. There are three dominant backgrounds. The first one is associated to $c\bar{c}$ continuum events in which both charm quarks decay semi-leptonically, the second one arises from $B\bar{B}$ events with two leptons either from semi-leptonic B or D decays, and the third one is due to $B \rightarrow J/\psi (\psi(2S)) X_s$ backgrounds. The semi-leptonic backgrounds can be suppressed by missing energy information and vertex quality requirement, while the $B \rightarrow J/\psi (\psi(2S)) X_s$ backgrounds can be eliminated by applying appropriate cuts on the invariant mass of the di-lepton system.

The partial branching ratios in the low- q^2 and high- q^2 regions are under good theoretical control (see (36) and (38)) and thus precise measurements of the di-lepton spectra will allow to put stringent constraints on the Wilson coefficients C_9 and C_{10} . We define the following q^2 regions $1 \text{ GeV}^2 < q^2 < 3.5 \text{ GeV}^2$ (low1), $3.5 \text{ GeV}^2 < q^2 < 6 \text{ GeV}^2$ (low2) and $q^2 > 14.4 \text{ GeV}^2$ (high). Given the large data sample expected at Belle II the reduction of systematic uncertainties is crucial. Thanks to the large branching fractions of the $B \rightarrow K^{(*)} \ell^+ \ell^-$ modes and the good ΔE resolution compared to $B \rightarrow X_s \gamma$, missing-mode and fragmentation uncertainties can be reduced by adding additional reconstructed decays, such as three-kaon modes, to the data sample. **[Uli: Changed sentence. Check that this is what was/is meant.]** In the high (low) q^2 region, these uncertainties are expected to be as small as 1% (as large as 4%) due to the lower (higher) multiplicity of X_s decays while K^*-X_s transition uncertainty could be as large as 2% (as small as 1%) due to the larger (smaller) fraction of K^* . **[Uli: Maybe simplify sentence a bit?]** With 50 ab^{-1} of data we expect total uncertainties of 6.6%, 6.4% and 4.7% for the partial branching ratios in the low1, low2 and high region as defined above.

Belle II measurements of the forward-backward asymmetry A_{FB} in $B \rightarrow X_s \ell^+ \ell^-$ are expected to provide the most stringent limits on the Wilson coefficients C_9 and C_{10} . Since large parts of the theoretical and experimental systematic uncertainties cancel out in A_{FB} the corresponding measurements will be statistically limited. The expected uncertainties on A_{FB} in the low1, low2 and high region are 3.1%, 2.6% and 2.4%, respectively, assuming the SM.

A helicity decomposition of $B \rightarrow X_s \ell^+ \ell^-$ provides the three observables H_i defined in (33). While H_A and the combination $H_T + H_L$ have been measured (cf. (34)) independent measurements of H_T and H_L have not been performed by BaBar and Belle, but will be possible

at Belle II. As for the measurements of the branching ratios, the experimental determinations of the coefficients H_i will be systematically limited until 10 ab^{-1} have been collected. Considering normalized observables might help to reduce the systematic uncertainties.

Measurement of the CP asymmetries in $B \rightarrow X_s \ell^+ \ell^-$ can be used to search for new source of CP violation. Not only the rate asymmetry, but also the CP asymmetry of angular distributions, such as forward-backward CP asymmetry ($A_{\text{FB}}^{\text{CP}}$) are useful [182]. Since the denominator of the $A_{\text{FB}}^{\text{CP}}$ can be zero if A_{FB} for \bar{B} and B are zero or have opposite sign, we consider the difference of the A_{FB} between \bar{B} and B mesons defined as $\Delta_{\text{CP}}(A_{\text{FB}}) = A_{\text{FB}}^{\bar{B}} - A_{\text{FB}}^B$.

[Uli: To be continued?]

1.3.3. Exclusive $b \rightarrow q \ell^+ \ell^-$ Decays. (Contributing author: W. Altmannshofer, U. Haisch and D. Straub)

The $\bar{B} \rightarrow \bar{K}^* (\rightarrow \bar{K} \pi) \ell^+ \ell^-$ transition is completely described in terms of twelve angular coefficient functions I_j [183?]. These quantities encode the angular distribution of the exclusive decay. They can be expressed in terms of helicity (or transversity) amplitudes that depend on the di-lepton invariant mass squared, the Wilson coefficients $C_7, C_9, C_{10}, C_S, C_P$ and their chirality-flipped counterparts as well as the $B \rightarrow K^*$ form factors that arise from the matrix elements $\langle K^* | Q_i | B \rangle$. The situation is much simpler for the $B \rightarrow K \ell^+ \ell^-$ decay which gives rise to only three observables, namely the branching ratio, the forward-backward asymmetry A_{FB} and the flat term F_H [184].

The self-tagging nature of the $\bar{B} \rightarrow \bar{K}^* (\rightarrow \bar{K} \pi) \ell^+ \ell^-$ decay means that it is possible to determine both CP-averaged and CP-asymmetric quantities that depend on the coefficients [183]

$$S_j = (I_j + \bar{I}_j) \Big/ \frac{d\Gamma}{dq^2}, \quad A_j = (I_j - \bar{I}_j) \Big/ \frac{d\Gamma}{dq^2}, \quad (40)$$

respectively. Here \bar{I}_j denote the angular coefficient functions of the CP-conjugated $B \rightarrow K^* (\rightarrow K \pi) \ell^+ \ell^-$ decay. The two most measured angular observables are the forward-backward asymmetry and the K^* longitudinal polarization fraction:

$$A_{\text{FB}} = \frac{3}{4} S_{6s} + \frac{3}{8} S_{6c}, \quad F_L = -S_{2c}. \quad (41)$$

By exploiting symmetry relations it is also possible to construct CP-averaged observables that are largely insensitive to form-factor uncertainties [185?, 186]. These are

$$P_1 = \frac{S_3}{2S_{2s}}, \quad P_2 = \frac{S_{6s}}{8S_{2s}}, \quad P_3 = -\frac{S_9}{4S_{2s}}, \quad (42)$$

as well as

$$\begin{aligned} P'_4 &= \frac{S_4}{2\sqrt{-S_{2s}S_{2c}}}, & P'_5 &= \frac{S_5}{2\sqrt{-S_{2s}S_{2c}}}, \\ P'_6 &= \frac{S_7}{2\sqrt{-S_{2s}S_{2c}}}, & P'_8 &= \frac{S_8}{2\sqrt{-S_{2s}S_{2c}}}. \end{aligned} \quad (43)$$

The above definitions of the coefficients S_j and the observables P_i and P'_i correspond to those used by LHCb [2]. Analog CP-violating observables P_i^{CP} and P'_i^{CP} can be defined by simply replacing the coefficient S_j in the numerator of P_i and P'_i by the corresponding

coefficient A_j . Notice that the observables P_1 and P_2 are commonly also called $A_T^{(2)} = P_1$ [?] and $A_T^{\text{Re}} = 2P_2$ [187].

In order to illustrate the importance of Belle II measurements of the observables defined in (41) to (43), we consider the two cases P_1 and P'_5 . At small di-lepton masses the angular variable P_1 is sensitive to the photon polarization. In fact, in the heavy-quark and large-energy limit and ignoring α_s and m_s/m_b suppressed effects, one finds

$$P_1 \simeq \frac{2\text{Re}(C_7 C'_7)}{|C_7|^2 + |C'_7|^2}. \quad (44)$$

To maximize the sensitivity to the virtual photon, it is necessary to go to very small q^2 which is only possible in the case of the decay $B \rightarrow K^* e^+ e^-$. Precision measurement of P_1 (as well as of $P_3^{\text{CP}} \propto \text{Im}(C_7 C'_7)$) in the di-electron channel are thus essential for probing possible BSM effects related to the right-handed magnetic penguin operator Q'_7 [115, 132, 188]. Consequently, decays like $B \rightarrow K^* e^+ e^-$ emerge as highly relevant for the Belle II programme.

The angular observable P'_5 is instead a sensitive probe of the semi-leptonic operators Q_9 and Q_{10} and their interference with Q_7 . In the same approximation that led to (44), one obtains the expression

$$P'_5 \simeq \frac{\text{Re}(C_{10}^* C_{9,\perp} + C_{9,\parallel}^* C_{10})}{\sqrt{(|C_{9,\perp}|^2 + |C_{10}|^2)(|C_{9,\parallel}|^2 + |C_{10}|^2)}}, \quad (45)$$

if only contributions from SM operators are included. Here

$$C_{9,\perp} = C_9^{\text{eff}}(q^2) + \frac{2m_b m_B}{q^2} C_7^{\text{eff}}, \quad C_{9,\parallel} = C_9^{\text{eff}}(q^2) + \frac{2m_b}{m_B} C_7^{\text{eff}}. \quad (46)$$

Importantly the above results for P_1 and P'_5 are correct only in the infinite heavy-quark limit. While in the case of (44) the leading power-corrections are formally of $\mathcal{O}(\Lambda_{\text{QCD}}^2/m_b^2)$, in the case of (45) a rather complex structure of Λ_{QCD}/m_b terms arises (see [115] for details). Since at present the relevant power corrections can only be modeled, assumption-free extractions of C_9 and C_{10} as well as their chirality-flipped partners from measurements of P'_5 and other angular observables are not possible.

Additional information on C_9 , C_{10} , C'_9 and C'_{10} can fortunately be gleaned from the lepton flavor universality ratios

$$R_H[q_0, q_1] = \frac{\int_{q_0^2}^{q_1^2} dq^2 \frac{d\Gamma(B \rightarrow H \mu^+ \mu^-)}{dq^2}}{\int_{q_0^2}^{q_1^2} dq^2 \frac{d\Gamma(B \rightarrow H e^+ e^-)}{dq^2}}, \quad (47)$$

with $H = K, K^*$. The SM predictions for these ratios are 1 with high precision. Phase space effects are small and can be taken into account. Theoretical uncertainties from CKM factors as well as from form factors and other hadronic effects cancel in the ratio. Corrections due to collinear photon emissions have been studied recently and appear to be well described by existing Monte Carlo tools [189]. Any deviation in R_H from the SM prediction exceeding the few percent level would thus be a sign of new physics.

808 Including only the dominant linear BSM contributions from interference with the SM, the
 809 ratios R_K and R_{K^*} can be approximated by [190]

$$R_K[1, 6] \simeq 1 + \Delta_+, \quad R_{K^*}[1, 6] \simeq 1 + \Delta_+ - p(\Delta_+ - \Delta_-), \quad (48)$$

810 with

$$\Delta_{\pm} = \frac{2}{|C_9^{\text{SM}}|^2 + |C_{10}^{\text{SM}}|^2} \left\{ \sum_{i=9,10} \text{Re} \left[C_i^{\text{SM}} \left(C_i^{\text{NP}\mu} \pm C_i^{\prime\mu} \right) \right] - (\mu \rightarrow e) \right\}, \quad (49)$$

811 and $p \simeq 0.86$ is the so-called polarization fraction of the K^* meson [184, 190]. The labels
 812 “SM” and “NP” denote the SM and new-physics contributions, respectively, and the index μ
 813 or e indicates the flavor content of the corresponding operator. Under the assumption that
 814 new physics modifies the di-muon channels only and that the relevant corrections are real,
 815 one obtains numerically

$$R_K[1, 6] \simeq 1 + 0.24 \left(C_{LL}^{\text{NP}\mu} + C_{RL}^{\mu} \right), \quad (50)$$

$$R_{K^*}[1, 6] \simeq 1 + 0.24 \left(C_{LL}^{\text{NP}\mu} - C_{RL}^{\mu} \right) + 0.07 C_{RL}^{\mu},$$

816 where we have introduced the chiral Wilson coefficients

$$C_{LL}^{\text{NP}\ell} = C_9^{\text{NP}\ell} - C_{10}^{\text{NP}\ell}, \quad C_{RL}^{\ell} = C_9^{\prime\ell} - C_{10}^{\prime\ell}. \quad (51)$$

817 From (50) one observes that R_K only probes the combination $C_{LL}^{\text{NP}\ell} + C_{RL}^{\ell}$ of Wilson coef-
 818 ficients, while R_{K^*} is mostly sensitive to $C_{LL}^{\text{NP}\ell} - C_{RL}^{\ell}$. The observables R_K and R_{K^*} thus
 819 provide complementary information as they constrain different chirality structures of possible
 820 lepton flavor universality violating new physics in rare B decays. Notice furthermore that
 821 measurements of lepton flavor universality double ratios such as $R_K/R_{K^*} \simeq 1 + 0.41 C_{RL}^{\mu}$
 822 directly probe right-handed currents in a theoretically clean way [190].

823 Belle II will also be able to perform lepton flavor universality tests using angular observ-
 824 ables. Suitable variables include differences of angular observables in $B \rightarrow K^* \mu^+ \mu^-$ and
 825 $B \rightarrow K^* e^+ e^-$ [191, 192], for instance $\Delta_{\text{A}_{\text{FB}}} = \text{A}_{\text{FB}}(B \rightarrow K^* \mu^+ \mu^-) - \text{A}_{\text{FB}}(B \rightarrow K^* e^+ e^-)$ or
 826 $Q_i = P_i^{\mu} - P_i^e$. The differences in angular observables are predicted to be zero in the SM
 827 with high accuracy. Non-zero values would therefore again be an indication of new physics.

828 The recent LHCb measurements of $R_K[1, 6] = 0.745^{+0.090}_{-0.074} \pm 0.036$ [4] and $R_{K^*}[1.1, 6] =$
 829 $0.69^{+0.11}_{-0.07} \pm 0.05$ [5] deviate by 2.6σ and 2.4σ from their SM values. Previous measurements
 830 from BaBar [193] and Belle [194] have considerably larger uncertainties and are compatible
 831 with both the SM prediction and the LHCb results. New physics that only modifies the
 832 $b \rightarrow s \mu^+ \mu^-$ transition but leaves $b \rightarrow s e^+ e^-$ unaffected can explain the deviations seen in
 833 the lepton flavor universality ratios R_K and R_{K^*} and simultaneously address other B -physics
 834 anomalies, like the discrepancy in P_5' [2] and the too low $B_s \rightarrow \phi \mu^+ \mu^-$ branching ratio [123].
 835 Independent validations of the deviations observed in P_5' , R_K and R_{K^*} are needed to build
 836 a solid case for new physics. In the near future, Belle II is the only experiment that can
 837 perform such cross-checks.

838 1.3.4. Measurement of $B \rightarrow K^{(*)} \ell^+ \ell^-$. (Contributing author: A. Ishikawa and S. Wehle)

839

840 The $b \rightarrow s \ell^+ \ell^-$ transition has first been observed in 2001 by Belle in the $B \rightarrow K \ell^+ \ell^-$
 841 channel [195]. Two years later in 2003, Belle then observed the $B \rightarrow K^* \ell^+ \ell^-$ mode [196].

These observations opened the door for new-physics searches via EW penguin B decays. The branching ratio and forward-backward asymmetry as a function of q^2 in $B \rightarrow K^{(*)}\ell^+\ell^-$ are important observables and several experiments have by now measured them [6–8, 194, 197–199]. Due to the spin structure of the K^* meson, a full angular analysis of $B \rightarrow K^*\ell^+\ell^-$ with optimized observables is a very powerful way to search for new physics. These optimized angular observables are less sensitive to form factor uncertainties that plague the theory calculations.

$B \rightarrow K^\mu^+\mu^-$ channel.* In 2013, the LHCb collaboration announced the observation of a tension in the optimized observable P'_5 with 1 fb^{-1} of data [200]. This tension has been confirmed two years later when LHCb presented their $B \rightarrow K^*\mu^+\mu^-$ angular analysis based on the full LHC Run I data set of 3 fb^{-1} [2]. Belle has recently also reported results of a angular analysis with its full data set using both charged and neutral B mesons decaying to $K^*e^+e^-$ and $K^*\mu^+\mu^-$ [3]. The Belle results are consistent with the angular analyses by LHCb, which considered alone show a 3.3σ discrepancy from the SM [201].

The observed deviations make further independent measurements of the angular distributions in $B \rightarrow K^*\mu^+\mu^-$ mandatory. Our extrapolations for Belle II are based on the systematic uncertainties obtained at Belle. For example, the difference between simulation and data was estimated directly from $B \rightarrow J/\psi K^*$ decays as measured by Belle. Since at Belle II the mis-modelling in the simulation will be improved such a approach should lead to conservative projections. The uncertainty due to peaking backgrounds can be reduced by including the individual components in the fitted model. The individual components, which may be small, are more reliably modelled in a larger data set. The uncertainty that is associated to the efficiency modelling can be reduced by adding correlation between q^2 and the helicity angle $\cos\theta_l$ in the efficiency function. The helicity angle θ_l is defined as the angle between the positively (negatively) charged lepton in the rest frame of the di-lepton system and the direction of the B (\bar{B}) meson. We find that with 2.8 fb^{-1} of Belle II data, the uncertainty on P'_5 in the $4\text{ GeV}^2 < q^2 < 8\text{ GeV}^2$ bin **[Uli: Personally I would give the numbers for the $4\text{ GeV}^2 < q^2 < 6\text{ GeV}^2$ bin since it is theoretically cleaner.]** using both muon and electron modes will be comparable to the 3.0 fb^{-1} LHCb result [2] that uses the muon mode only. A naive extrapolation then leads to the conclusion that the accuracy that can be achieved on the optimized observables at Belle II with 50 ab^{-1} is just by 20% lower than the precision that LHCb is expected to reach with 50 fb^{-1} of data. We add that at Belle II the iTOP and ARICH might be able to identify low momentum muons, which may increase the available data in the low- q^2 region. Our projections do not included such possible improvements.

*$B \rightarrow K^*e^+e^-$ channel.* As mentioned before, a angular analysis of $B \rightarrow K^*e^+e^-$ at very low q^2 is a sensitive probe of the photon polarization [115, 132, 187, 188]. In fact, angular observables such as P_1 and P_3^{CP} or $A_T^{(2)}$ and A_T^{Im} **[Uli: Should mention at least some of these observables in the theory part.]** are functions of different combinations of real and imaginary parts of C_7 and C'_7 and hence together with $S_{K^*\gamma}$ and $\text{Br}(B \rightarrow X_s\gamma)$ form a basis of clean observables that allow to completely determine the contributions to Q_7 and Q'_7 from experiment.

LHCb has measured the angular observables using 3 fb^{-1} of data [139]. They reconstructed 124 signal events for the q^2 range from 0.002 GeV^2 to 1.12 GeV^2 where the lower bound is

limited by angular resolution on $\tilde{\phi}$, $\tilde{\phi}$, where $\tilde{\phi} = \phi + \phi$ if $\phi < 0$. At Belle II, the resolution in $\tilde{\phi}$ is better than that at a forward spectrometer, such as LHCb [AI: need check], and the reconstruction efficiency of the electron mode is higher than that of the muon mode at low q^2 . These features will allow for precise Belle II measurement of $B \rightarrow K^* e^+ e^-$ in the low q^2 -region. The number of reconstructed signal events in the q^2 range [Uli: Which range?] will be 202 ± 21 (2020 ± 66) events with 5 fb^{-1} (50 fb^{-1}). [Uli: Add a sentence or two to describe prospects better.]

1.3.5. $b \rightarrow q\tau^+\tau^-$ and Lepton Flavor Non-Universality. (Contributing authors: W. Altmannshofer and J. Kamenik)

B -meson decays to $\tau^+\tau^-$ final states are experimentally largely uncharted territory. While a few bounds like $\text{Br}(B_d \rightarrow \tau^+\tau^-) < 1.3 \cdot 10^{-3}$ [202] and $\text{Br}(B^+ \rightarrow K^+\tau^+\tau^-) < 2.25 \cdot 10^{-3}$ [203] do exist, they are all orders of magnitudes away from the corresponding SM predictions. In view of the fact that measurements of $\tau^+\tau^-$ final states remain a big challenge at LHCb, and that it is unclear whether a sensitivity beyond $\mathcal{O}(10^{-3})$ can be reached [204], Belle II might be the only next-generation machine that allows to explore these modes in some depths.

Purely Leptonic Modes. The most recent SM predictions for the branching ratios of the purely leptonic $B_s \rightarrow \tau^+\tau^-$ and $B_d \rightarrow \tau^+\tau^-$ decays include NNLO QCD corrections and NLO EW corrections [17, 19, 205]. They are given by

$$\begin{aligned}\text{Br}_{B_s\tau^+\tau^-}^{\text{SM}} &= (7.73 \pm 0.49) \cdot 10^{-7}, \\ \text{Br}_{B_d\tau^+\tau^-}^{\text{SM}} &= (2.22 \pm 0.19) \cdot 10^{-8}.\end{aligned}\tag{52}$$

These SM predictions refer to the average time-integrated branching ratios. The uncertainties are dominated by CKM elements and the B -meson decay constants f_{B_q} . The used input parameters are collected in [205].

Semi-Leptonic Modes. Predictions for exclusive semi-leptonic decays depend on form factors. In the semi-tauonic decays the di-lepton invariant mass, q^2 , is restricted to the range from $4m_\tau^2 \simeq 12.6 \text{ GeV}^2$ to $(m_B - m_H)^2$, where $H = \pi, K, K^*, \dots$. To avoid contributions from the resonant decay through the narrow $\psi(2S)$ charmonium resonance, $B \rightarrow H\psi(2S)$ with $\psi(2S) \rightarrow \tau^+\tau^-$, SM predictions are typically restricted to a di-tau invariant mass $q^2 > 15 \text{ GeV}^2$. In this kinematic regime, lattice computations are expected to provide reliable results for the form factors (see the discussion in Section 1.1.1).

Combining the uncertainties from the relevant CKM elements and form factors leads to SM predictions for the branching ratios of the semi-tauonic decays with an accuracy of around 10% to 15%. The presence of broad charmonium resonances above the open charm threshold is a source of additional uncertainty. Possible effects of the broad resonances are typically taken into account by assigning an additional error of a few percent following [206], which is subdominant compared to the CKM and form factor uncertainties.

SM predictions for the decay $B \rightarrow \pi\tau^+\tau^-$ have very recently been presented in [29, 207] using form factors from the Fermilab/MILC collaboration [28, 29]. Results are given for the branching ratios and the “flat term” in the angular distributions (cf. [184, 207] for the

definition of the latter observable)

$$\begin{aligned}\text{Br}_{\pi^+\tau^+\tau^-}^{\text{SM}} &= (4.29 \pm 0.39) \cdot 10^{-9}, \\ \text{Br}_{\pi^0\tau^+\tau^-}^{\text{SM}} &= (1.99 \pm 0.18) \cdot 10^{-9}, \\ F_{H,\pi\tau^+\tau^-}^{\text{SM}} &= 0.80 \pm 0.02,\end{aligned}\tag{53}$$

where the prediction for $F_{H,\pi\tau^+\tau^-}^{\text{SM}}$ holds for both B^+ and B^0 and all errors quoted in [29, 207] have been added in quadrature to obtain the final uncertainties. The above predictions correspond to a di-tau invariant mass $15 \text{ GeV}^2 < q^2 < 22 \text{ GeV}^2$. Predictions for additional q^2 bins are available in [29, 207]. The dominant uncertainties in the branching ratios come from the $B \rightarrow \pi$ form factors and the CKM input. Those uncertainties cancel to a large extent in the flat term.

Also for the $B \rightarrow K\tau^+\tau^-$ decays, SM predictions have been given in [207], using recent lattice determination of the $B \rightarrow K$ form factors from the Fermilab/MILC collaboration [31]. The SM predictions for the branching ratios and the flat terms read

$$\begin{aligned}\text{Br}_{K^+\tau^+\tau^-}^{\text{SM}} &= (1.22 \pm 0.10) \cdot 10^{-7}, \\ \text{Br}_{K^0\tau^+\tau^-}^{\text{SM}} &= (1.13 \pm 0.09) \cdot 10^{-7}, \\ F_{H,K\tau^+\tau^-}^{\text{SM}} &= 0.87 \pm 0.02,\end{aligned}\tag{54}$$

where we added all uncertainties quoted in [207] in quadrature. As in the case of the $B \rightarrow \pi\tau^+\tau^-$ decays, the value of $F_{H,K\tau^+\tau^-}^{\text{SM}}$ applies to the charged and neutral channel and the above predictions refer to a q^2 range $15 \text{ GeV}^2 < q^2 < 22 \text{ GeV}^2$. Predictions for additional q^2 bins can be found in [207]. Again, the dominant source of uncertainty in the branching ratio arises from the $B \rightarrow K$ form factors and from the CKM elements, while in the flat terms these errors largely cancel.

The SM predictions for the $B \rightarrow K^*\tau^+\tau^-$ branching ratios read [?]

$$\begin{aligned}\text{Br}_{K^{*+}\tau^+\tau^-}^{\text{SM}} &= (0.99 \pm 0.12) \cdot 10^{-7}, \\ \text{Br}_{K^{*0}\tau^+\tau^-}^{\text{SM}} &= (0.91 \pm 0.11) \cdot 10^{-7},\end{aligned}\tag{55}$$

where the di-tau invariant mass ranges from 15 GeV^2 to the kinematic endpoint around 19.2 GeV^2 . The used $B \rightarrow K^*$ form factors are based on a combined fit of lattice and LCSR results [38].

The SM prediction for the $B_s \rightarrow \phi\tau^+\tau^-$ branching ratio is given by [?]

$$\text{Br}_{\phi\tau^+\tau^-}^{\text{SM}} = (0.73 \pm 0.09) \cdot 10^{-7},\tag{56}$$

where the di-tau invariant mass ranges from 15 GeV^2 to the kinematic endpoint at roughly 18.9 GeV^2 . The used $B_s \rightarrow \phi$ form factors are based on a combined fit of lattice and LCSR results [38].

Lepton Flavor Universality Ratios. We define the lepton flavor universality ratios $R_H^{\ell\ell'}[q_0, q_1]$ in analogy to (47). In these ratios uncertainties from CKM elements drop out. Also form factor uncertainties cancel almost exactly in ratios involving electrons and muons, while in ratios with taus, these uncertainties get reduced.

952 The SM predictions from [207] read

$$\begin{aligned} (R_{\pi}^{\mu\tau})_{\text{SM}} &= 1.18 \pm 0.06, \\ (R_K^{\mu\tau})_{\text{SM}} &= 0.87 \pm 0.02, \end{aligned} \quad (57)$$

953 for $15 \text{ GeV}^2 < q^2 < 22 \text{ GeV}^2$. For the $B \rightarrow K^*$ decays we find [?]]

$$(R_{K^*}^{\mu\tau})_{\text{SM}} = 2.44 \pm 0.09, \quad (58)$$

954 where $15 \text{ GeV}^2 < q^2 < 19.2 \text{ GeV}^2$. Within the quoted uncertainties the results (57) and (58)
955 apply to both charged and neutral decays.

956 *Probing BSM Physics.* Since the $b \rightarrow q\tau^+\tau^-$ decays involve third-generation fermions in
957 the final state, one can envisage new-physics scenarios — such as models with extended
958 Higgs or gauge sectors or scenarios with leptoquarks — that give rise to effects in the $\tau^+\tau^-$
959 modes, while leaving the e^+e^- and/or $\mu^+\mu^-$ channels unaltered. In a model-independent
960 approach, tau-specific new physics in rare B -meson decays can be described by an effective
961 Hamiltonian that contains besides the operators Q_7, Q_9, Q_{10} introduced in (3) and (4) their
962 chirality-flipped partners Q'_7, Q'_9, Q'_{10} as well as

$$\begin{aligned} Q_S &= (\bar{q}_L b_R)(\bar{\tau}_R \tau_L), \\ Q'_S &= (\bar{q}_R b_L)(\bar{\tau}_L \tau_R). \end{aligned} \quad (59)$$

963 To constrain all possible $\tau^+\tau^-$ operators, one should try to measure/bound both purely
964 leptonic and semi-leptonic modes, since they have different blind directions in parameter
965 space [208, 209]. In this respect it is also interesting to note that $b \rightarrow s\nu\bar{\nu}$ decays can constrain
966 the operator combinations containing a left-handed tau current $Q_9 - Q_{10}$ and $Q'_9 - Q'_{10}$,
967 due to $SU(2)_L$ invariance. On the other hand, $b \rightarrow s\nu\bar{\nu}$ is blind to the orthogonal directions
968 $Q_9 + Q_{10}$ and $Q'_9 + Q'_{10}$, that contain right-handed tau currents.

969 Many BSM models can lead to modifications in the $b \rightarrow q\tau^+\tau^-$ channels. Interestingly,
970 several models that address the LHCb anomalies in the $b \rightarrow s\mu^+\mu^-$ sector [2, 4, 121–123, 200,
971 210] or the evidence of lepton flavor universality violation in $B \rightarrow D^{(*)}\ell\nu$ decays [211–214],
972 predict characteristic deviations in $b \rightarrow s\tau^+\tau^-$ transitions from the SM predictions.

973 The model proposed in [215] contains a Z' boson, associated to the gauge symmetry of
974 muon-number minus tau-number, $L_\mu - L_\tau$. Given the current anomalies in the $b \rightarrow s\mu^+\mu^-$
975 sector, the model predicts a suppression of all semi-leptonic $b \rightarrow s\mu^+\mu^-$ decays by about
976 20% [191]. The $L_\mu - L_\tau$ symmetry implies that all semi-leptonic $b \rightarrow s\tau^+\tau^-$ decays are
977 instead enhanced. Translating the predictions for $b \rightarrow s\mu^+\mu^-$ transitions found in the
978 minimal flavor violation (MFV) scenario of [191] to the tau sector using [?], we find

$$\begin{aligned} \text{Br}_{K^+\tau^+\tau^-}^{L_\mu - L_\tau} &= (1.46 \pm 0.13) \cdot 10^{-7}, \\ \text{Br}_{K^0\tau^+\tau^-}^{L_\mu - L_\tau} &= (1.35 \pm 0.12) \cdot 10^{-7}, \\ \text{Br}_{K^{*+}\tau^+\tau^-}^{L_\mu - L_\tau} &= (1.53 \pm 0.23) \cdot 10^{-7}, \\ \text{Br}_{K^{*0}\tau^+\tau^-}^{L_\mu - L_\tau} &= (1.40 \pm 0.21) \cdot 10^{-7}, \end{aligned} \quad (60)$$

979 where the $K^{+,0}$ branching ratios refer to the q^2 region $15 \text{ GeV}^2 < q^2 < 22 \text{ GeV}^2$, while the K^*
980 rates correspond to $15 \text{ GeV}^2 < q^2 < 19.2 \text{ GeV}^2$. The $B_s \rightarrow \tau^+\tau^-$ decay remains SM-like in
981 the $L_\mu - L_\tau$ framework.

In the scenarios discussed in [216–218], the current B physics anomalies are addressed by BSM physics in the form of left-handed currents involving mainly the third generation. In these scenarios the $b \rightarrow s\tau^+\tau^-$ decays can in principle be enhanced by an order of magnitude compared to the SM predictions. Left-handed currents imply a strong correlation between $b \rightarrow s\tau^+\tau^-$ and $b \rightarrow s\nu\bar{\nu}$ decays, see also the discussion in Section 1.4.3 below. Using the current upper bound on $\text{Br}(B^+ \rightarrow K^+\nu\bar{\nu}) < 1.6 \cdot 10^{-7}$ [219], one finds the following maximal values for the tauonic branching ratios [?]

$$\begin{aligned} \text{Br}_{K^+\tau^+\tau^-}^{\text{LH}} &< 24.5 \cdot 10^{-7}, \\ \text{Br}_{K^0\tau^+\tau^-}^{\text{LH}} &< 22.5 \cdot 10^{-7}, \\ \text{Br}_{K^{*+}\tau^+\tau^-}^{\text{LH}} &< 22.8 \cdot 10^{-7}, \\ \text{Br}_{K^{*0}\tau^+\tau^-}^{\text{LH}} &< 20.1 \cdot 10^{-7}, \\ \text{Br}_{B_s\tau^+\tau^-}^{\text{LH}} &< 1.5 \cdot 10^{-5}. \end{aligned} \tag{61}$$

The q^2 regions are chosen as in (60). Enhancements beyond the above bounds are possible in the presence of right-handed currents [220]. Measurement of $b \rightarrow s, d\tau^+\tau^-$ modes are thus likely to play an important role in the search for lepton non-universality and indirectly may also provide useful information on lepton flavor violation.

1.3.6. Tests of Lepton Flavor Universality in $b \rightarrow s\ell^+\ell^-$ and $B_q \rightarrow \tau^+\tau^-$. (Contributing authors: A. Ishikawa and S. Wehle)

The LHCb measurement of the ratio $R_K[1,6]$ as defined in (47) deviates by 2.6σ from its SM value [4]. This anomaly can be explained by new physics that only modifies the $b \rightarrow s\mu^+\mu^-$ transition but leaves $b \rightarrow se^+e^-$ unaffected, which implies a violation of lepton flavor universality.

At Belle II, all the ratios R_K , R_{K^*} and R_{X_s} can be measured precisely in both the low- q^2 and high- q^2 region. This is possible since, in contrast to LHCb where the radiative photon recovery is difficult, the reconstruction efficiency for electrons is comparable to that for muons thanks to the better electromagnetic calorimeter. By taking the ratio between the muon and electron mode, almost all systematic uncertainties cancel out. The dominant source of uncertainty is hence due to the imperfect lepton identification which is expected to lead to a relative error of 0.4%. Given the smallness of this uncertainty, Belle II measurements of R_K , R_{K^*} and R_{X_s} will all be statistically dominated. It thus follows that with 20 ab^{-1} of data, Belle II should be able to confirm the R_K anomaly observed by LHCb with a significance of 5σ , if it is indeed due to new physics. We add that measurements of the observables $Q_{4,5} = P_{4,5}'^\mu - P_{4,5}'^e$ [192], which have been recently performed by Belle for the first time [3], are also statistically dominated at Belle II.

Studies of the $B^+ \rightarrow K^+\tau^+\tau^-$ and $B_{d,s} \rightarrow \tau^+\tau^-$ decay modes are interesting because they allow to search for new physics which affects EW penguin B decays involving third-generation leptons. Since the final states contains multiple neutrinos, a tagging of the other B meson is needed to search for these decays. Recently, Belle demonstrated that hadronic B_s tagging is possible, showing that the tagging efficiency is about two times better than that in the case of B_d mesons [?]. **[Uli: Spires does not know this reference.]** A further improvement

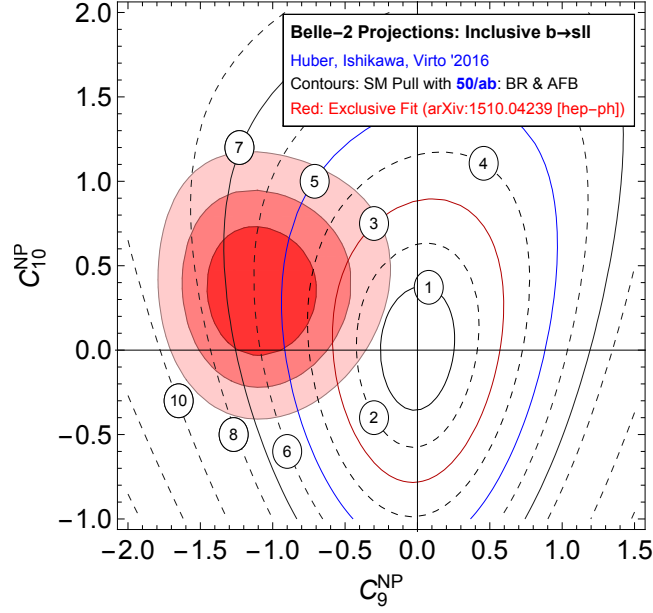


Fig. 4: Exclusion contours in the $C_9^{\text{NP}} - C_{10}^{\text{NP}}$ plane resulting from future inclusive $b \rightarrow s\ell^+\ell^-$ measurements at Belle II. For comparison the constraints on C_9^{NP} and C_{10}^{NP} following from the global fit presented in [221] is also shown.

of the hadronic tagging efficiency by a factor of two can be achieved with the full event interpretation. [Uli: Explain or link to technical section.] After tagging the other B meson, the tau leptons are reconstructed from single prong decays. Even with the improved reconstruction techniques, observations of the SM branching ratios of $B^+ \rightarrow K^+\tau^+\tau^-$ and $B_{d,s} \rightarrow \tau^+\tau^-$ are unlikely. The expected upper limits on the branching ratios that Belle II should be able to place are of order 10^{-5} and 10^{-4} for B_d and B_s decays, respectively.

1.3.7. Future Interplay of Inclusive and Exclusive $b \rightarrow s\ell^+\ell^-$ Measurements. (Contributing authors: T. Huber, A. Ishikawa and J. Virto)

In the following, we will study the phenomenological impact that future Belle II measurements of the branching fraction and forward-backward asymmetry in $B \rightarrow X_s\ell^+\ell^-$ with 50 ab^{-1} of integrated luminosity may have. We consider three q^2 bins, namely $[1, 3.5]\text{ GeV}^2$, $[3.5, 6]\text{ GeV}^2$ and $> 14.4\text{ GeV}^2$, and derive model-independent constraints on the Wilson coefficients of the operators Q_9 and Q_{10} introduced in (4). In particular, we will ask the following question: if the true values of the new-physics contributions are C_9^{NP} and C_{10}^{NP} , respectively, with which significance will Belle II be able to exclude the SM?

This question is answered by the contours shown in Figure 4, which have been obtained from a χ^2 fit based on the theory predictions of [163], but including an extra 5% uncertainty to account for non-perturbative effects [178]. Consider for example a point in the $C_9^{\text{NP}} - C_{10}^{\text{NP}}$ plane which resides on the contour labeled “5”. If this point represent the true values of the new-physics contributions then a fit including only the measurements $\text{Br}(B \rightarrow X_s\ell^+\ell^-)$ and $A_{\text{FB}}(B \rightarrow X_s\ell^+\ell^-)$ will result in a pull of the SM with respect to the best fit point by 5σ .

The figure thus allows to determine the significance with which future Belle II measurements of $B \rightarrow X_s \ell^+ \ell^-$ can exclude the SM, depending on which are the true values of the Wilson coefficients C_9 and C_{10} .

For comparison, the 1σ , 2σ and 3σ regions in the $C_9^{\text{NP}} - C_{10}^{\text{NP}}$ plane that are obtained from the global analysis [221] are also shown in Figure 4 as red contours. One can see that Belle II would exclude the SM by more than 5σ if the central value $C_9^{\text{NP}} = -1$ preferred by the global fit turns out to be correct. This nicely illustrates the interplay and complementarity between inclusive and exclusive measurements, and shows that Belle II can play a decisive role in the search for new physics via $b \rightarrow s \ell^+ \ell^-$ transitions.

[Uli: This contribution could go to new-physics section?]

1.4. Double-radiative decays

(Contributing authors: C. Bobeth and A. Kokulu)

$B_q \rightarrow \gamma\gamma$ Decays. In the SM, the branching ratios of the $B_q \rightarrow \gamma\gamma$ decays scale as the involved CKM elements $|V_{td}|^2$ and $|V_{ts}|^2$, predicting an enhancement of the $B_s \rightarrow \gamma\gamma$ decay over the $B_d \rightarrow \gamma\gamma$ decay by a factor of $|V_{ts}/V_{td}|^2 \simeq 20$. Using the full data set at $\Upsilon(5S)$ [222], Belle obtained the following 90% CL upper limit

$$\text{Br}(B_s \rightarrow \gamma\gamma)_{\text{exp}} < 3.1 \cdot 10^{-6}, \quad (62)$$

on the branching ratio of $B_s \rightarrow \gamma\gamma$. The searches for $B_d \rightarrow \gamma\gamma$ at $\Upsilon(4S)$ resulted instead in the 90% CL upper limits

$$\text{Br}(B_d \rightarrow \gamma\gamma)_{\text{exp}} < \begin{cases} 3.2 \cdot 10^{-7}, \\ 6.2 \cdot 10^{-7}, \end{cases} \quad (63)$$

from the full data set of BaBar [223], and a partial data set of 104 fb^{-1} of Belle [224] out of the available 711 fb^{-1} . The corresponding SM predictions are given by [225]

$$\begin{aligned} \text{Br}(B_s \rightarrow \gamma\gamma)_{\text{SM}} &\in [0.5, 3.7] \cdot 10^{-6}, \\ \text{Br}(B_d \rightarrow \gamma\gamma)_{\text{SM}} &\in [1.0, 9.8] \cdot 10^{-8}, \end{aligned} \quad (64)$$

and are either close to or only by an order of magnitude below the bounds (62) and (63). The above comparison shows that Belle II will be able to discover $B_d \rightarrow \gamma\gamma$ with the anticipated 50 times larger data set at $\Upsilon(4S)$. Furthermore, an appropriately large $\Upsilon(5S)$ data set could provide an observation of $B_s \rightarrow \gamma\gamma$.

From a theoretical point of view, double radiative $B_q \rightarrow \gamma\gamma$ decays are complementary to the corresponding radiative inclusive $B \rightarrow X_q \gamma$ decay. They depend on the same Wilson coefficient C_7 of the photonic dipole operator (3), but the contribution of four-quark operators in $B_q \rightarrow \gamma\gamma$ is different compared to $B \rightarrow X_q \gamma$. This feature provides a complementary test of the Wilson coefficient C_7 which plays an important role in many BSM models.

As will be explained in more detail below, the main source of theoretical uncertainty in the QCDF approach arises due to the first negative moment, λ_B , of the B -meson distribution amplitude. This hadronic parameter can be determined from the radiative leptonic decay $B \rightarrow \ell \bar{\nu}_\ell \gamma$ [226, 227]. **For the definition and a detailed discussion of the phenomenological impact on two-body hadronic decays, see Section ??.**

1076 The amplitude of the $\bar{B} \rightarrow \gamma(k_1, \epsilon_1) \gamma(k_2, \epsilon_2)$ decays — hereafter B stands for both B_q —
 1077 has the general structure

$$\mathcal{A} = A_+ [2(k_1 \cdot \epsilon_2)(k_2 \cdot \epsilon_1) - m_B^2(\epsilon_1 \cdot \epsilon_2)] - A_- 2i \varepsilon_{\mu\nu\alpha\beta} k_1^\mu k_2^\nu \epsilon_1^\alpha \epsilon_2^\beta. \quad (65)$$

1078 The CP properties of the corresponding two-photon final states are indicated by the sub-
 1079 scripts \pm on the amplitudes A_\pm . The parallel spin polarization of the photons is described
 1080 by A_+ , whereas the perpendicular one is encoded in A_- .

The decay rate is obtained after summation over photon polarizations

$$\Gamma(\bar{B} \rightarrow \gamma\gamma) = \frac{m_B^3}{16\pi} (|A_+|^2 + |A_-|^2). \quad (66)$$

In the absence of methods to tag the flavor of the initial B meson, the CP-averaged branching ratio must be considered instead

$$\overline{\text{Br}}_{\gamma\gamma} = \frac{\tau_B}{2} [\Gamma(\bar{B} \rightarrow \gamma\gamma) + \Gamma(B \rightarrow \gamma\gamma)], \quad (67)$$

where $\Gamma(B \rightarrow \gamma\gamma)$ is determined from (66) using the amplitudes \bar{A}_\pm of the CP-conjugated decay $B \rightarrow \gamma\gamma$. Further, for the case of untagged B_s decays the sizable decay width leads to rapid mixing and requires to perform a time-integration [228] in order to obtain the experimentally measured CP-averaged and time-integrated branching ratio

$$\langle \overline{\text{Br}}_{\gamma\gamma} \rangle = \frac{1 + y_s A_{\Delta\Gamma}}{1 - y_s^2} \overline{\text{Br}}_{\gamma\gamma}. \quad (68)$$

1081 It depends on $y_s = \Delta\Gamma_s/(2\Gamma_s) = 0.075 \pm 0.012$, where $\Gamma_s = 1/\tau_{B_s}$ the inverse of the lifetime,
 1082 the CP-averaged branching ratio (67) at time $t = 0$ and the mass-eigenstate rate asymmetry
 1083 $A_{\Delta\Gamma}(B \rightarrow \gamma\gamma)$. The latter can be determined in an untagged but time-dependent analysis
 1084 via a measurement of the effective lifetime [228].

1085 Direct CP violation can be tested by a tagged measurement of

$$r_{\text{CP}} = \frac{|\mathcal{A}|^2 - |\bar{\mathcal{A}}|^2}{|\mathcal{A}|^2 + |\bar{\mathcal{A}}|^2}, \quad (69)$$

$$r_{\text{CP}}^\pm = \frac{|A_\pm|^2 - |\bar{A}_\pm|^2}{|A_\pm|^2 + |\bar{A}_\pm|^2},$$

1086 where extractions of r_{CP}^\pm also require the determination of the photon polarizations.

1087 A systematic analysis of these decays in the heavy quark limit $m_b \gg \Lambda_{\text{QCD}}$ has been first
 1088 given in [225]. In this limit, the hadronic matrix elements of operators Q_i of the effective
 1089 Hamiltonian (1) factorize

$$\langle \gamma\gamma | Q_i | \bar{B} \rangle = f_B \int_0^1 d\omega T_i^{\mu\nu}(\omega) \phi_B^+(\omega) \epsilon_{1\mu} \epsilon_{2\nu}. \quad (70)$$

1090 The $T_i^{\mu\nu}$ are perturbatively calculable SD functions, whereas the non-perturbative effects
 1091 are contained in the B -meson decay constant f_B and the leading light-cone distribution
 1092 amplitude (LCDA) of the B meson in HQET, denoted as ϕ_B^+ . The latter depend on the light-
 1093 cone momentum ω of the spectator quark inside the B meson. Within the QCD factorization
 1094 setup [225], only the first negative moment,

$$\frac{1}{\lambda_B} = \int_0^1 d\omega \frac{\phi_B^+(\omega)}{\omega}, \quad (71)$$

1095 of the LCDA of the B meson appears.

The leading-power contribution arises from the emission of a hard photon from the B -meson spectator quark for the matrix element of the photonic dipole operator Q_7 ,

$$A_{\pm} = \frac{G_F}{\sqrt{2}} \frac{\alpha}{3\pi} f_B \sum_{p=u,c} \lambda_p^{(q)} A_{\pm}^p, \quad (72)$$

$$A_{\pm}^p = -C_7^{\text{eff}} \frac{m_B}{\lambda_B},$$

where C_7^{eff} is the effective coupling of this operator at the low-energy scale μ_b . At this order in the power expansion, one has $(r_{\text{CP}}^{\pm})_{\text{SM}} = 0$. Furthermore, since $\overline{\text{Br}}_{\gamma\gamma} \propto (f_B/\lambda_B)^2$ and given the accuracy of lattice predictions for f_B , in the case of the branching ratios the main theoretical uncertainty comes from λ_B .

At the subleading order in the power expansion, there are two types of contributions to the matrix element of Q_7 : (i) higher-twist contributions and (ii) the one-particle reducible (1PR) diagram where the photon is emitted from the b -quark line. Both corrections naively represent a correction of $\mathcal{O}(\Lambda_{\text{QCD}}/m_b) = \mathcal{O}(10\%)$ and have so far been neglected in the theoretical predictions.

One-particle-irreducible (1PI) contributions of the four-quark operators in the effective Hamiltonian (1) also arise at $\mathcal{O}(\Lambda_{\text{QCD}}/m_b)$. The corresponding matrix elements were shown to factorize in the heavy-quark limit to NLO in QCD, leading to $\langle \gamma\gamma | Q_i | \bar{B} \rangle = f_B T_i^{\mu\nu} \epsilon_{1\mu} \epsilon_{2\nu}$, independent of ω . Numerically the largest contributions stem from the current-current operators $Q_{1,2}^p$. They give an additional contribution to the coefficient A_{\pm}^p appearing in (72). One obtains

$$A_{\pm}^p = -C_7^{\text{eff}} \frac{m_B}{\lambda_B} - \frac{2}{3} (C_1^p + N_c C_2^p) g(z_p), \quad (73)$$

where $C_{1,2}^p$ are the Wilson coefficients of $Q_{1,2}^p$ at the scale μ_b and $N_c = 3$. The function $g(z_p)$ with $z_p = m_p^2/m_b^2$ develops an imaginary part only for $p = c$ when setting m_u to zero, which provides the leading contribution to r_{CP}^- . The quantity r_{CP}^+ on the other hand still remains zero. The QCD penguin operators Q_{3-6} contribute equally to the u -quark and c -quark sectors and their overall effect is very small [229]. Including all relevant effects, the CP asymmetries in the SM have been estimated as [208, 225, 230]

$$(r_{\text{CP}}^s)_{\text{SM}} \simeq 0.5\%, \quad (r_{\text{CP}}^-)_{\text{SM}}^s \simeq 0.4\%,$$

$$(r_{\text{CP}}^d)_{\text{SM}} \simeq -5\%, \quad (r_{\text{CP}}^-)_{\text{SM}}^d \simeq -10\%, \quad (74)$$

while $(r_{\text{CP}}^{\pm})_{\text{SM}}^{s,d} \simeq 0\%$. Notice that the predictions for B_d are larger than those for B_s as a result of the CKM hierarchies (2).

The dependence of the branching ratios on λ_B cancels almost completely in their ratio, leading to

$$\frac{\text{Br}(B_s \rightarrow \gamma\gamma)_{\text{SM}}}{\text{Br}(B_d \rightarrow \gamma\gamma)_{\text{SM}}} \propto \left| \frac{V_{ts}}{V_{td}} \right|^2 \frac{\tau_{B_s} f_{B_s}^2 m_{B_s}^3}{\tau_{B_d} f_{B_d}^2 m_{B_d}^3}. \quad (75)$$

Compared to λ_B , other parametric uncertainties due to the CKM elements and f_B are currently subdominant. Higher-order radiative QCD effects are estimated via factorisation-scale variation to be of $\mathcal{O}(30\%)$, and subleading power corrections are expected to be of $\mathcal{O}(10\%)$ [225].

1119 In BSM models, the $B_q \rightarrow \gamma\gamma$ decays can receive two types of non-standard contributions:

- 1120 (i) Modifications of the Wilson coefficient C_7 , which will also leave an imprint in $B \rightarrow X_q\gamma$.
- 1121 (ii) Modifications of the 1PI contributions due to four-fermion operators $b \rightarrow qf\bar{f}$, where f
- 1122 stands for the five possible light quarks or the three charged leptons.

1123 The first type has been studied in various models such as the two-Higgs-doublet-model
 1124 of type II (2HDM-II) [231, 232], the minimal supersymmetric SM (MSSM) [233] and universal
 1125 extra dimensions [234]. However, due to strong constraints on C_7 from $B \rightarrow X_q\gamma$, large
 1126 modifications of $\text{Br}(B_q \rightarrow \gamma\gamma)$ are by now already excluded.

1127 The complementarity of $B_q \rightarrow \gamma\gamma$ comes therefore mainly from the second type of modifi-
 1128 cations due to non-standard four-fermion operators $b \rightarrow qf\bar{f}$ with vectorial and scalar Dirac
 1129 structures, which contribute differently to $B_q \rightarrow \gamma\gamma$ and $B \rightarrow X_q\gamma$ [208], turning it into an
 1130 interesting probe of such effects. Experimentally least constrained are the $b \rightarrow s\tau^+\tau^-$ oper-
 1131 ators, which have been studied model-independently in [208]. Currently large deviations
 1132 from $(r_{\text{CP}})_{\text{SM}}^s$ are still allowed. Concerning the rate it might be enhanced up to a factor of
 1133 order two, depending also on the exact value of λ_B , which determines the relative size of
 1134 four-fermion operators versus the contribution of Q_7 . Such effects arise for example in SUSY
 1135 with broken R -parity [235] or leptoquark scenarios [208].

1136 1.4.1. Searches for $B_q \rightarrow \gamma\gamma$. (Contributing authors: A. Ishikawa)

1137
 1138 Since the final states do not have charged particles, the $B_s \rightarrow \gamma\gamma$ and $B_d \rightarrow \gamma\gamma$ decays have
 1139 so far only been searched for at e^+e^- colliders [222–224]. The obtained upper limits (62)
 1140 and (63) are several times larger than the corresponding SM predictions (64). Given its
 1141 large data set, Belle II will be able to observe the $B_q \rightarrow \gamma\gamma$ decays and perform new-physics
 1142 searches through precise measurements of these unique transitions.

1143 The reconstruction of $B_q \rightarrow \gamma\gamma$ decays is straightforward. Two isolated clusters in the
 1144 calorimeter, whose shower shapes are consistent with an electromagnetic shower, are com-
 1145 bined to reconstruct the B -meson candidates. The B meson is identified through the ΔE and
 1146 M_{bc} distributions. Since the calorimeter is about 16 radiation lengths, the ΔE distribution
 1147 has a longer tail to lower ΔE values due to shower leakage. The dominant backgrounds are
 1148 off-timing Bhabha events on top of hadronic events and continuum events with initial state
 1149 radiation. The former can be reduced by requiring the hit timing differences of the clusters
 1150 and trigger **[Uli: What is the requirement?]**, while the latter can be suppressed by the
 1151 use of event shape variables.

1152 Assuming that $\text{Br}(B_d \rightarrow \gamma\gamma) = 3.1 \cdot 10^{-8}$, the decay should be observed with an integrated
 1153 luminosity of 12 ab^{-1} and the relative uncertainty on the branching ratio is expected to be
 1154 9.6% **[Uli: Maybe just say 10%]** with 50 ab^{-1} of data. The given uncertainty is statistically
 1155 dominated. After an observation, the direct CP violation can be measured using flavor
 1156 tagging. With 50 ab^{-1} it should be possible to measure $A_{\text{CP}}(B_d \rightarrow \gamma\gamma)$ with a precision
 1157 of 25%.

1158 The data taking strategy at $\Upsilon(5S)$ is not determined yet. If we assume that 15 ab^{-1}
 1159 data will be accumulated, the data sample will contain about $8.8 \cdot 10^8 B_s^{(*)0} \bar{B}_s^{(*)0}$ pairs. To
 1160 observe the $B_s \rightarrow \gamma\gamma$ decay, 6 ab^{-1} of integrated luminosity are needed and the precision
 1161 on the branching ratio will be around 13% with the full data set. The achievable precision

is again statistics limited. Since flavor tagging of B_s mesons is difficult due to fast B_s - \bar{B}_s oscillations and the worse proper-time resolution compared to the B_d case, a measurement of the direct CP asymmetry of $B_s \rightarrow \gamma\gamma$ seems very difficult. An exception could be provided by CP tagging of the other B_s meson in the $\Upsilon(5S) \rightarrow B_s^0 \bar{B}_s^0$ or $\Upsilon(5S) \rightarrow B_s^{*0} \bar{B}_s^{*0}$ processes. Further studies of the CP tagging efficiency using full event interpretation are needed to clarify this issue.

1.4.2. $B \rightarrow X_s \gamma\gamma$ decay. Compared to $B \rightarrow X_s \gamma$, the double-radiative process $B \rightarrow X_s \gamma\gamma$ is suppressed by an additional factor of $\alpha/(4\pi)$, which leads to the naive expectation $\text{Br}(B \rightarrow X_s \gamma\gamma)_{\text{SM}} = \mathcal{O}(10^{-7})$. Given its small branching ratio it is unsurprising that the mode $B \rightarrow X_s \gamma\gamma$ has not been observed so far.

Even though it is very rare compared to the single radiative $B \rightarrow X_s \gamma$ decay, the double-radiative process has some features that make it worthwhile to study it at Belle II. These features are:

- (i) In contrast to $B \rightarrow X_s \gamma$, the current-current operators $Q_{1,2}$ contribute to $B \rightarrow X_s \gamma\gamma$ via 1PI diagrams already at LO. As a result, measurements of the double-radiative decay mode would allow to put bounds on these 1PI corrections.
- (ii) For $B \rightarrow X_s \gamma\gamma$ one can study more complicated distributions such as $d^2\Gamma/(dE_1 dE_2)$, where $E_{1,2}$ are the final state photon energies, or a forward-backward asymmetry (A_{FB}) that can provide additional sensitivity to BSM physics.

In order to exploit these features in a clean way, SM predictions beyond the LO are needed. A first step towards achieving NLO accuracy has been made in [236, 237] by the calculation of the (Q_7, Q_7) interference contribution to the differential distributions at $\mathcal{O}(\alpha_s)$. In the latter works it has been shown that the NLO corrections associated to (Q_7, Q_7) are large and can amount to a relative change of around $\pm 50\%$ compared to the corresponding LO predictions [238–241]. Further progress towards $B \rightarrow X_s \gamma\gamma$ at NLO was made recently in [242] by providing the (Q_8, Q_8) self-interference contribution. Although these corrections should be suppressed relative to those from (Q_7, Q_7) by $|C_8^{\text{eff}} Q_8 / C_7^{\text{eff}}|^2 \simeq 3\%$ the appearance of collinear logarithms $\ln(m_s/m_b)$ could upset this naive expectation. One important outcome of the work [242] is that the logarithmically-enhanced contributions stay small in the full phase-space, and as a result the (Q_8, Q_8) interference represents only a subleading NLO correction. The NLO calculation of the numerically important (Q_7, Q_7) interference contribution has very recently been extended to the case of a non-zero s -quark mass [243].

Including all known perturbative corrections the state-of-the-art SM prediction reads [243]

$$\text{Br}(B \rightarrow X_s \gamma\gamma)_{\text{SM}}^{c=0.02} = (0.9 \pm 0.3) \cdot 10^{-7}, \quad (76)$$

where c represents a cut on the phase-space (for details see [243]) which guarantees that the two photons are not soft and also not parallel to each other. The quoted uncertainty is dominated by the error due to scale variations $\mu_b \in [m_b/2, 2m_b]$. Since scale ambiguities represent the largest theoretical uncertainty at present, a more reliable SM prediction can only be achieved by calculating further NLO corrections such as for instance the $(Q_{1,2}, Q_7)$ interference term. We add that LD resonant [240] and spectator quark [244] effects are small and have therefore not been included in (76).

The inclusive $B \rightarrow X_s \gamma\gamma$ decay has also been examined in extensions of the SM. Predictions for $\text{Br}(B \rightarrow X_s \gamma\gamma)$ and A_{FB} have been obtained in 2HDMs [239, 241] and in the framework of

R -parity violating SUSY [235]. In all cases it has been found that $\mathcal{O}(1)$ effects in $B \rightarrow X_s \gamma \gamma$ can arise in the models under consideration.

[Uli: Drop?]

1.4.3. $B \rightarrow K^{(*)} \nu \bar{\nu}$ Transitions and Missing Energy Signals. (Contributing authors: C. Smith and D. Straub)

The $B \rightarrow K^{(*)} \nu \bar{\nu}$ decays provide clean testing grounds for new dynamics modifying the $b \rightarrow s$ transition [220, 245, 246]. Unlike in other B -meson decays, factorization of hadronic and leptonic currents is exact in the case of $B \rightarrow K^{(*)} \nu \bar{\nu}$ because the neutrinos are electrically neutral. Given the small perturbative and parametric uncertainties, measurements of the $B \rightarrow K^{(*)} \nu \bar{\nu}$ decay rates would hence in principle allow to extract the $B \rightarrow K^{(*)}$ form factors to high accuracy.

Closely related to the $B \rightarrow K^{(*)} \nu \bar{\nu}$ modes are the B decays that lead to an exotic final state X , since the missing energy signature is the same. Studies of such signals are very interesting in the dark matter context and may allow to illuminate the structure of the couplings between the dark and SM sectors [247].

$B \rightarrow K^{(*)} \nu \bar{\nu}$ in the SM. Due to the exact factorization, the precision of the SM prediction for the branching ratios of $B \rightarrow K^{(*)} \nu \bar{\nu}$ is mainly limited by the $B \rightarrow K^{(*)}$ form factors and by the knowledge of the relevant CKM elements. The relevant Wilson coefficient is known in the SM, including NLO QCD and NLO EW correction to a precision of better than 2% [15, 16, 18]. Concerning the form factors, combined fits using results from LCSRs at low q^2 and lattice QCD at high q^2 can improve the theoretical predictions.

Using $|\lambda_t^{(s)}| = (4.06 \pm 0.16) \cdot 10^{-2}$ for the relevant CKM elements, obtained using unitarity and an average of inclusive and exclusive tree-level determinations of V_{cb} , as well as a combined fit to LCSR [38] and lattice QCD [248] results for the $B \rightarrow K^*$ form factors, one obtains the following SM prediction for the $B \rightarrow K^* \nu \bar{\nu}$ branching ratio [?]

$$\text{Br}(B \rightarrow K^* \nu \bar{\nu})_{\text{SM}} = (9.6 \pm 0.9) \cdot 10^{-6}. \quad (77)$$

An angular analysis of the angle spanned by the B meson and the K^+ meson resulting from the $K^* \rightarrow K^+ \pi^-$ decay gives access to an additional observable, the K^* longitudinal polarization fraction F_L , which is sensitive to right-handed currents [245]. For the low number of events expected at Belle II, such an analysis can still be feasible using a principal moment analysis [249].

The $B \rightarrow K$ form factors are known to an even better precision from lattice QCD. Extrapolating the lattice result to the full q^2 range, one arrives at [?]

$$\text{Br}(B^+ \rightarrow K^+ \nu \bar{\nu})_{\text{SM}} = (4.6 \pm 0.5) \cdot 10^{-6}. \quad (78)$$

Since the isospin asymmetry vanishes for both decays (except for a presumably negligible difference in the charged and neutral form factors), the B^0 vs. B^+ branching ratios can be trivially obtained by rescaling with the appropriate lifetimes — once the tree-level $B^+ \rightarrow \tau^+ \nu_\tau$ ($\tau^+ \rightarrow K^+ \bar{\nu}_\tau$) contribution is properly taken into account [246].

BSM Physics in $B \rightarrow K^{()} \nu \bar{\nu}$.* Within the SM, the $B \rightarrow K^{(*)} \nu \bar{\nu}$ decays are mediated by the effective operator (5) which involves a sum over the three neutrino flavors $\ell = e, \mu, \tau$.

In BSM scenarios, there can be a left-handed operator for each neutrino flavor as well as right-handed one of the form

$$Q_R^\ell = (\bar{s}_R \gamma_\mu b_R)(\bar{\nu}_{\ell L} \gamma^\mu \nu_{\ell L}). \quad (79)$$

In total there can hence be six different operators.

The two branching ratios give access to two combinations of the six Wilson coefficients, namely

$$\begin{aligned} \frac{\text{Br}(B \rightarrow K \nu \bar{\nu})}{\text{Br}(B \rightarrow K \nu \bar{\nu})_{\text{SM}}} &= \frac{1}{3} \sum_{\ell} (1 - 2\eta_{\ell}) \epsilon_{\ell}^2, \\ \frac{\text{Br}(B \rightarrow K^* \nu \bar{\nu})}{\text{Br}(B \rightarrow K^* \nu \bar{\nu})_{\text{SM}}} &= \frac{1}{3} \sum_{\ell} (1 + \kappa_{\eta} \eta_{\ell}) \epsilon_{\ell}^2, \end{aligned} \quad (80)$$

where κ_{η} is a ratio of binned form factors [220] and

$$\begin{aligned} \epsilon_{\ell} &= \frac{\sqrt{|C_L^{\ell}|^2 + |C_R^{\ell}|^2}}{|C_L^{\text{SM}}|}, \\ \eta_{\ell} &= \frac{-\text{Re}(C_L^{\ell} C_R^{\ell*})}{|C_L^{\ell}|^2 + |C_R^{\ell}|^2}. \end{aligned} \quad (81)$$

While in principle, no general constraint on the size of BSM effects in $B \rightarrow K^{(*)} \nu \bar{\nu}$ decays can be derived from other processes, in practice in many models there is a relation between semi-leptonic decays with neutrinos and the ones with charged leptons in the final state. This is because $SU(2)_L$ gauge symmetry relates left-handed neutrinos and charged leptons. This relation can be most conveniently studied in the SM effective field theory (SMEFT) [250, 251], based on an OPE in powers of the inverse new-physics scale. The relevant dimension-six operators read

$$\begin{aligned} Q_{Hq}^{(1)} &= (\bar{q}_L \gamma_\mu q_L) H^\dagger i D^\mu H, \\ Q_{Hq}^{(3)} &= (\bar{q}_L \gamma_\mu \tau^a q_L) H^\dagger i D^\mu \tau^a H, \\ Q_{Hd} &= (\bar{d}_R \gamma_\mu d_R) H^\dagger i D^\mu H, \\ Q_{ql}^{(1)} &= (\bar{q}_L \gamma_\mu q_L) (\bar{l}_L \gamma^\mu l_L), \\ Q_{ql}^{(3)} &= (\bar{q}_L \gamma_\mu \tau^a q_L) (\bar{l}_L \gamma^\mu \tau^a l_L), \\ Q_{dl} &= (\bar{d}_R \gamma_\mu d_R) (\bar{l}_L \gamma^\mu l_L), \end{aligned} \quad (82)$$

where H denotes the Higgs doublet field, while q_L and l_L are the quark and lepton doublets, respectively, and we have suppressed flavor indices. The generators of $SU(2)_L$ are denoted by τ^a . The SMEFT Wilson coefficients can be matched onto the low-energy Wilson

coefficients $C_{L,R}^\ell$ and the ones relevant for $b \rightarrow s\ell^+\ell^-$ transitions as follows [220, 252?]]

$$\begin{aligned}
C_L &\propto C_{ql}^{(1)} - C_{ql}^{(3)} + C_Z, \\
C_R &\propto C_{dl} + C'_Z, \\
C_9 &\propto C_{qe} + C_{ql}^{(1)} + C_{ql}^{(3)} - \zeta C_Z, \\
C'_9 &\propto C_{de} + C_{dl} - \zeta C'_Z, \\
C_{10} &\propto C_{qe} - C_{ql}^{(1)} - C_{ql}^{(3)} + C_Z, \\
C'_{10} &\propto C_{de} - C_{dl} + C'_Z,
\end{aligned} \tag{83}$$

where

$$C_Z = \frac{1}{2} \left(C_{Hq}^{(1)} + C_{Hq}^{(3)} \right), \quad C'_Z = \frac{1}{2} C_{Hd}, \tag{84}$$

and $\zeta = 1 - 4s_w^2 \simeq 0.08$ is the accidentally small vector coupling of the Z boson to charged leptons with s_w the sine of the weak mixing angle. While in full generality, these relations are not very useful due to the larger number of operators in the SMEFT, they become useful in models where only a subset of the SMEFT operators are generated. For instance, in models with an additional $SU(2)_L$ -singlet neutral heavy gauge boson (Z'), one has $C_{ql}^{(3)} = 0$. If in addition Z - Z' mixing is small, one obtains the prediction

$$C_L = \frac{C_9 - C_{10}}{2}, \quad C_R = \frac{C'_9 - C'_{10}}{2}. \tag{85}$$

In the opposite limit of a new-physics model where only the coefficients C_Z and C'_Z are generated, one obtains

$$C_L = C_{10}, \quad C_9 = -\zeta C_{10}, \tag{86}$$

and

$$C_R = C'_{10}, \quad C'_9 = -\zeta C'_{10}. \tag{87}$$

In both cases, the existing data on $b \rightarrow s\ell^+\ell^-$ transitions limit the size of possible BSM effects in $B \rightarrow K^{(*)}\nu\bar{\nu}$. However, in models where new physics enters in the pattern $C_{ql}^{(1)} = -C_{ql}^{(3)}$, large modifications are possible without any constraint from $b \rightarrow s\ell^+\ell^-$ processes. Indeed such a pattern is realized in a particular leptoquark model [220] up to loop effects [253]. Finally, we stress that the constraints from $b \rightarrow s\ell^+\ell^-$ processes can be weakened by the contributions of additional operators not relevant in $b \rightarrow s\nu\bar{\nu}$, like dipole operators or operators involving right-handed leptons.

In the discussion after (82), we have neglected lepton flavor so far. In fact, in the $B \rightarrow K^{(*)}\nu\bar{\nu}$ decays all three neutrino flavors contribute and cannot be distinguished experimentally. In $b \rightarrow s\ell^+\ell^-$ transitions, on the other hand, the most precise measurements have been done with muons, and the modes with electrons in the final state are less strongly constrained. Finally, $b \rightarrow s\tau^+\tau^-$ decays have not been observed at all to date due to the difficulty posed by the identification of tau leptons. This highlights another important feature of the $B \rightarrow K^{(*)}\nu\bar{\nu}$ decays: if new physics couples mostly to the third generation of leptons (and lepton neutrinos), it could cause large enhancements of the $B \rightarrow K^{(*)}\nu\bar{\nu}$ branching ratios without strongly affecting $b \rightarrow se^+e^-$ or $b \rightarrow s\mu^+\mu^-$ decays. Such a dominant coupling to third-generation lepton flavor has been put forward to explain various anomalies in B physics recently [216, 218], cf. the related discussion in Section 1.3.5.

$B \rightarrow K^{(*)}\nu\bar{\nu}$ experimental prospects:. (Contributing authors: A. Ishikawa, E. Manoni) 1288

From the experimental point of view, searches of the $B \rightarrow K^{(*)}\nu\bar{\nu}$ charged and neutral 1289
channels have been performed by both Belle and Babar using hadronic tagging [219, 254] 1290
and semileptonic tagging [255, 256]. The resulting upper limits at 90% of confidence level are 1291
a factor of 2-5 above the Standard Model predictions [220] for K^+ , K^{*+} , and K^{*0} channels. 1292
If new physics does not contribute to $b \rightarrow s\nu\bar{\nu}$ transitions and the Standard Model prediction 1293
holds, the $B \rightarrow K^{(*)}\nu\bar{\nu}$ decays will be able to be observed at Belle II. 1294

Assuming the same performance as Belle for semileptonic tagging analysis, we have esti- 1295
mated the sensitivities of $B \rightarrow K^+\nu\nu$ and $B \rightarrow K^{*0}\nu\nu$ by combining the hadronic tagging 1296
and semileptonic tagging analysis. The two decay modes will be observed with about 18 ab^{-1} 1297
and the sensitivities of the BF will be 12% and 11% for $B \rightarrow K^+\nu\nu$ and $B \rightarrow K^{*0}\nu\nu$ with 1298
 50 ab^{-1} . Once the K^* modes are observed, measurements of differential BF and K^* polar- 1299
ization are important subjects. We performed the toy MC studies and we can measure the 1300
 F_L with uncertainty of 0.11 when the input F_L value is 0.47 [220]. 1301

In order to evaluate the impact of machine background on $B \rightarrow K^{(*)}\nu\bar{\nu}$ searches, we studied 1302
signal and generic MC samples (from the MC5 central campaign, described in the “Belle 1303
II Simulation” section), in two configuration: physics events superimposed to the nominal 1304
machine background (“BGx1” configuration), physics events without machine background 1305
 (“BGx0” configuration). To investigate this, we considered the $B^\pm \rightarrow K^{*\pm}\nu\bar{\nu}$ channel with 1306
 $K^{*\pm}$ reconstructed in the $K^\pm\pi^0$ final state. 1307

The used generic MC samples consist on a mixture of B^+B^- , $B^0\bar{B}^0$, $u\bar{u}$, $d\bar{d}$, $c\bar{c}$, and $s\bar{s}$ 1308
corresponding to 1 ab^{-1} . About 1 million signal MC events, with $K^{*\pm}$ decaying to both $K^\pm\pi^0$ 1309
and $K_S^0\pi^\pm$, have also been generated. The signal signature in the recoil of a B reconstructed 1310
in hadronic final states are searched. To do that the official FEI algorithm ?? with ad-hoc 1311
refinements on particle identification and cluster cleaning, as done for the $B \rightarrow \tau\nu$ analysis 1312
documented in ??, are used. 1313

We select $\Upsilon(4S)$ candidates in which the B_{tag} probability given by FEI is higher than 0.5%. 1314
Moreover, no extra-tracks (tracks not associated to the signal B meson nor to the tag side B 1315
meson) should be reconstructed. We select the best $\Upsilon(4S)$ candidate in the event according 1316
to the highest B_{tag} signal probability and the smallest difference between the reconstructed 1317
 K^* mass and the PDG value. 1318

Once the best $B\bar{B}$ pair is selected, we exploit variables related to the B_{tag} kinematics 1319
(M_{bc} and ΔE variables) in order to remove mis-reconstructed candidates. Both requirements 1320
suppress events in which B_{tag} ’s originate from wrong combination of charged and neutral 1321
particles, both in $B\bar{B}$ and $q\bar{q}$ events. 1322

The continuum events can be further reduced by considering event shape variables such 1323
as R_2 , the normalized second Fox-Wolfram moment. The goodness of the strange mesons 1324
reconstructed in the signal side is checked through a selection requirement on the difference 1325
between the reconstructed mass and the PDG value. Properties of the missing energy in the 1326
signal side are also exploited. We define the missing 4-momentum in the CM frame as the 1327
difference of the $\Upsilon(4S)$ 4-momentum and the sum of the B_{tag} and K^* 4-momenta. Since 1328
no extra-tracks are allowed, the missing momentum is related to actual neutrinos, extra- 1329
neutrals, and particles escaping the detector acceptance. One of the most powerfull selection 1330

variables of the analysis is the sum of the missing energy and of the module of the missing 3-momentum in the CM frame ($E_{miss}^* + cp_{miss}^*$) which is require to be greater than 4.5 GeV .

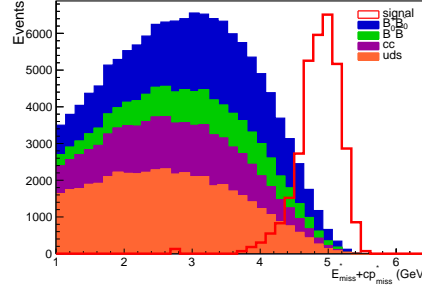


Fig. 5: Distribution of $E_{miss}^* + cp_{miss}^*$ for the signal (red) and for the generic MC samples (see legenda), for the $K^{*+} \rightarrow K^+\pi^0$ channel in the “BGx1” configuration after all the selection criteria applied but the ones on $E_{miss}^* + cp_{miss}^*$ and E_{ECL} . The number of generic MC events corresponds to an integrated luminosity of 1 ab^{-1} while the signal normalization is arbitrary.

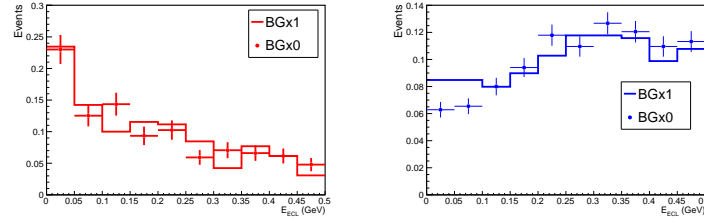


Fig. 6: Distribution of the E_{ECL} , normalized to unitary area, for the for the “BGx0” (dots) and “BGx1” (line) configurations for the $K^{*+} \rightarrow K^+\pi^0$ channel after all the selection criteria. Left: signal MC sample. Right: charged B^+B^- sample.

Figure 5 shows the $E_{miss}^* + cp_{miss}^*$ distributions for the $K^{*+} \rightarrow K^+\pi^0$ channel, for signal and generic MC samples in the “BGx1” configuration. The quantity $E_{miss}^* + cp_{miss}^*$ is much less correlated to the $\nu\bar{\nu}$ invariant mass than E_{miss}^* or p_{miss}^* alone, making it suitable for a model-independent analysis. A signal region in the extra-neutral energy deposited in the calorimeter (E_{ECL}) is also defined, requiring $E_{ECL} < 0.5$ GeV . The distributions for signal MC and the dominant source of background surviving the selection, namely charged $B\bar{B}$ decays, are shown in Figure 6 in both “BGx1” and “BGx0” configurations. In Table 2 a comparison of the selection performances considering the two machine background configurations are reported. As can be noticed, both efficiency and background contamination is higher for the “BGx0” case. This is due to the fact that the optimisation of the selection at reconstruction level has been optimised using the “BGx1” sample and also that for the “BGx0” configuration we have used a FEI training performed on the sample with machine background superimposed. The overall signal significance is higher in the background-free sample as expected. From this study we can conclude that, with the machine background

	“BGx0”	“BGx1”
N_{bkg}	6415 ± 80	3678 ± 61
ε (10^{-4})	10.3 ± 0.3	5.38 ± 0.23
$N_{sig}/\sqrt{N_{bkg}}$	0.16	0.15
UL (10^{-4})	2.6	3.8

Table 2: Number of generic events (N_{bkg}), signal selection efficiency (ε), signal significance ($N_{sig}/\sqrt{N_{bkg}}$ with arbitrary normalization of the signal), and expected upper limit (UL) at 90% C.L. extracted with a bayesian approach, for “BGx0” and “BGx1” configurations. The errors reported and the ones used in the UL estimation are statistical only.

campaign used in the MC5 production cycle, the detector performances and the reconstruction algorithms are robust against machine background. This has been tested on a K^{*+} final state with both a neutral particle and a charged tracks. In this respect, the analysis of final states with $K^{*+} \rightarrow K_S^0(\pi^+\pi^-)\pi^+$ and $K^{*0} \rightarrow K^+\pi^-$, reconstructed with track only, should give similar or better results.

Related $B \rightarrow X\nu\bar{\nu}$ Decays. The processes $B_s \rightarrow \phi\nu\bar{\nu}$ or $B_s \rightarrow \eta^{(\prime)}\nu\bar{\nu}$ are based on the same quark-level transition as $B \rightarrow K^{(*)}\nu\bar{\nu}$ and only differ in their form factors. In addition, there are also exclusive decays based on the $b \rightarrow d\nu\bar{\nu}$ transition, e.g. $B \rightarrow \rho\nu\bar{\nu}$, $B \rightarrow \omega\nu\bar{\nu}$ or $B \rightarrow \pi\nu\bar{\nu}$. In the SM, the SD contribution to these decay rates are parametrically suppressed by $|V_{td}/V_{ts}|^2 \simeq 0.05$ with respect to the $b \rightarrow s\nu\bar{\nu}$ modes and thus challenging to detect. Further, charged modes are polluted by the large Cabibbo-allowed tree-level contribution $B^+ \rightarrow \tau^+\nu_\tau$ ($\tau^+ \rightarrow (\pi, \rho)^+\bar{\nu}_\tau$). Still, order-of-magnitude enhancements of these modes relative to the SM expectations are not excluded in a model-independent fashion.

Non-Standard Invisible Final States. The successes of the SM do not rule out the presence of new light particles. Indeed, if they are sufficiently weakly interacting with SM particles, they could have evaded direct detection until now. One could think for example of the extreme situation in which a unique new particle, fully neutral under the whole SM gauge group, is added to the SM. Our only window to discover such a particle would be its gravitational interactions, and there would be no hope of an earth-based discovery in the foreseeable future. In a more realistic setting though, new neutral light particles would be accompanied by new dynamics at some scale. Presumably, this new dynamics would also affect the SM, and would thus indirectly couple the visible and hidden sectors.

There are many examples of such BSM models. The most well-known example is the axion [257–260], introduced to cure the strong CP problem of the SM. More crucially, there are now very strong indications that the universe is filled with dark matter, so there should be at least one new electrically neutral colourless particle, possibly lighter than the EW scale. Once opening that door, it is not such a drastic step to imagine a whole dark sector, i.e. a set of darkly interacting dark particles only loosely connected to our own visible sector. For a recent review, including further physical motivations from string theory or extra dimensional settings, see for instance [261].

1377 *Experimental Searches.* New light states would show up as missing energy in some process
1378 $A \rightarrow BX_{\text{dark}}$, with A and B some SM particle states and X_{dark} representing one or more
1379 dark particles. Because of their very weak couplings, high luminosity is crucial to have any
1380 hope of discovery, and except in some special circumstances colliders cannot compete with
1381 low-energy experiments yet.

1382 Several B decay modes offer unique windows for the search of new dark state with masses
1383 up to a few GeV. Specifically, the most promising processes are

$$\begin{aligned}
B &\rightarrow X_{\text{dark}} , \\
B &\rightarrow (\pi, \rho) X_{\text{dark}} , \\
B &\rightarrow (K, K^*) X_{\text{dark}} ,
\end{aligned} \tag{88}$$

1384 with X_{dark} made of at least two dark particles for the first mode, but possibly only one
1385 for the others. This also includes situations in which the dark particle is not stable but has
1386 cascade decays in the hidden sector, e.g. $X_{\text{dark}} \rightarrow Y_{\text{dark}} Y_{\text{dark}}$.

1387 In this context, the SM decays with $X_{\text{SM}} = \nu\bar{\nu}$ act as an irreducible background. The
1388 relevant branching ratios are smaller than about 10^{-9} for the fully invisible mode, and 10^{-5}
1389 for those with π , ρ , K , or K^* . It is important to stress though that the kinematics may
1390 be different. The differential rate $d\Gamma/dq_X^2$ with q_X^2 the missing invariant mass, depends on
1391 the nature of X_{dark} and may strongly deviate from that with X_{SM} . This is obvious if X_{dark}
1392 is a single particle, in which case $d\Gamma/dq_X^2$ would show a peak at $q_X^2 = m_X^2$, or when X_{dark}
1393 is made of two states Y with $m_Y^2 \gg 0$ since $d\Gamma/dq_Y^2$ would vanish below $q_Y^2 = 4m_Y^2$.
1394 More generally, $d\Gamma/dq^2$ strongly depend on the Dirac structure(s) involved in the effective
1395 couplings of the dark states to the SM quark current $b \rightarrow q$, and thereby on whether these
1396 states are scalar, fermion or vector particles.

1397 This caveat concerning the differential rate must be kept in mind when reinterpreting the
1398 bounds on the branching ratios for $B \rightarrow (\pi, \rho, K, K^*)\nu\bar{\nu}$ as bounds on the production of new
1399 light states. Not only are those limits obtained from measurements over a fraction of the
1400 phase-space, but the SM differential rate is explicitly assumed in the extrapolation. To be
1401 consistent, it is thus compulsory to use the same cuts on the produced meson momentum
1402 as in the experimental analysis. In this respect, it should be remarked that some recent
1403 experimental results [219] do perform differential analyses over the whole q^2 range. Those
1404 are the data most suitable to look for new light states.

1405 Finally, it should be mentioned that these modes also constrain indirectly other observ-
1406 ables. For example, since the branching ratios $\text{Br}(B^+ \rightarrow K^{*+} J/\psi) = (0.143 \pm 0.008)\%$ or
1407 $\text{Br}(B^+ \rightarrow \rho^+ \bar{D}) = (1.34 \pm 0.18)\%$ [262] being significantly larger than those for the decays
1408 with missing energy (88), the latter modes indirectly bound $J/\psi \rightarrow X_{\text{dark}}$ or $\bar{D} \rightarrow X_{\text{dark}}$
1409 whenever $m_{J/\psi}^2$ or $m_{\bar{D}}^2$ falls within the missing invariant mass window of the experimental
1410 search. This method has been used, and is the best available, for charmonium but remains
1411 to be applied for charmed mesons. It is not so promising for $K_{L,S} \rightarrow X_{\text{dark}}$ because the B
1412 decay branching ratios involving kaons are not much enhanced compared to those with a
1413 neutrino pair, and because the reach on $B(K \rightarrow X_{\text{dark}})$ would in any case be very far from
1414 the 10^{-10} achievable for the golden mode $B(K \rightarrow \pi X_{\text{dark}})$.

	neutral	
	flavor-blind	flavored
ϕ : scalar	$\Lambda H^\dagger H \phi$	$\frac{1}{\Lambda} \bar{Q} \gamma_\mu Q \partial^\mu \phi$
ψ : spin 1/2	$H \bar{\psi} L$	$\frac{1}{\Lambda^2} \bar{D} Q \bar{\psi} L$
V^μ : vector	$H^\dagger D_\mu H V^\mu$	$\bar{Q} \gamma_\mu Q V^\mu$
V^μ : gauge	$B_{\mu\nu} V^{\mu\nu}$	$\frac{1}{\Lambda^2} H \bar{D} \sigma_{\mu\nu} Q V^{\mu\nu}$
Ψ^μ : spin 3/2	$\frac{1}{\Lambda} D_\mu H \bar{\Psi}^\mu L$	$\frac{1}{\Lambda^3} \bar{D} D_\mu Q \bar{\Psi}^\mu L$
	charged	
	flavor-blind	flavored
ϕ : scalar	$H^\dagger H \phi^\dagger \phi$	$\frac{1}{\Lambda^2} \bar{Q} \gamma_\mu Q \phi^\dagger \partial^\mu \phi$
ψ : spin 1/2	$\frac{1}{\Lambda^2} H^\dagger D_\mu H \bar{\psi} \gamma^\mu \psi$	$\frac{1}{\Lambda^2} \bar{Q} \gamma_\mu Q \bar{\psi} \gamma^\mu \psi$
V^μ : vector	$H^\dagger H V_\mu V^\mu$	$\frac{1}{\Lambda^2} \bar{Q} \gamma_\mu Q V_\nu V^{\mu\nu}$
V^μ : gauge	$\frac{1}{\Lambda^2} H^\dagger H V_{\mu\nu} V^{\mu\nu}$	$\frac{1}{\Lambda^4} \bar{Q} \gamma_\mu D^\nu Q V^{\mu\rho} V_{\rho\nu}$
Ψ^μ : spin 3/2	$\frac{1}{\Lambda} H^\dagger H \bar{\Psi}_\mu \Psi^\mu$	$\frac{1}{\Lambda^2} \bar{Q} \gamma_\mu Q \bar{\Psi}_\rho \gamma^\mu \Psi^\rho$

Table 3: Example of leading operators under various assumptions on the nature of the dark state. For more information and references see [247, 264].

Theoretical Classification and Expectations. To organise the search for new light states as model-independently as possible, the strategy is to construct the equivalent of the SMEFT operator basis [250, 251, 263] once the SM particle content is extended, and then constrain all the operators involving the new state(s). This program is more involved than it seems. Clearly, the leading operators one has to consider, the so-called portals, strongly depend on generic assumptions on the nature of the new state. For example, its spin has to be specified, as well as whether it carries a dark charge and needs to be produced in pairs.

Importantly, the dimension of the leading effective operators depend on these assumptions. For instance, some of the leading interactions of the SM fields with a dark scalar, spin 1/2 or 3/2 fermion or vector boson are shown in Table 3, where Λ denotes the scale of the heavy BSM dynamics linking the dark and visible sectors [247, 264]. For each type of new particle, we separate the case in which it is neutral or charged under some dark symmetry, and then further distinguish the overall leading operators to those involving the quark currents. Indeed, from the point of view of flavor physics, whether the dark states couple dominantly to Higgs or gauge bosons, hence are flavor-blind, or when they couple to quarks and leptons, whether they are able to directly induce the flavor transition is crucial. Even if it is not favourable from a dimensionality point of view to couple X_{dark} directly to quarks, failure to

do so means that the flavor transition must still proceed through the SM weak interaction, and ends up suppressed by G_F and CKM factors. From these considerations, three classes of scenarios for a generic effective coupling of X_{dark} to quarks can be identified. We refer to [247] for the full classification of the effective operators, and here only illustrate these three classes for the case of the production of a dark fermion pair.

First, consider the SM contributions which constitutes the irreducible background for BSM production of dark states. It can be embodied into the generic dimension-six effective operators

$$\mathcal{H}_{\text{eff}} = \sum_{q=s,d} \frac{c^{bq}}{\Lambda^2} \bar{b} \Gamma q \bar{\nu} \Gamma \nu, \quad (89)$$

where Γ represents all possible Dirac structures and c^{bq} denote the Wilson coefficients. We recall that in the SM one has $\Lambda \simeq m_W$, $c_{\text{SM}}^{bs} \simeq \alpha_w/(4\pi) \lambda$ and $c_{\text{SM}}^{bd} \simeq \alpha_w/(4\pi) \lambda^3$ with $\alpha_w = g^2/(4\pi)$ the $SU(2)_L$ coupling constant.

For the first scenario, imagine that the production of a dark fermion pair proceeds through the flavor-changing operator $\bar{Q}^I \gamma_\mu Q^J \bar{\psi} \gamma^\mu \psi$ shown in Table 3, where Q is a left-handed quark doublet and I, J denote flavor indices. The BSM rate will be of the order of the SM $b \rightarrow q \nu \bar{\nu}$ rate when

$$\frac{c_{\text{dark}}^{bq}}{\Lambda^2} \simeq G_F \frac{\alpha_w}{4\pi} \lambda_t^{(q)}. \quad (90)$$

Provided the Wilson coefficient c_{dark}^{bq} is $\mathcal{O}(1)$, the reach in Λ is rather high, i.e. about 40 TeV (20 TeV) for $b \rightarrow d$ ($b \rightarrow s$) transitions.

On the contrary, for the second scenario, imagine that the leading coupling is flavor-blind, say $H^\dagger D_\mu H \bar{\psi} \gamma^\mu \psi \supset v^2 \bar{\psi} \gamma_\mu \psi Z^\mu$ with $v \simeq 246$ GeV the Higgs vacuum expectation value. Then, the production of new states is driven by the SM Z penguin. As a result, the relation (90) takes the form

$$c_{\text{dark}}^{HH} \frac{v^2}{\Lambda^2} G_F \frac{\alpha_w}{4\pi} \lambda_t^{(q)} \simeq G_F \frac{\alpha_w}{4\pi} \lambda_t^{(q)}. \quad (91)$$

In this case, the reach in Λ is around the EW scale at best, i.e. when $c_{\text{dark}}^{HH} = \mathcal{O}(1)$, and is in general not competitive with other searches using EW precision observables, invisible Higgs boson decay or other flavor-blind searches. Note that even very low-energy probes are sensitive to $v^2 \bar{\psi} \gamma_\mu \psi Z^\mu$ since the Z boson couples to all SM fermions. A similar conclusion is valid for all the flavor blind operators, even when those arise at a much lower order and appear superficially less suppressed by the new-physics scale Λ than those involving quark fields.

In between these two extreme situations, there is a third scenario. If the dark state couples dominantly to top-quark pairs, then all the flavor-blind low-energy searches would be inefficient, while high-energy collider searches relying for example on the associated productions of a top quark and a dark state would not be competitive yet. In this case, the FCNC processes still represent our best window, even if the reach in the BSM scale Λ would not be much higher than the EW scale.

[Uli: Section still too long!]

1.4.4. Search for $B_q \rightarrow \nu \bar{\nu}$ or Invisible Final States. (Contributing authors: A. Ishikawa)

The $B_d \rightarrow \nu\bar{\nu}$ decay and B_d -meson decays to invisible final states were searched for by BaBar with semi-leptonic tagging [265] and by Belle using hadronic tagging [266]. The resulting 90% CL upper limits on the branching ratios are $1.7 \cdot 10^{-5}$ and $1.3 \cdot 10^{-4}$, respectively. The $B_s \rightarrow \nu\bar{\nu}$ decay has instead not been searched for yet.

Since there are no charged tracks nor photons in the final states, only the tag-side B mesons can be used for the searches. The Belle analysis used an old hadronic tagging without hierarchical reconstruction method [267], which can increase the tagging efficiency by a factor of two. And another factor of two improvement can be obtained by introducing the FEL. Requirements on event shape variables using multivariate techniques to suppress continuum and $\tau^+\tau^-$ backgrounds are promising to improve the sensitivity further. In combination, an improvement by a factor of five on the efficiency of the hadronic tagging analysis is expected at Belle II. Such an improvement is still not sufficient to beat the semi-leptonic tagging analysis, which is expected to provide upper limits on the branching ratios that are three times better than those following from hadronic tagging. By combining hadronic and semi-leptonic tagging, Belle II is expected to set an upper limit on $\text{Br}(B_d \rightarrow \nu\bar{\nu})$ of $1.5 \cdot 10^{-6}$ with 50 ab^{-1} of integrated luminosity.

The hadronic B_s tagging efficiency using a hierarchical reconstruction method gives an efficiency that is two times better than that for B_d . The semi-leptonic tagging is not tried yet, however it is expected that the tagging efficiency is smaller than that for B_d , since the dominant semi-leptonic decay $B_d^0 \rightarrow D^{*-}\ell^+\nu$ is clean due to the small mass splitting of D^{*-} and $\bar{D}^0\pi^-$. We conservatively assume that the semileptonic B_s tagging is three times worse than that for B_d . By combining the hadronic and semi-leptonic tagging, it is expected that an upper limit on $\text{Br}(B_s \rightarrow \nu\bar{\nu})$ of $8.4 \cdot 10^{-6}$ can be set with the full data set of 15 ab^{-1} collected at $\Upsilon(5S)$.

1.5. Conclusions

To conclude, the study of radiative and EW penguin B decays is an important area for precision flavor physics. This has been established by an effort within the theory community and experimental results from BaBar, Belle and most recently LHCb. The Belle II program for these modes aims at processes complementary to the physics program at the upgraded LHCb experiment as well as competitive measurements and updates to key observables. A summary of sensitivities mentioned throughout this chapter is presented in Tables ?? and ??.

[Uli: Links to tables do not work.] [Uli: Extend conclusions a bit?]

Observables	Belle 0.71 ab ⁻¹	Belle II 5 ab ⁻¹	Belle II 50 ab ⁻¹
$B(B \rightarrow X_s \gamma)_{\text{inc}}^{\text{lep-tag}}$	7.3%	4.8%	3.9%
$B(B \rightarrow X_s \gamma)_{\text{inc}}^{\text{had-tag}}$	13%	7.0%	4.2%
$B(B \rightarrow X_s \gamma)_{\text{sum-of-ex}}$	10.5%	7.3%	5.7%
$\Delta_{0+}(B \rightarrow X_s \gamma)_{\text{sum-of-ex}}$	2.4%	0.94%	0.69%
$\Delta_{0+}(B \rightarrow X_{s+d} \gamma)_{\text{inc}}^{\text{had-tag}}$	9.0%	2.6%	0.85%
$A_{CP}(B \rightarrow X_s \gamma)_{\text{sum-of-ex}}$	1.6%	0.56%	0.19%
$A_{CP}(B \rightarrow X_{s+d} \gamma)_{\text{inc}}^{\text{lep-tag}}$	4.0%	1.5%	0.48%
$A_{CP}(B \rightarrow X_{s+d} \gamma)_{\text{inc}}^{\text{had-tag}}$	8.0%	2.2%	0.70%
$\Delta A_{CP}(B \rightarrow X_s \gamma)_{\text{sum-of-ex}}$	3.1%	1.2%	0.37%
$\Delta A_{CP}(B \rightarrow X_{s+d} \gamma)_{\text{inc}}^{\text{had-tag}}$	16%	4.3%	1.3%
$B(B \rightarrow X_d \gamma)_{\text{sum-of-ex}}$	30%	20%	14%
$\Delta_{0+}(B \rightarrow X_d \gamma)_{\text{sum-of-ex}}$	30%	11%	3.6%
$A_{CP}(B^+ \rightarrow X_{ud}^+ \gamma)_{\text{sum-of-ex}}$	42%	16%	5.1%
$A_{CP}(B^0 \rightarrow X_{dd}^0 \gamma)_{\text{sum-of-ex}}$	84%	32%	10%
$A_{CP}(B \rightarrow X_d \gamma)_{\text{sum-of-ex}}$	38%	14%	4.6%
$\Delta A_{CP}(B \rightarrow X_d \gamma)_{\text{sum-of-ex}}$	93%	36%	11%
$\Delta_{0+}(B \rightarrow K^* \gamma)$	2.0%	0.70%	0.53%
$A_{CP}(B^0 \rightarrow K^{*0} \gamma)$	1.7%	0.58%	0.21%
$A_{CP}(B^+ \rightarrow K^{*+} \gamma)$	2.4%	0.81%	0.29%
$\Delta A_{CP}(B \rightarrow K^* \gamma)$	2.9%	0.98%	0.36%
$S_{CP}(B^0 \rightarrow K^{*0} \gamma)$	29%	9.0%	3.0%
$\Delta_{0+}(B \rightarrow \rho \gamma)$	18%	5.4%	1.9%
$A_{CP}(B^0 \rightarrow \rho^0 \gamma)$	44%	12%	3.8%
$A_{CP}(B^+ \rightarrow \rho^+ \gamma)$	30%	9.6%	3.0%
$\Delta A_{CP}(B \rightarrow \rho \gamma)$	53%	16%	4.8%
$S_{CP}(B^0 \rightarrow \rho^0 \gamma)$	63%	19%	6.4%
$ V_{td}/V_{ts} $	12%	8.2%	7.6%
$B(B^0 \rightarrow \gamma \gamma)$	<740%	30%	9.6%
$A_{CP}(B^0 \rightarrow \gamma \gamma)$	–	78%	25%

Table 4: Sensitivities of observables for the radiative B decays. Some sensitivities at Belle are extrapolated to 0.71 ab⁻¹.

References

- [1] R. Aaij et al., LHCb, JHEP, **08**, 131 (2013), 1304.6325.
- [2] Roel Aaij et al., LHCb, JHEP, **02**, 104 (2016), arXiv:1512.04442.
- [3] S. Wehle et al., Belle, Phys. Rev. Lett., **118**(11), 111801 (2017), arXiv:1612.05014.
- [4] Roel Aaij et al., LHCb, Phys. Rev. Lett., **113**, 151601 (2014), arXiv:1406.6482.
- [5] R. Aaij et al., LHCb (2017), arXiv:1705.05802.
- [6] Vardan Khachatryan et al., CMS, Phys. Lett., **B753**, 424–448 (2016), arXiv:1507.08126.
- [7] Measurement of the P_1 and P'_5 angular parameters of the decay $B^0 \rightarrow K^{*0} \mu^+ \mu^-$ in proton-proton collisions at $\sqrt{s} = 8$ TeV, Technical Report CMS-PAS-BPH-15-008, CERN, Geneva (2017).
- [8] Angular analysis of $B_d^0 \rightarrow K^* \mu^+ \mu^-$ decays in pp collisions at $\sqrt{s} = 8$ TeV with the ATLAS detector, Technical Report ATLAS-CONF-2017-023, CERN, Geneva (Apr 2017).
- [9] Gerhard Buchalla, Andrzej J. Buras, and Markus E. Lautenbacher, Rev. Mod. Phys., **68**, 1125–1144

Observables	Belle 0.71 ab ⁻¹	Belle II 5 ab ⁻¹	Belle II 50 ab ⁻¹
$B(B \rightarrow X_s \ell^+ \ell^-) (1.0 < q^2 < 3.5 \text{ GeV}^2)$	29%	13%	6.6%
$B(B \rightarrow X_s \ell^+ \ell^-) (3.5 < q^2 < 6.0 \text{ GeV}^2)$	24%	11%	6.4%
$B(B \rightarrow X_s \ell^+ \ell^-) (q^2 > 14.4 \text{ GeV}^2)$	23%	10%	4.7%
$A_{CP}(B \rightarrow X_s \ell^+ \ell^-) (1.0 < q^2 < 3.5 \text{ GeV}^2)$	26%	9.7 %	3.1 %
$A_{CP}(B \rightarrow X_s \ell^+ \ell^-) (3.5 < q^2 < 6.0 \text{ GeV}^2)$	21%	7.9 %	2.6 %
$A_{CP}(B \rightarrow X_s \ell^+ \ell^-) (q^2 > 14.4 \text{ GeV}^2)$	21%	8.1 %	2.6 %
$A_{FB}(B \rightarrow X_s \ell^+ \ell^-) (1.0 < q^2 < 3.5 \text{ GeV}^2)$	26%	9.7%	3.1%
$A_{FB}(B \rightarrow X_s \ell^+ \ell^-) (3.5 < q^2 < 6.0 \text{ GeV}^2)$	21%	7.9%	2.6%
$A_{FB}(B \rightarrow X_s \ell^+ \ell^-) (q^2 > 14.4 \text{ GeV}^2)$	19%	7.3%	2.4%
$\Delta_{CP}(A_{FB}) (1.0 < q^2 < 3.5 \text{ GeV}^2)$	52%	19%	6.1%
$\Delta_{CP}(A_{FB}) (3.5 < q^2 < 6.0 \text{ GeV}^2)$	42%	16%	5.2%
$\Delta_{CP}(A_{FB}) (q^2 > 14.4 \text{ GeV}^2)$	38%	15%	4.8%
$A_T^{(2)} (0.002 < q^2 < 1.12 \text{ GeV}^2)$	–	0.21	0.066
$A_T^{\text{Im}} (0.002 < q^2 < 1.12 \text{ GeV}^2)$	–	0.20	0.064
$B(B^+ \rightarrow K^+ \nu \bar{\nu})$	< 450%	38%	12%
$B(B^0 \rightarrow K^{*0} \nu \bar{\nu})$	< 180%	35%	11%
$F_L(B^0 \rightarrow K^{*0} \nu \bar{\nu})$	–	–	0.11
$B(B^0 \rightarrow \nu \bar{\nu}) \times 10^6$	< 14	< 5.0	< 1.5
$B(B^+ \rightarrow K^+ \tau^+ \tau^-) \times 10^5$	< 32	< 6.5	< 2.0
$B(B^0 \rightarrow \tau^+ \tau^-) \times 10^5$	< 140	< 30	< 9.6

Table 5: Sensitivities of lepton flavor conserving observables for the electroweak penguin B decays except for the $B \rightarrow K^* \ell^+ \ell^-$ decay.

- (1996), arXiv:hep-ph/9512380. 1512
- [10] Konstantin G. Chetyrkin, Mikolaj Misiak, and Manfred Munz, Phys. Lett., **B400**, 206–219, [Erratum: 1513
Phys. Lett. B425,414(1998)] (1997), arXiv:hep-ph/9612313. 1514
- [11] Michal Czakon, Ulrich Haisch, and Mikolaj Misiak, JHEP, **03**, 008 (2007), arXiv:hep-ph/0612329. 1515
- [12] Christoph Bobeth, Mikolaj Misiak, and Jorg Urban, Nucl. Phys., **B574**, 291–330 (2000), arXiv:hep- 1516
ph/9910220. 1517
- [13] Paolo Gambino, Martin Gorbahn, and Ulrich Haisch, Nucl. Phys., **B673**, 238–262 (2003), arXiv:hep- 1518
ph/0306079. 1519
- [14] Martin Gorbahn and Ulrich Haisch, Nucl. Phys., **B713**, 291–332 (2005), arXiv:hep-ph/0411071. 1520
- [15] Mikolaj Misiak and Jorg Urban, Phys. Lett., **B451**, 161–169 (1999), arXiv:hep-ph/9901278. 1521
- [16] Gerhard Buchalla and Andrzej J. Buras, Nucl. Phys., **B548**, 309–327 (1999), arXiv:hep-ph/9901288. 1522
- [17] Thomas Hermann, Mikolaj Misiak, and Matthias Steinhauser, JHEP, **12**, 097 (2013), arXiv:1311.1347. 1523
- [18] Joachim Brod, Martin Gorbahn, and Emmanuel Stamou, Phys. Rev., **D83**, 034030 (2011), 1524
arXiv:1009.0947. 1525
- [19] Christoph Bobeth, Martin Gorbahn, and Emmanuel Stamou, Phys. Rev., **D89**(3), 034023 (2014), 1526
arXiv:1311.1348. 1527
- [20] B. Blok, L. Koyrakh, Mikhail A. Shifman, and A. I. Vainshtein, Phys. Rev., **D49**, 3356, [Erratum: 1528
Phys. Rev. D50, 3572 (1994)] (1994), arXiv:hep-ph/9307247. 1529
- [21] Aneesh V. Manohar and Mark B. Wise, Phys. Rev., **D49**, 1310–1329 (1994), arXiv:hep-ph/9308246. 1530
- [22] Matthias Neubert, Phys. Rev., **D49**, 3392–3398 (1994), arXiv:hep-ph/9311325. 1531
- [23] Matthias Neubert, Phys. Rev., **D49**, 4623–4633 (1994), arXiv:hep-ph/9312311. 1532
- [24] Ikaros I. Y. Bigi, Mikhail A. Shifman, N. G. Uraltsev, and A. I. Vainshtein, Int. J. Mod. Phys., **A9**, 1533
2467–2504 (1994), arXiv:hep-ph/9312359. 1534
- [25] Seung J. Lee, Matthias Neubert, and Gil Paz, Phys. Rev., **D75**, 114005 (2007), arXiv:hep-ph/0609224. 1535
- [26] Michael Benzke, Seung J. Lee, Matthias Neubert, and Gil Paz, JHEP, **08**, 099 (2010), arXiv:1003.5012. 1536

Observables	Belle 0.71 ab ⁻¹	Belle II 5 ab ⁻¹	Belle II 50 ab ⁻¹
$F_L (1 < q^2 < 2.5 \text{ GeV}^2)$	0.19	0.063	0.025
$F_L (2.5 < q^2 < 4 \text{ GeV}^2)$	0.17	0.057	0.022
$F_L (4 < q^2 < 6 \text{ GeV}^2)$	0.14	0.046	0.018
$F_L (q^2 > 14.2 \text{ GeV}^2)$	0.088	0.027	0.009
$P_1 (1 < q^2 < 2.5 \text{ GeV}^2)$	0.59	0.24	0.078
$P_1 (2.5 < q^2 < 4 \text{ GeV}^2)$	0.53	0.21	0.071
$P_1 (4 < q^2 < 6 \text{ GeV}^2)$	0.43	0.17	0.057
$P_1 (q^2 > 14.2 \text{ GeV}^2)$	0.33	0.12	0.040
$P_2 (1 < q^2 < 2.5 \text{ GeV}^2)$	0.32	0.12	0.040
$P_2 (2.5 < q^2 < 4 \text{ GeV}^2)$	0.30	0.11	0.036
$P_2 (4 < q^2 < 6 \text{ GeV}^2)$	0.24	0.090	0.029
$P_2 (q^2 > 14.2 \text{ GeV}^2)$	0.086	0.034	0.011
$P_3 (1 < q^2 < 2.5 \text{ GeV}^2)$	0.32	0.12	0.040
$P_3 (2.5 < q^2 < 4 \text{ GeV}^2)$	0.30	0.11	0.036
$P_3 (4 < q^2 < 6 \text{ GeV}^2)$	0.24	0.090	0.029
$P_3 (q^2 > 14.2 \text{ GeV}^2)$	0.18	0.068	0.022
$P'_4 (1 < q^2 < 2.5 \text{ GeV}^2)$	0.50	0.18	0.056
$P'_4 (2.5 < q^2 < 4 \text{ GeV}^2)$	0.45	0.15	0.049
$P'_4 (4 < q^2 < 6 \text{ GeV}^2)$	0.34	0.12	0.040
$P'_4 (q^2 > 14.2 \text{ GeV}^2)$	0.26	0.099	0.032
$P'_5 (1 < q^2 < 2.5 \text{ GeV}^2)$	0.47	0.17	0.054
$P'_5 (2.5 < q^2 < 4 \text{ GeV}^2)$	0.42	0.15	0.049
$P'_5 (4 < q^2 < 6 \text{ GeV}^2)$	0.34	0.12	0.040
$P'_5 (q^2 > 14.2 \text{ GeV}^2)$	0.23	0.088	0.027
$P'_6 (1 < q^2 < 2.5 \text{ GeV}^2)$	0.50	0.17	0.054
$P'_6 (2.5 < q^2 < 4 \text{ GeV}^2)$	0.45	0.15	0.049
$P'_6 (4 < q^2 < 6 \text{ GeV}^2)$	0.36	0.12	0.040
$P'_6 (q^2 > 14.2 \text{ GeV}^2)$	0.27	0.10	0.032
$P'_8 (1 < q^2 < 2.5 \text{ GeV}^2)$	0.51	0.19	0.061
$P'_8 (2.5 < q^2 < 4 \text{ GeV}^2)$	0.47	0.17	0.056
$P'_8 (4 < q^2 < 6 \text{ GeV}^2)$	0.38	0.14	0.045
$P'_8 (q^2 > 14.2 \text{ GeV}^2)$	0.27	0.10	0.032

Table 6: Sensitivities of lepton flavor conserving observables for the $B \rightarrow K^* \ell^+ \ell^-$ decay.

- 1537 [27] Sinya Aoki et al., Eur. Phys. J., **C74**, 2890 (2014), arXiv:1310.8555.
1538 [28] Jon A. Bailey et al., Fermilab Lattice, MILC, Phys. Rev., **D92**(1), 014024 (2015), arXiv:1503.07839.
1539 [29] Jon A. Bailey et al., Fermilab Lattice, MILC, Phys. Rev. Lett., **115**(15), 152002 (2015),
1540 arXiv:1507.01618.
1541 [30] Chris Bouchard, G. Peter Lepage, Christopher Monahan, Heechang Na, and Junko Shigemitsu,
1542 HPQCD, Phys. Rev. Lett., **111**(16), 162002, [Erratum: Phys. Rev. Lett. 112, no. 14, 149902 (2014)]
1543 (2013), arXiv:1306.0434.
1544 [31] Jon A. Bailey et al., Phys. Rev., **D93**(2), 025026 (2016), arXiv:1509.06235.
1545 [32] Ronald R. Horgan, Zhao Feng Liu, Stefan Meinel, and Matthew Wingate, Phys. Rev., **D89**(9), 094501
1546 (2014), arXiv:1310.3722.
1547 [33] Jonathan Flynn, Andreas Jüttner, Taichi Kawanai, Edwin Lizarazo, and Oliver Witzel, Hadronic

Observables	Belle 0.71 ab^{-1}	Belle II 5 ab^{-1}	Belle II 50 ab^{-1}
$R_K (1 < q^2 < 6 \text{ GeV}^2)$	28%	11%	3.6%
$R_K (q^2 > 14.4 \text{ GeV}^2)$	30%	12%	3.6%
$R_{K^*} (1 < q^2 < 6 \text{ GeV}^2)$	26%	10%	3.2%
$R_{K^*} (q^2 > 14.4 \text{ GeV}^2)$	24%	9.2%	2.8%
$R_{X_s} (1 < q^2 < 6 \text{ GeV}^2)$	32%	12%	4.0%
$R_{X_s} (q^2 > 14.4 \text{ GeV}^2)$	28%	11%	3.4%
$Q_{F_L} (1 < q^2 < 6 \text{ GeV}^2)$	0.20	0.068	0.026
$Q_{F_L} (4 < q^2 < 8 \text{ GeV}^2)$	0.20	0.068	0.026
$Q_{F_L} (q^2 > 14.2 \text{ GeV}^2)$	0.19	0.059	0.020
$Q_1 (1 < q^2 < 6 \text{ GeV}^2)$	0.64	0.26	0.086
$Q_1 (4 < q^2 < 8 \text{ GeV}^2)$	0.95	0.35	0.12
$Q_1 (q^2 > 14.2 \text{ GeV}^2)$	0.73	0.26	0.088
$Q_2 (1 < q^2 < 6 \text{ GeV}^2)$	0.35	0.13	0.044
$Q_2 (4 < q^2 < 8 \text{ GeV}^2)$	0.21	0.081	0.026
$Q_2 (q^2 > 14.2 \text{ GeV}^2)$	0.19	0.075	0.024
$Q_3 (1 < q^2 < 6 \text{ GeV}^2)$	0.64	0.24	0.079
$Q_3 (4 < q^2 < 8 \text{ GeV}^2)$	0.46	0.18	0.059
$Q_3 (q^2 > 14.2 \text{ GeV}^2)$	0.40	0.15	0.048
$Q_4 (1 < q^2 < 6 \text{ GeV}^2)$	0.57	0.19	0.062
$Q_4 (4 < q^2 < 8 \text{ GeV}^2)$	0.42	0.15	0.051
$Q_4 (q^2 > 14.2 \text{ GeV}^2)$	0.57	0.22	0.070
$Q_5 (1 < q^2 < 6 \text{ GeV}^2)$	0.51	0.18	0.059
$Q_5 (4 < q^2 < 8 \text{ GeV}^2)$	0.46	0.16	0.053
$Q_5 (q^2 > 14.2 \text{ GeV}^2)$	0.51	0.19	0.059
$Q_6 (1 < q^2 < 6 \text{ GeV}^2)$	0.55	0.18	0.059
$Q_6 (4 < q^2 < 8 \text{ GeV}^2)$	0.48	0.17	0.055
$Q_6 (q^2 > 14.2 \text{ GeV}^2)$	0.59	0.22	0.070
$Q_8 (1 < q^2 < 6 \text{ GeV}^2)$	0.55	0.21	0.066
$Q_8 (4 < q^2 < 8 \text{ GeV}^2)$	0.46	0.17	0.055
$Q_8 (q^2 > 14.2 \text{ GeV}^2)$	0.59	0.22	0.070

Table 7: Sensitivities of LFV observables for the electroweak penguin B decays.

Observables	Belle 0.12 ab^{-1}	Belle II 0.5 ab^{-1}	Belle II 5 ab^{-1}
$B(B_s \rightarrow \gamma\gamma)$	<250%	73%	23%
$B(B_s \rightarrow \tau^+\tau^-) \times 10^4$	< 70	< 24	< 8.1
$B(B_s \rightarrow \nu\bar{\nu}) \times 10^5$	< 9.7	< 4.5	< 1.5

Table 8: Sensitivities of observables for the radiative and electroweak penguin B_s decays.

- form factors for rare semileptonic B decays, In *Proceedings, 33rd International Symposium on Lattice Field Theory (Lattice 2015)* (2015), arXiv:1511.06622.
- [34] M. Beneke, G. Buchalla, M. Neubert, and C. T. Sachrajda, Phys. Rev. Lett., **83**, 1914–1917 (1999), arXiv:hep-ph/9905312.
- [35] M. Beneke, G. Buchalla, M. Neubert, and Christopher T. Sachrajda, Nucl. Phys., **B606**, 245–321 (2001), arXiv:hep-ph/0104110.
- [36] A. Khodjamirian and R. Rückl, Adv. Ser. Direct. High Energy Phys., **15**, 345–401 (1998), arXiv:hep-ph/9801443.
- [37] Patricia Ball and Roman Zwicky, Phys. Rev., **D71**, 014029 (2005), arXiv:hep-ph/0412079.
- [38] Aoife Bharucha, David M. Straub, and Roman Zwicky (2015), arXiv:1503.05534.
- [39] Bernard Aubert et al., BaBar, Phys. Rev., **D77**, 051103 (2008), arXiv:0711.4889.
- [40] P. del Amo Sanchez et al., BaBar, Phys. Rev., **D82**, 051101 (2010), arXiv:1005.4087.
- [41] J. P. Lees et al., BaBar, Phys. Rev., **D86**, 052012 (2012), arXiv:1207.2520.
- [42] J. P. Lees et al., BaBar, Phys. Rev. Lett., **109**, 191801 (2012), arXiv:1207.2690.
- [43] T. Saito et al., Belle, Phys. Rev., **D91**(5), 052004 (2015), arXiv:1411.7198.
- [44] A. Abdesselam et al., Measurement of the inclusive $B \rightarrow X_{s+d}\gamma$ branching fraction, photon energy spectrum and HQE parameters, In *38th International Conference on High Energy Physics (ICHEP 2016) Chicago, IL, USA, August 03-10, 2016* (2016), arXiv:1608.02344.
- [45] Michal Czakon, Paul Fiedler, Tobias Huber, Mikolaj Misiak, Thomas Schutzmeier, and Matthias Steinhauser, JHEP, **04**, 168 (2015), arXiv:1503.01791.
- [46] M. Misiak et al., Phys. Rev. Lett., **114**(22), 221801 (2015), arXiv:1503.01789.
- [47] Oliver Buchmüller and Henning Flächer, Phys. Rev., **D73**, 073008 (2006), arXiv:hep-ph/0507253.
- [48] Gil Paz, Theory of Inclusive Radiative B Decays, In *CKM unitarity triangle. Proceedings, 6th International Workshop, CKM 2010, Warwick, UK, September 6-10, 2010* (2010), arXiv:1011.4953.
- [49] Florian U. Bernlochner, Heiko Lacker, Zoltan Ligeti, Iain W. Stewart, Frank J. Tackmann, and Kerstin Tackmann, Status of SIMBA, In *CKM unitarity triangle. Proceedings, 6th International Workshop, CKM 2010, Warwick, UK, September 6-10, 2010* (2011), arXiv:1101.3310.
- [50] Florian U. Bernlochner, Heiko Lacker, Zoltan Ligeti, Iain W. Stewart, Frank J. Tackmann, and Kerstin Tackmann, SIMBA, PoS, **ICHEP2012**, 370 (2013), arXiv:1303.0958.
- [51] Andreas Crivellin and Lorenzo Mercolli, Phys. Rev., **D84**, 114005 (2011), arXiv:1106.5499.
- [52] H. M. Asatrian and C. Greub, Phys. Rev., **D88**(7), 074014 (2013), arXiv:1305.6464.
- [53] Paolo Gambino and Mikolaj Misiak, Nucl. Phys., **B611**, 338–366 (2001), arXiv:hep-ph/0104034.
- [54] G. Buchalla, G. Isidori, and S. J. Rey, Nucl. Phys., **B511**, 594–610 (1998), arXiv:hep-ph/9705253.
- [55] Maciej Kaminski, Mikolaj Misiak, and Michal Poradzinski, Phys. Rev., **D86**, 094004 (2012), arXiv:1209.0965.
- [56] Tobias Huber, Michal Poradzinski, and Javier Virto, JHEP, **01**, 115 (2015), arXiv:1411.7677.
- [57] Ian Richard Blokland, A. Czarnecki, M. Misiak, M. Slusarczyk, and F. Tkachov, Phys. Rev., **D72**, 033014 (2005), arXiv:hep-ph/0506055.
- [58] Kirill Melnikov and Alexander Mitov, Phys. Lett., **B620**, 69–79 (2005), arXiv:hep-ph/0505097.
- [59] H. M. Asatrian, T. Ewerth, H. Gabrielyan, and C. Greub, Phys. Lett., **B647**, 173–178 (2007), arXiv:hep-ph/0611123.
- [60] Thorsten Ewerth, Phys. Lett., **B669**, 167–172 (2008), arXiv:0805.3911.
- [61] H. M. Asatrian, T. Ewerth, A. Ferroglia, C. Greub, and G. Ossola, Phys. Rev., **D82**, 074006 (2010), arXiv:1005.5587.
- [62] Zoltan Ligeti, Michael E. Luke, Aneesh V. Manohar, and Mark B. Wise, Phys. Rev., **D60**, 034019 (1999), arXiv:hep-ph/9903305.
- [63] Andrea Ferroglia and Ulrich Haisch, Phys. Rev., **D82**, 094012 (2010), arXiv:1009.2144.
- [64] Mikolaj Misiak and Michal Poradzinski, Phys. Rev., **D83**, 014024 (2011), arXiv:1009.5685.
- [65] Stanley J. Brodsky, G. Peter Lepage, and Paul B. Mackenzie, Phys. Rev., **D28**, 228 (1983).
- [66] Kay Bieri, Christoph Greub, and Matthias Steinhauser, Phys. Rev., **D67**, 114019 (2003), arXiv:hep-ph/0302051.
- [67] R. Boughezal, M. Czakon, and T. Schutzmeier, JHEP, **09**, 072 (2007), arXiv:0707.3090.
- [68] Mikolaj Misiak and Matthias Steinhauser, Nucl. Phys., **B764**, 62–82 (2007), arXiv:hep-ph/0609241.
- [69] Mikolaj Misiak and Matthias Steinhauser, Nucl. Phys., **B840**, 271–283 (2010), arXiv:1005.1173.
- [70] J. Charles et al., Phys. Rev., **D91**(7), 073007 (2015), arXiv:1501.05013.
- [71] Thorsten Ewerth, Paolo Gambino, and Soumitra Nandi, Nucl. Phys., **B830**, 278–290 (2010), arXiv:0911.2175.
- [72] Andrea Alberti, Paolo Gambino, and Soumitra Nandi, JHEP, **01**, 147 (2014), arXiv:1311.7381.
- [73] Ikaros I. Y. Bigi, N. G. Uraltsev, and A. I. Vainshtein, Phys. Lett., **B293**, 430–436, [Erratum: Phys. Lett. B297,477(1992)] (1992), arXiv:hep-ph/9207214.

- [74] Adam F. Falk, Michael E. Luke, and Martin J. Savage, Phys. Rev., **D49**, 3367–3378 (1994), arXiv:hep-ph/9308288. 1608
- [75] Christian W. Bauer, Phys. Rev., **D57**, 5611–5619, [Erratum: Phys. Rev.D60,099907(1999)] (1998), arXiv:hep-ph/9710513. 1609
- [76] Thomas Mannel, Sascha Turczyk, and Nikolai Uraltsev, JHEP, **11**, 109 (2010), arXiv:1009.4622. 1611
- [77] Thomas Becher and Matthias Neubert, Phys. Lett., **B637**, 251–259 (2006), arXiv:hep-ph/0603140. 1612
- [78] Keith S. M. Lee and Iain W. Stewart, Nucl. Phys., **B721**, 325–406 (2005), arXiv:hep-ph/0409045. 1613
- [79] Stefan W. Bosch, Matthias Neubert, and Gil Paz, JHEP, **11**, 073 (2004), arXiv:hep-ph/0409115. 1614
- [80] M. Beneke, F. Campanario, T. Mannel, and B. D. Pecjak, JHEP, **06**, 071 (2005), arXiv:hep-ph/0411395. 1615
- [81] Christian W. Bauer, Michael E. Luke, and Thomas Mannel, Phys. Rev., **D68**, 094001 (2003), arXiv:hep-ph/0102089. 1616
- [82] Gil Paz, JHEP, **06**, 083 (2009), arXiv:0903.3377. 1617
- [83] Bjorn O. Lange, Matthias Neubert, and Gil Paz, Phys. Rev., **D72**, 073006 (2005), arXiv:hep-ph/0504071. 1618
- [84] Bjorn O. Lange, Matthias Neubert, and Gil Paz, JHEP, **0510**, 084 (2005), hep-ph/0508178. 1619
- [85] Bjorn O. Lange, JHEP, **01**, 104 (2006), arXiv:hep-ph/0511098. 1620
- [86] Ahmed Ali and C. Greub, Phys. Lett., **B361**, 146–154 (1995), arXiv:hep-ph/9506374. 1621
- [87] Anton Kapustin, Zoltan Ligeti, and H. David Politzer, Phys. Lett., **B357**, 653–658 (1995), arXiv:hep-ph/9507248. 1622
- [88] John F. Donoghue and Alexey A. Petrov, Phys. Rev., **D53**, 3664–3671 (1996), arXiv:hep-ph/9510227. 1623
- [89] M. B. Voloshin, Phys. Lett., **B397**, 275–278 (1997), arXiv:hep-ph/9612483. 1624
- [90] Zoltan Ligeti, Lisa Randall, and Mark B. Wise, Phys. Lett., **B402**, 178–182 (1997), arXiv:hep-ph/9702322. 1625
- [91] Aaron K. Grant, A. G. Morgan, S. Nussinov, and R. D. Peccei, Phys. Rev., **D56**, 3151–3154 (1997), arXiv:hep-ph/9702380. 1626
- [92] Michael Benzke, Seung J. Lee, Matthias Neubert, and Gil Paz, Phys. Rev. Lett., **106**, 141801 (2011), arXiv:1012.3167. 1627
- [93] Joao M. Soares, Nucl. Phys., **B367**, 575–590 (1991). 1628
- [94] Ahmed Ali, H. Asatrian, and C. Greub, Phys. Lett., **B429**, 87–98 (1998), arXiv:hep-ph/9803314. 1629
- [95] Alexander L. Kagan and Matthias Neubert, Phys. Rev., **D58**, 094012 (1998), arXiv:hep-ph/9803368. 1630
- [96] Tobias Hurth, Enrico Lunghi, and Werner Porod, Nucl. Phys., **B704**, 56–74 (2005), arXiv:hep-ph/0312260. 1631
- [97] Paolo Gambino, Kristopher J. Healey, and Sascha Turczyk, Phys. Lett., **B763**, 60–65 (2016), arXiv:1606.06174. 1632
- [98] Mikolaj Misiak, Acta Phys. Polon., **B40**, 2987–2996 (2009), arXiv:0911.1651. 1633
- [99] J. P. Lees et al., BaBar, Phys. Rev., **D86**, 112008 (2012), arXiv:1207.5772. 1634
- [100] A. Limosani et al., Belle, Phys. Rev. Lett., **103**, 241801 (2009), arXiv:0907.1384. 1635
- [101] S. Chen et al., CLEO, Phys. Rev. Lett., **87**, 251807 (2001), arXiv:hep-ex/0108032. 1636
- [102] Bernard Aubert et al., BaBar, Phys. Rev., **D72**, 052004 (2005), arXiv:hep-ex/0508004. 1637
- [103] L. Pesantez et al., Belle, Phys. Rev. Lett., **114**(15), 151601 (2015), arXiv:1501.01702. 1638
- [104] J. P. Lees et al., BaBar, Phys. Rev., **D90**(9), 092001 (2014), arXiv:1406.0534. 1639
- [105] S. Nishida et al., Belle, Phys. Rev. Lett., **93**, 031803 (2004), arXiv:hep-ex/0308038. 1640
- [106] Stefan W. Bosch and Gerhard Buchalla, Nucl. Phys., **B621**, 459–478 (2002), arXiv:hep-ph/0106081. 1641
- [107] M. Beneke, T. Feldmann, and D. Seidel, Nucl. Phys., **B612**, 25–58 (2001), arXiv:hep-ph/0106067. 1642
- [108] M. Beneke, Th. Feldmann, and D. Seidel, Eur. Phys. J., **C41**, 173–188 (2005), arXiv:hep-ph/0412400. 1643
- [109] Maria Dimou, James Lyon, and Roman Zwicky, Phys. Rev., **D87**(7), 074008 (2013), arXiv:1212.2242. 1644
- [110] Ahmed Ali and Vladimir M. Braun, Phys. Lett., **B359**, 223–235 (1995), arXiv:hep-ph/9506248. 1645
- [111] A. Khodjamirian, G. Stoll, and D. Wyler, Phys. Lett., **B358**, 129–138 (1995), arXiv:hep-ph/9506242. 1646
- [112] James Lyon and Roman Zwicky, Phys. Rev., **D88**(9), 094004 (2013), arXiv:1305.4797. 1647
- [113] Roel Aaij et al., LHCb, Phys. Rev. Lett., **112**(16), 161801 (2014), arXiv:1402.6852. 1648
- [114] Damir Becirevic, Emi Kou, Alain Le Yaouanc, and Andrey Tayduganov, JHEP, **08**, 090 (2012), arXiv:1206.1502. 1649
- [115] Sebastian Jäger and Jorge Martin Camalich, Phys. Rev., **D93**(1), 014028 (2016), arXiv:1412.3183. 1650
- [116] Martino Borsato, *Study of the $B^0 \rightarrow K^{*0} e^+ e^-$ decay with the LHCb detector and development of a novel concept of PID detector: the Focusing DIRC*, PhD thesis, Santiago de Compostela U. (2015). 1651
- [117] Ayan Paul and David M. Straub, JHEP, **04**, 027 (2017), arXiv:1608.02556. 1652
- [118] Patricia Ball, Gareth W. Jones, and Roman Zwicky, Phys. Rev., **D75**, 054004 (2007), arXiv:hep-ph/0612081. 1653
- [119] R Aaij et al., LHCb, Phys. Rev., **D85**, 112013 (2012), arXiv:1202.6267. 1654
- [120] R Aaij et al., LHCb, Nucl. Phys., **B867**, 1–18 (2013), arXiv:1209.0313. 1655

-
- [121] Sebastien Descotes-Genon, Joaquim Matias, and Javier Virto, Phys. Rev., **D88**, 074002 (2013), arXiv:1307.5683.
- [122] Wolfgang Altmannshofer and David M. Straub, Implications of $b \rightarrow s$ measurements, In *Proceedings, 50th Rencontres de Moriond Electroweak interactions and unified theories*, pages 333–338 (2015), arXiv:1503.06199.
- [123] Roel Aaij et al., LHCb, JHEP, **09**, 179 (2015), arXiv:1506.08777.
- [124] Ahmed Ali and A. Y. Parkhomenko, Eur. Phys. J., **C23**, 89–112 (2002), arXiv:hep-ph/0105302.
- [125] Alexander L. Kagan and Matthias Neubert, Phys. Lett., **B539**, 227–234 (2002), arXiv:hep-ph/0110078.
- [126] Y. Amhis et al., Heavy Flavor Averaging Group (2012), arXiv:1207.1158.
- [127] David Atwood, Michael Gronau, and Amarjit Soni, Phys. Rev. Lett., **79**, 185–188 (1997), arXiv:hep-ph/9704272.
- [128] Franz Muheim, Yuehong Xie, and Roman Zwicky, Phys. Lett., **B664**, 174–179 (2008), arXiv:0802.0876.
- [129] Emi Kou, Cai-Dian Lü, and Fu-Sheng Yu, JHEP, **12**, 102 (2013), arXiv:1305.3173.
- [130] Naoyuki Haba, Hiroyuki Ishida, Tsuyoshi Nakaya, Yasuhiro Shimizu, and Ryo Takahashi, JHEP, **03**, 160 (2015), arXiv:1501.00668.
- [131] Benjamin Grinstein, Yuval Grossman, Zoltan Ligeti, and Dan Pirjol, Phys. Rev., **D71**, 011504 (2005), arXiv:hep-ph/0412019.
- [132] S. Jäger and J. Martin Camalich, JHEP, **05**, 043 (2013), arXiv:1212.2263.
- [133] Patricia Ball and Roman Zwicky, JHEP, **04**, 046 (2006), arXiv:hep-ph/0603232.
- [134] A. Khodjamirian, Th. Mannel, A. A. Pivovarov, and Y. M. Wang, JHEP, **09**, 089 (2010), arXiv:1006.4945.
- [135] Patricia Ball and Roman Zwicky, Phys. Lett., **B642**, 478–486 (2006), arXiv:hep-ph/0609037.
- [136] Michael Gronau, Yuval Grossman, Dan Pirjol, and Anders Ryd, Phys. Rev. Lett., **88**, 051802 (2002), arXiv:hep-ph/0107254.
- [137] Michael Gronau and Dan Pirjol, Phys. Rev., **D66**, 054008 (2002), arXiv:hep-ph/0205065.
- [138] E. Kou, A. Le Yaouanc, and A. Tayduganov, Phys. Rev., **D83**, 094007 (2011), arXiv:1011.6593.
- [139] Roel Aaij et al., LHCb, JHEP, **04**, 064 (2015), arXiv:1501.03038.
- [140] Fady Bishara and Dean J. Robinson, JHEP, **09**, 013 (2015), arXiv:1505.00376.
- [141] David Atwood, Tim Gershon, Masashi Hazumi, and Amarjit Soni, Phys. Rev., **D71**, 076003 (2005), arXiv:hep-ph/0410036.
- [142] R. Ammar et al., CLEO, Phys. Rev. Lett., **71**, 674–678 (1993).
- [143] Wolfgang Altmannshofer and David M. Straub, Eur. Phys. J., **C75**(8), 382 (2015), arXiv:1411.3161.
- [144] Kazuo Abe et al., Belle, Phys. Rev. Lett., **96**, 221601 (2006), arXiv:hep-ex/0506079.
- [145] Y. Ushiroda et al., Belle, Phys. Rev. Lett., **100**, 021602 (2008), arXiv:0709.2769.
- [146] N. Taniguchi et al., Belle, Phys. Rev. Lett., **101**, 111801, [Erratum: Phys. Rev. Lett.101,129904(2008)] (2008), arXiv:0804.4770.
- [147] Bernard Aubert et al., BaBar, Phys. Rev., **D78**, 112001 (2008), arXiv:0808.1379.
- [148] A. J. Bevan et al., Belle, BaBar, Eur. Phys. J., **C74**, 3026 (2014), arXiv:1406.6311.
- [149] R Aaij et al., LHCb, JHEP, **1307**, 084 (2013), arXiv:1305.2168.
- [150] Keith S. M. Lee, Zoltan Ligeti, Iain W. Stewart, and Frank J. Tackmann, Phys. Rev., **D75**, 034016 (2007), arXiv:hep-ph/0612156.
- [151] Ahmed Ali, T. Mannel, and T. Morozumi, Phys. Lett., **B273**, 505–512 (1991).
- [152] H. H. Asatryan, H. M. Asatryan, C. Greub, and M. Walker, Phys. Rev., **D65**, 074004 (2002), arXiv:hep-ph/0109140.
- [153] H. H. Asatryan, H. M. Asatryan, C. Greub, and M. Walker, Phys. Lett., **B507**, 162–172 (2001), arXiv:hep-ph/0103087.
- [154] H. H. Asatryan, H. M. Asatryan, C. Greub, and M. Walker, Phys. Rev., **D66**, 034009 (2002), arXiv:hep-ph/0204341.
- [155] A. Ghinculov, T. Hurth, G. Isidori, and Y. P. Yao, Nucl. Phys., **B648**, 254–276 (2003), arXiv:hep-ph/0208088.
- [156] H. M. Asatryan, K. Bieri, C. Greub, and A. Hovhannisyanyan, Phys. Rev., **D66**, 094013 (2002), arXiv:hep-ph/0209006.
- [157] H. M. Asatryan, H. H. Asatryan, A. Hovhannisyanyan, and V. Poghosyan, Mod. Phys. Lett., **A19**, 603–614 (2004), arXiv:hep-ph/0311187.
- [158] A. Ghinculov, T. Hurth, G. Isidori, and Y. P. Yao, Nucl. Phys., **B685**, 351–392 (2004), arXiv:hep-ph/0312128.
- [159] Christoph Greub, Volker Pilipp, and Christof Schupbach, JHEP, **12**, 040 (2008), arXiv:0810.4077.
- [160] Christoph Bobeth, Paolo Gambino, Martin Gorbahn, and Ulrich Haisch, JHEP, **04**, 071 (2004), arXiv:hep-ph/0312090.
- [161] Tobias Huber, Enrico Lunghi, Mikolaj Misiak, and Daniel Wyler, Nucl. Phys., **B740**, 105–137 (2006),

- arXiv:hep-ph/0512066. 1730
- [162] Tobias Huber, Tobias Hurth, and Enrico Lunghi, Nucl. Phys., **B802**, 40–62 (2008), arXiv:0712.3009. 1731
- [163] Tobias Huber, Tobias Hurth, and Enrico Lunghi, JHEP, **06**, 176 (2015), arXiv:1503.04849. 1732
- [164] Ahmed Ali, G. Hiller, L. T. Handoko, and T. Morozumi, Phys. Rev., **D55**, 4105–4128 (1997), arXiv:hep-ph/9609449. 1733
- [165] Jiunn-Wei Chen, Gautam Rupak, and Martin J. Savage, Phys. Lett., **B410**, 285–289 (1997), arXiv:hep-ph/9705219. 1734
- [166] Gerhard Buchalla and Gino Isidori, Nucl. Phys., **B525**, 333–349 (1998), arXiv:hep-ph/9801456. 1735
- [167] Christian W. Bauer and Craig N. Burrell, Phys. Rev., **D62**, 114028 (2000), arXiv:hep-ph/9911404. 1736
- [168] Zoltan Ligeti and Frank J. Tackmann, Phys. Lett., **B653**, 404–410 (2007), arXiv:0707.1694. 1737
- [169] Bernard Aubert et al., BaBar, Phys. Rev. Lett., **93**, 081802 (2004), arXiv:hep-ex/0404006. 1738
- [170] J.P. Lees et al., BaBar (2013), arXiv:1312.5364. 1739
- [171] J. Kaneko et al., Belle, Phys. Rev. Lett., **90**, 021801 (2003), arXiv:hep-ex/0208029. 1740
- [172] M. Iwasaki et al., Belle, Phys. Rev., **D72**, 092005 (2005), arXiv:hep-ex/0503044. 1741
- [173] Y. Sato et al., Belle, Phys. Rev., **D93**(3), 032008, [Addendum: Phys. Rev.D93,no.5,059901(2016)] (2016), arXiv:1402.7134. 1742
- [174] Keith S. M. Lee and Iain W. Stewart, Phys. Rev., **D74**, 014005 (2006), arXiv:hep-ph/0511334. 1743
- [175] Keith S. M. Lee, Zoltan Ligeti, Iain W. Stewart, and Frank J. Tackmann, Phys. Rev., **D74**, 011501 (2006), arXiv:hep-ph/0512191. 1744
- [176] Keith S. M. Lee and Frank J. Tackmann, Phys. Rev., **D79**, 114021 (2009), arXiv:0812.0001. 1745
- [177] G. Bell, M. Beneke, T. Huber, and Xin-Qiang Li, Nucl. Phys., **B843**, 143–176 (2011), arXiv:1007.3758. 1746
- [178] Tobias Hurth, Subleading-power factorization in inclusive $b \rightarrow sll$, talk at workshop on rare b decays: Theory and experiment (). 1747
- [179] F. Krüger and L. M. Sehgal, Phys. Lett., **B380**, 199–204 (1996), arXiv:hep-ph/9603237. 1748
- [180] H. M. Asatrian, K. Bieri, C. Greub, and M. Walker, Phys. Rev., **D69**, 074007 (2004), arXiv:hep-ph/0312063. 1749
- [181] Dirk Seidel, Phys. Rev., **D70**, 094038 (2004), arXiv:hep-ph/0403185. 1750
- [182] Gerhard Buchalla, Gudrun Hiller, and Gino Isidori, Phys. Rev., **D63**, 014015 (2000), arXiv:hep-ph/0006136. 1751
- [183] Wolfgang Altmannshofer, Patricia Ball, Aoife Bharucha, Andrzej J. Buras, David M. Straub, and Michael Wick, JHEP, **01**, 019 (2009), arXiv:0811.1214. 1752
- [184] Christoph Bobeth, Gudrun Hiller, and Giorgi Piranishvili, JHEP, **12**, 040 (2007), arXiv:0709.4174. 1753
- [185] Sebastien Descotes-Genon, Joaquim Matias, Marc Ramon, and Javier Virto, JHEP, **01**, 048 (2013), arXiv:1207.2753. 1754
- [186] Sebastien Descotes-Genon, Tobias Hurth, Joaquim Matias, and Javier Virto, JHEP, **05**, 137 (2013), arXiv:1303.5794. 1755
- [187] Damir Becirevic and Elia Schneider, Nucl. Phys., **B854**, 321–339 (2012), arXiv:1106.3283. 1756
- [188] Yuval Grossman and Dan Pirjol, JHEP, **06**, 029 (2000), arXiv:hep-ph/0005069. 1757
- [189] Marzia Bordone, Gino Isidori, and Andrea Pattori, Eur. Phys. J., **C76**(8), 440 (2016), arXiv:1605.07633. 1758
- [190] Gudrun Hiller and Martin Schmaltz, JHEP, **02**, 055 (2015), arXiv:1411.4773. 1759
- [191] Wolfgang Altmannshofer and Itay Yavin, Phys. Rev., **D92**(7), 075022 (2015), arXiv:1508.07009. 1760
- [192] Bernat Capdevila, Sebastien Descotes-Genon, Joaquim Matias, and Javier Virto, JHEP, **10**, 075 (2016), arXiv:1605.03156. 1761
- [193] J. P. Lees et al., BaBar, Phys. Rev., **D86**, 032012 (2012), arXiv:1204.3933. 1762
- [194] J.-T. Wei et al., Belle, Phys.Rev.Lett., **103**, 171801 (2009), arXiv:0904.0770. 1763
- [195] Kazuo Abe et al., Belle, Phys. Rev. Lett., **88**, 021801 (2002), arXiv:hep-ex/0109026. 1764
- [196] A. Ishikawa et al., Belle, Phys. Rev. Lett., **91**, 261601 (2003), arXiv:hep-ex/0308044. 1765
- [197] T. Aaltonen et al., CDF, Phys.Rev.Lett., **108**, 081807 (2012), arXiv:1108.0695. 1766
- [198] J. P. Lees et al., BaBar, Phys. Rev., **D93**(5), 052015 (2016), arXiv:1508.07960. 1767
- [199] Roel Aaij et al., LHCb, JHEP, **11**, 047 (2016), arXiv:1606.04731. 1768
- [200] R Aaij et al., LHCb, Phys. Rev. Lett., **111**, 191801 (2013), arXiv:1308.1707. 1769
- [201] Wolfgang Altmannshofer, Christoph Niehoff, Peter Stangl, and David M. Straub (2017), arXiv:1703.09189. 1770
- [202] Kristof De Bruyn, Search for the rare decays $B_{(s)}^0 \rightarrow \tau^+ \tau^-$, Technical Report LHCb-CONF-2016-011. CERN-LHCb-CONF-2016-011, CERN, Geneva (Sep 2016). 1771
- [203] J. P. Lees et al., BaBar (2016), arXiv:1605.09637. 1772
- [204] A. Mord, LHCb (). 1773
- [205] Christoph Bobeth, Martin Gorbahn, Thomas Hermann, Mikolaj Misiak, Emmanuel Stamou, and Matthias Steinhauser, Phys. Rev. Lett., **112**, 101801 (2014), arXiv:1311.0903. 1774

-
- [206] M. Beylich, G. Buchalla, and T. Feldmann, *Eur. Phys. J.*, **C71**, 1635 (2011), arXiv:1101.5118.
- [207] Daping Du, A. X. El-Khadra, Steven Gottlieb, A. S. Kronfeld, J. Laiho, E. Lunghi, R. S. Van de Water, and Ran Zhou, *Phys. Rev.*, **D93**(3), 034005 (2016), arXiv:1510.02349.
- [208] Christoph Bobeth and Ulrich Haisch, *Acta Phys. Polon.*, **B44**, 127–176 (2013), arXiv:1109.1826.
- [209] Ulrich Haisch, (No) New physics in B_s mixing and decay, In *2012 Electroweak Interactions and Unified Theories*, pages 219–226 (2012), arXiv:1206.1230.
- [210] Wolfgang Altmannshofer and David M. Straub, *Eur. Phys. J.*, **C73**, 2646 (2013), arXiv:1308.1501.
- [211] Roel Aaij et al., LHCb, *Phys. Rev. Lett.*, **115**(11), 111803, [Addendum: *Phys. Rev. Lett.* **115**, no.15, 159901 (2015)] (2015), arXiv:1506.08614.
- [212] J. P. Lees et al., BaBar, *Phys. Rev. Lett.*, **109**, 101802 (2012), arXiv:1205.5442.
- [213] J. P. Lees et al., BaBar, *Phys. Rev.*, **D88**(7), 072012 (2013), arXiv:1303.0571.
- [214] M. Huschle et al., Belle, *Phys. Rev.*, **D92**(7), 072014 (2015), arXiv:1507.03233.
- [215] Wolfgang Altmannshofer, Stefania Gori, Maxim Pospelov, and Itay Yavin, *Phys. Rev.*, **D89**, 095033 (2014), arXiv:1403.1269.
- [216] Sheldon L. Glashow, Diego Guadagnoli, and Kenneth Lane, *Phys. Rev. Lett.*, **114**, 091801 (2015), arXiv:1411.0565.
- [217] Bhuvanajyoti Bhattacharya, Alakabha Datta, David London, and Shanmuka Shivashankara, *Phys. Lett.*, **B742**, 370–374 (2015), arXiv:1412.7164.
- [218] Admir Greljo, Gino Isidori, and David Marzocca, *JHEP*, **07**, 142 (2015), arXiv:1506.01705.
- [219] J. P. Lees et al., BaBar, *Phys. Rev.*, **D87**(11), 112005 (2013), arXiv:1303.7465.
- [220] Andrzej J. Buras, Jennifer Girrbach-Noe, Christoph Niehoff, and David M. Straub, *JHEP*, **02**, 184 (2015), arXiv:1409.4557.
- [221] Sebastien Descotes-Genon, Lars Hofer, Joaquim Matias, and Javier Virto, *JHEP*, **06**, 092 (2016), arXiv:1510.04239.
- [222] D. Dutta et al., Belle, *Phys. Rev.*, **D91**(1), 011101 (2015), arXiv:1411.7771.
- [223] P. del Amo Sanchez et al., BaBar, *Phys. Rev.*, **D83**, 032006 (2011), arXiv:1010.2229.
- [224] S. Villa et al., Belle, *Phys. Rev.*, **D73**, 051107 (2006), arXiv:hep-ex/0507036.
- [225] Stefan W. Bosch and Gerhard Buchalla, *JHEP*, **08**, 054 (2002), arXiv:hep-ph/0208202.
- [226] M. Beneke and J. Rohrwild, *Eur. Phys. J.*, **C71**, 1818 (2011), arXiv:1110.3228.
- [227] V. M. Braun and A. Khodjamirian, *Phys. Lett.*, **B718**, 1014–1019 (2013), arXiv:1210.4453.
- [228] Kristof De Bruyn, Robert Fleischer, Robert Knegjens, Patrick Koppenburg, Marcel Merk, and Niels Tuning, *Phys. Rev.*, **D86**, 014027 (2012), arXiv:1204.1735.
- [229] Stefan W. Bosch, *Exclusive radiative decays of B mesons in QCD factorization*, PhD thesis, Munich, Max Planck Inst. (2002), arXiv:hep-ph/0208203.
- [230] Joanne L. Hewett, D. G. Hitlin, T. Abe, K. Agashe, J. Albert, A. Ali, D. Atwood, C. Bauer, C. Bernard, I. Bigi, et al., editors, *The Discovery potential of a Super B Factory. Proceedings, SLAC Workshops, Stanford, USA, 2003* (2004), arXiv:hep-ph/0503261.
- [231] T. M. Aliev and G. Turan, *Phys. Rev.*, **D48**, 1176–1184 (1993).
- [232] T. M. Aliev, G. Hiller, and E. O. Iltan, *Nucl. Phys.*, **B515**, 321–341 (1998), arXiv:hep-ph/9708382.
- [233] S. Bertolini and J. Matias, *Phys. Rev.*, **D57**, 4197–4204 (1998), arXiv:hep-ph/9709330.
- [234] Ikaros I. Bigi, George Chiladze, Gela Devidze, Christoph Hanhart, Akaki Lipartelian, and Ulf-G. Meissner, *GESJ Phys.*, **2006N1**, 57–79 (2006), arXiv:hep-ph/0603160.
- [235] Alexander Gemintern, Shaouly Bar-Shalom, and Gad Eilam, *Phys. Rev.*, **D70**, 035008 (2004), arXiv:hep-ph/0404152.
- [236] H. M. Asatrian, C. Greub, A. Kokulu, and A. Yeghiazaryan, *Phys. Rev.*, **D85**, 014020 (2012), arXiv:1110.1251.
- [237] H. M. Asatrian and C. Greub, *Phys. Rev.*, **D89**(9), 094028 (2014), arXiv:1403.4502.
- [238] H. Simma and D. Wyler, *Nucl. Phys.*, **B344**, 283–316 (1990).
- [239] L. Reina, G. Ricciardi, and A. Soni, *Phys. Lett.*, **B396**, 231–237 (1997), arXiv:hep-ph/9612387.
- [240] L. Reina, G. Ricciardi, and A. Soni, *Phys. Rev.*, **D56**, 5805–5815 (1997), arXiv:hep-ph/9706253.
- [241] Jun-jie Cao, Zhen-jun Xiao, and Gong-ru Lu, *Phys. Rev.*, **D64**, 014012 (2001), arXiv:hep-ph/0103154.
- [242] H. M. Asatrian, C. Greub, and A. Kokulu, *Phys. Rev.*, **D93**(1), 014037 (2016), arXiv:1511.00153.
- [243] H. M. Asatrian, C. Greub, and A. Kokulu, *Phys. Rev.*, **D95**(5), 053006 (2017), arXiv:1611.08449.
- [244] Chia-Hung V. Chang, Guey-Lin Lin, and York-Peng Yao, *Phys. Lett.*, **B415**, 395–401 (1997), arXiv:hep-ph/9705345.
- [245] Wolfgang Altmannshofer, Andrzej J. Buras, David M. Straub, and Michael Wick, *JHEP*, **04**, 022 (2009), arXiv:0902.0160.
- [246] Jernej F. Kamenik and Christopher Smith, *Phys. Lett.*, **B680**, 471–475 (2009), arXiv:0908.1174.
- [247] Jernej F. Kamenik and Christopher Smith, *JHEP*, **03**, 090 (2012), arXiv:1111.6402.
- [248] R. R. Horgan, Z. Liu, S. Meinel, and M. Wingate, *PoS, LATTICE2014*, 372 (2015), arXiv:1501.00367.
- [249] Frederik Beaujean, Marcin Marcin Chrzasczcz, Nicola Serra, and Danny van Dyk, *Phys. Rev.*, **D91**(11),

- 114012 (2015), arXiv:1503.04100. 1851
- [250] W. Buchmuller and D. Wyler, Nucl. Phys., **B268**, 621–653 (1986). 1852
- [251] B. Grzadkowski, M. Iskrzynski, M. Misiak, and J. Rosiek, JHEP, **10**, 085 (2010), arXiv:1008.4884. 1853
- [252] Rodrigo Alonso, Benjamin Grinstein, and Jorge Martin Camalich, Phys. Rev. Lett., **113**, 241802 (2014), arXiv:1407.7044. 1854
- [253] Martin Bauer and Matthias Neubert, Phys. Rev. Lett., **116**(14), 141802 (2015), arXiv:1511.01900. 1855
- [254] O. Lutz et al., Belle Collaboration, Phys.Rev., **D87**, 111103 (2013), arXiv:1303.3719. 1856
- [255] J. Grygier et al., Belle (2017), arXiv:1702.03224. 1857
- [256] P. del Amo Sanchez et al., BaBar, Phys. Rev., **D82**, 112002 (2010), arXiv:1009.1529. 1858
- [257] R. D. Peccei and Helen R. Quinn, Phys. Rev. Lett., **38**, 1440–1443 (1977). 1859
- [258] R. D. Peccei and Helen R. Quinn, Phys. Rev., **D16**, 1791–1797 (1977). 1860
- [259] Steven Weinberg, Phys. Rev. Lett., **40**, 223–226 (1978). 1861
- [260] Frank Wilczek, Phys. Rev. Lett., **40**, 279–282 (1978). 1862
- [261] Joerg Jaeckel and Andreas Ringwald, Ann. Rev. Nucl. Part. Sci., **60**, 405–437 (2010), arXiv:1002.0329. 1863
- [262] K. A. Olive et al., Particle Data Group, Chin. Phys., **C38**, 090001 (2014). 1864
- [263] Steven Weinberg, Phys. Rev. Lett., **43**, 1566–1570 (1979). 1865
- [264] Jernej F. Kamenik and Christopher Smith, Phys. Rev., **D85**, 093017 (2012), arXiv:1201.4814. 1866
- [265] J. P. Lees et al., BaBar, Phys. Rev., **D86**, 051105 (2012), arXiv:1206.2543. 1867
- [266] C. L. Hsu et al., Belle, Phys. Rev., **D86**, 032002 (2012), arXiv:1206.5948. 1868
- [267] Michael Feindt, Fabian Keller, Michal Kreps, Thomas Kuhr, Sebastian Neubauer, Daniel Zander, and Anze Zupanc, Nucl. Instrum. Meth., **A654**, 432–440 (2011), arXiv:1102.3876. 1869
- 1870
- 1871